Characterization of key mechanisms involved in transmigration and invasion of mesenchymal stem cells

Improvement of transendothelial migration via focussed

ultrasound-mediated microbubble stimulation

Inaugural-Dissertation

zur

Erlangung des Doktorgrades

der Mathematisch-Naturwissenschaftlichen Fakultät

der Universität zu Köln

vorgelegt von

Caroline Steingen

aus Köln

Copy Team Cologne, Köln

2008

Berichterstatter: Prof. Dr. Wilhelm Bloch

                           Prof. Dr. Manolis Pasparakis

Tag der mündlichen Prüfung: 16. April 2008

Meinen Eltern

Carin & Rudi Steingen

und meiner lieben Oma

Kurzzusammenfassung

Adulte mesenchymale Stammzellen (MSCs) werden bereits für die Therapie verschiedener Krankheiten klinisch eingesetzt. Der erste Teil der vorliegenden Arbeit beschäftigt sich mit der Aufklärung von Schlüsselmechanismen, die an der Transmigration von MSCs über die Endothelbarriere und der Invasion in ein Ziel-gewebe beteiligt sind. Beide Prozesse sind die Grundvoraussetzung für eine erfolgreiche Stammzelltherapie, da MSCs stets das Blutgefäßsystem verlassen müssen, um in umgebendes Gewebe einzuwandern. Versuche mit verschiedenen Modelsystemen sowie *in vivo* Experimente ergaben, dass MSCs schnell Kontakt zur Endothelbarriere aufnehmen und anschließend die Blutbahn über folgende Schritte verlassen: (1) durch eine Integration in das Endothel, (2) durch die Transmigration über die Endothelbarriere, vermittelt durch die Ausbildung von Zellfortsätzen, (3) durch Penetration der Basalmembran und anschließende Invasion in das umgebende Gewebe.

Zudem konnte gezeigt werden, dass die Transmigration humaner MSCs durch die Interaktion der Oberflächenmoleküle VLA-4 und VCAM-1 vermittelt wird und in einer regionalen Ansammlung von β1-Integrinen resultiert. Desweiteren schütten MSCs aktive Matrix-Metalloproteinase (MMP)-2, nicht aber MMP-9 aus, um in Herzmuskel-gewebe einzudringen.

Die vorliegende Arbeit zeigt, dass sowohl der zeitliche Verlauf als auch die morpho-logischen Aspekte der Transmigration vom Phänotyp der Endothelzellen abhängig sind. Dies deutet auf Unterschiede in der Effizienz der Transmigration innerhalb des Gefäßsystems – abhängig vom Gefäßtyp – hin. Außerdem beschleunigt die Zugabe von Zytokinen, besonders VEGF und EPO, zu Beginn der Transmigration den Ablauf des Prozesses. Auch ergaben Versuche, dass MSCs, sobald sie Kontakt zu Endo-thelzellen aufnehmen, vermehrt Stickstoffmonoxid (NO) und reaktive Sauerstoff-Spezies (ROS) freisetzen. Veränderungen des NO- oder ROS-Haushaltes resultierten in Abweichungen der transmigratorischen Fähigkeit der MSCs.

Der letzte Teil der vorliegenden Arbeit beschäftigt sich mit zwei möglichen Ansätzen, die therapeutische Effizienz von MSCs zu erhöhen. Einerseits zeigte sich, dass eine genetische Modifikation der Stammzellen durch adenovirale Überexpression des Chemokin-Rezeptors CXCR4 keine Verbesserung ihrer transmigratorischen Aktivität zur Folge hat. Andererseits verbesserte eine gezielte Vorbehandlung des Endothels durch eine neuartige und nicht-invasive Technik, die Ultraschall-vermittelte Mikro-bläschen-Stimulierung (UMS), sowohl die Anlockung als auch die Transmigration und Invasion von MSCs in gesundes und ischämisches Herzmuskelgewebe. Diese regionale Verbesserung wurde vermutlich durch die Ultraschall-vermittelte Frei-setzung von Stickstoffmonoxid und Zytokinen, sowie die lokale Aktivierung von Matrix-Metalloproteinasen erzielt. Daher stellt die Ultraschall-vermittelte Mikrobläschen-Stimulierung eine zukunftsweisende Möglichkeit dar, die therapeutische Effizienz von MSCs lokal und nicht-invasiv zu erhöhen.

Abstract

Stem cell therapy using human adult mesenchymal stem cells (MSCs) has emerged as a novel strategy for the treatment of a variety of damaged tissues. For a successful systemic stem cell therapy MSCs have to exit the blood circulation by transmigrating across the endothelium and invading into the target tissue. Elevating our knowledge on these core processes might help to optimize stem cell based therapies. The first part of the present study provides insights into key mechanisms involved in the transmigration and invasion of MSCs. Different model systems as well as *in vivo* studies revealed that MSCs quickly come into contact with the endothelium and subsequently exit the blood circulation by (1) integrating into the endothelium, (2) transmigrating across the endothelial barrier *via* the insertion of plasmic podia, (3) penetrating the basement membrane and subsequently invading the surrounding tissue.

Additionally, it was proven that transmigration of human MSCs not only requires the interaction of very late antigen-4 (VLA-4, $\alpha4\beta1$ integrin) and its most important ligand vascular cell adhesion molecule-1 (VCAM-1), but also triggers a clustering of $\beta1$ integrins. Furthermore, upon invading into cardiac tissue MSCs secrete active matrix metalloproteinase (MMP)-2, but not MMP-9.

This study also demonstrates that both the time course and the morphological aspects of MSC transmigration differ depending on the endothelial phenotype, thus indicating, that a variable capacity for transendothelial migration exists within the vasculature. Furthermore, addition of cytokines, mainly vascular endothelial growth factor (VEGF) and erythropoietin (EPO), accelerate the transmigration of MSCs at early stages. Moreover, nitric oxide (NO) and reactive oxygen species (ROS) are released by MSCs upon contact with endothelial cells; manipulating the NO and ROS system by donors and inhibitors resulted in alterations of the transmigratory capacity of MSCs.

The second part of the study deals with two possible strategies to enhance the transmigration of MSCs and thereby their therapeutic effectiveness. First, the results demonstrate that genetic modification of MSCs using adenoviral overexpression of the chemokine receptor CXCR4 does not lead to an increase in the transmigration efficiency. Second, focussed pretreatment of the endothelium by a novel and non-invasive technique using ultrasound-mediated microbubble stimulation (UMS) induces a targeted improvement of MSC attraction, transmigration and invasion into non-ischemic as well as into ischemic myocardium. This effect was most likely due to the release of nitric oxide, cytokines and the regional activation of proteases. Thus, UMS represents a forward-looking possibility to increase the efficiency of MSC engraftment by modulating the process of transmigration in a targeted and non-invasive manner.

Table of contents

Table of figures

List of abbreviations

3D	three-dimensional
α-MEM	Minimum Essential Medium alpha Modification
Ad.CXCR4.GFP	CXCR4 and GFP expressing adenovirus
Ad.GFP	GFP expressing adenovirus
ANOVA	one-way analysis of variance
Ap	apex
APF	3´-(p-aminophenyl) fluorescein
AW	anterior wall
bFGF	basic fibroblastic growth factor
BP	bandpass emission filter
bp	base pair(s)
BSA	bovine serum albumin
CD	cluster of differentiation
cDNA	complementary DNA
CFU-F	colony forming unit-fibroblast assay
CMFDA	5-chloromethylfluorescein diacetate
CMV	cytomegalovirus
CXCR4	CXC chemokine receptor 4
DAB	diaminobenzidine
DAF	4-amino-5-methylamino-2`,7`-difluorofluorescein diacetate
DAPI	4´,6-diamidino-2-phenyl-indole
DEPC	diethylpyrocarbonate
DETA	diethylenetriamine
Dil-Ac-LDL	1,1'-dioctadecyl-3,3,3',3'-tetramethyl-indocarbocyanine perchlorate acetylated-low density lipoprotein
D-MEM	Dublecco`s Modified Eagle Medium
DMSO	dimethylsulfoxide
DNA	deoxyribonucleic acid
DNAse	deoxyribonuclease
dNTP	deoxyribonucleotide triphosphate
dT	deoxyribosylthymine nucleotide
DTT	dithiothreitol
e.g.	for example
EBs	embryoid bodies
ECD	energy-coupled dye
ECG	electrocardiogram
ECs	endothelial cells
EDTA	ethylene-diamine tetraacetic acid
ELISA	enzyme-linked immunosorbent assay
eNOS	endothelial nitric oxide synthase
EPO	erythropoietin

EtOH	ethanol
F	forward
FACS	fluorescence activated cell sorting
FCS	fetal calf serum
FITC	fluorescein isothiocyanate
Gel ZYM	active gelatinases detected by *in situ* zymography
GFP	green fluorescent protein
GM-CSF	granulocyte-macrophage colony-stimulating factor
HCAEC	human coronary artery endothelial cells
HEPES	4-(2-hydroxyethyl)-1-piperazineethanesulfonic acid
HFT	main dichroic beam splitter
HRP	horseradish peroxidase
HuAoEC	human aortic endothelial cells
HUVEC	human umbilical vein endothelial cells
I/R	ischemia followed by reperfusion
ICAM	intercellular adhesion molecule
IgG	immunoglobulin
IL	interleukin
kDa	kilodalton
LAD	left descending coronary artery
LIF	leukemia inhibition factor
L-NAME	N-nitro-L-arginine methyl ester
LP	longpass emission filter
LSM	laser scanning microscope
LV	left-ventricular cavity
mAb	anti-mouse antibody
MACS	magnet associated cell sorting
MAP	mitogen activated protein
MAPK	MAP kinase
MI	myocardial infarction
min	minute
M-MLV	moloney murine leukemia virus
MMP	matrix metalloproteinase
MOI	multiplicity of infection
MOPS	3-morpholinopropane-1-sulfonic acid
MSC	mesenchymal stem cell
n. s.	no significant difference
NAc	N-acetylcysteine
NFT	secondary dichroic beam splitter
NO	nitric oxide
NOS	nitric oxide synthase
PAGE	polyacrylamide-gelelectrophoresis
PBS	phosphate-buffered saline

PC	phycoerythrin-cyanine
PCR	polymerase chain reaction
PE tube	polyethylene tube
PE	phycoerythrin
PECAM	platelet-endothelial cell adhesion molecule
PFA	paraformaldehyde
Pfu	plaque-forming units
pH	*potentia hydrogenii*
PVDF	polyvinylidene fluoride
PW	posterior wall
R	reverse
RNA	ribonucleic acid
ROS	reactive oxygen species
rpm	revolutions per minute
RT-PCR	reverse transcription polymerase chain reaction
RV	right ventricle
SDF	stromal-derived growth factor
SDS	sodium dodecyl sulfate
sec	seconds
TAE	Tris-acetate-EDTA
TBS	Tris-buffered saline
TBST	Tris-buffered saline containing Tween 20
TGF	transforming growth factor
TNF-α	tumor necrosis factor alpha
Tris	2-Amino-2-(hydroxymethyl)propane-1,3-diol
TUNEL	terminal uridine desoxynucleotidyl transferas dUTP nick end labeling
U	unit
UMS	ultrasound-mediated microbubble stimulation
UV	ultraviolet light
v/v	volume per volume
VCAM	vascular cell adhesion molecule
VE-Cadherin	vascular endothelial Cadherin
VEGF	vascular endothelial growth factor
VLA	very late antigen
vs.	versus
w/v	weight per volume

1.   Introduction

Bone marrow-derived mesenchymal stem cells (MSCs) are adult stem cells that reside within the bone marrow compartment (Schmidt *et al.*, 2006b). MSCs can be isolated and expanded in culture and are described as multipotent because of their ability, even as clonally isolated cells, to differentiate into a variety of different cells (Tuan *et al.*, 2002; Pittenger *et al.*, 2004). Stem cell therapy using human adult bone marrow derived MSCs has emerged as a novel strategy for the treatment of a variety of damaged tissues as they possess a multi-lineage differentiation potential (Jiang *et al.*, 2002). The use of adult stem cells to regenerate damaged tissue not only circumvents the ethical and technical issues associated with the use of embryonic stem cells, but also allows the transplantation of autologous as well as allogeneic cells. As allogeneic MSCs inhibit T cell proliferation and maturation (Krampera *et al.*, 2003; Le Blanc *et al.*, 2003; Tse *et al.*, 2003b) they are not recognized by responder T cells and therefore not rejected by a recipient host. Thus, allogenic MSCs can be prepared in advance for any patient at the needed time (Pittenger *et al.*, 1999) and can be administered without immunosuppression (Krause *et al.*, 2007).

1.1   Sources, multipotency and markers of mesenchymal stem cells

MSCs, first identified by Friedenstein and co-workers in 1976 (Friedenstein *et al.*, 1976), have a fibroblastic morphology, possess a broad *ex vivo* expansive potential and can maintain an undifferentiated, stable phenotype over many generations (Pittenger *et al.*, 1999). Currently, bone marrow aspirate is considered to be the most accessible and enriched source of MSCs. Nevertheless, MSCs have also been isolated from several other sources, including adipose tissue (Zuk *et al.*, 2002; Lee *et al.*, 2004b), scalp tissue (Shih *et al.*, 2005), dermal tissue (Toma *et al.*, 2001) and peripheral blood (Fernandez *et al.*, 1997). In addition to adult tissues, MSCs were also identified in various fetal tissues, such as in the placenta (In 't Anker *et al.*, 2004), in umbilical veins and umbilical cord blood (Erices *et al.*, 2000). Although MSCs represent a very small fraction of cells – only about 0.001 to 0.01% of the cells isolated from a density gradient of a bone marrow aspirate belong to this population (Pittenger *et al.*, 1999) – they are easy and fast expandable *ex vivo*. Due to the plastic-adherence of MSCs, non-adherent contaminating hematopoietic cells can be easily removed after isolation. Human MSC populations can be distinguished from

hematopoietic stem cells and leukocytes by distinct cell surface markers. Considering their mesodermal origin, MSCs are known to be negative for the leukocyte common antigen CD45, for the lipopolysaccharide receptor CD14 and for CD34, a marker of human hematopoietic stem and progenitor cells. The collective presence of a combination of other markers, such as CD105 (endoglin or transforming growth factor TGF β1/3-receptor) and CD106 (vascular cell adhesion molecule-1, VCAM-1), albeit not specific to MSCs, defines the MSC cell population (Pittenger *et al.*, 1999).

As depicted in Figure 1, MSCs are capable of differentiating into various tissues of mesenchymal origin such as bone (Friedenstein *et al.*, 1987; Haynesworth *et al.*, 1992; Kuznetsov *et al.*, 1997; Meinel *et al.*, 2004a; Meinel *et al.*, 2004b), skeletal muscle cells and cardiomyocytes (Wang *et al.*, 2000; Goodell *et al.*, 2001; Toma *et al.*, 2002; De Bari *et al.*, 2003), cartilage (Friedenstein *et al.*, 1987; Li *et al.*, 2005b) or vascular endothelial cells (Reyes *et al.*, 2002; Koike *et al.*, 2004), but can also give rise to non-mesenchymal cells like neural cells (Azizi *et al.*, 1998; Kopen *et al.*, 1999).

1.2   Therapeutic usage of MSCs

The ability of MSCs to differentiate into various cells *in vivo* has understandably aroused great interest for the therapeutic treatment of a variety of diseases. Indeed, clinical benefit has been observed following the intravenous administration of heterogeneous populations of MSCs in patients with osteogenesis imperfecta (Horwitz *et al.*, 1999) or severe acute graft-versus-host disease (Le Blanc *et al.*, 2004). Moreover, due to the very limited ability of myocardial tissue to regenerate after a myocardial infarction, treatment with stem cells also seems to be a promising therapeutic approach in cardiology. Adult cardiomyocytes have essentially no regenerative capacity and although a cardiac stem cell has been described (Anversa *et al.*, 2002), its physiological role in repair after infarction appears minimal (Pittenger and Martin, 2004). Therefore, only an implantation of exogenous cells may allow replacement of damaged cardiac cells. Indeed, cellular transplantation, termed cellular cardiomyoplasty, has been investigated as a potential therapy for myocardial infarction in order to replace cardiomyocytes lost after ischemia (Bittner *et al.*, 1999; Jackson *et al.*, 2001; Orlic *et al.*, 2001a; Orlic *et al.*, 2001b; Nygren *et al.*, 2004). The first use of bone marrow cells for cardiomyoplasty was reported in 1999 by Tomita and co-workers at the University of Toronto (Tomita *et al.*, 1999). For a successful cardiomyoplasty, MSCs are a promising stem cell type, because they differentiate

into a cardiomyocyte-like phenotype when implanted in healthy myocardium (Pittenger *et al.*, 2000; Toma *et al.*, 2002). Furthermore, MSCs supply growth factors and cytokines, which help to repair the damaged tissue *via* paracrine effects (Pittenger and Martin, 2004; Mirotsou *et al.*, 2007). Thus, in several ongoing clinical trials, patients are treated with MSCs after a myocardial infarction (for review see (Laflamme *et al.*, 2005; Ohnishi *et al.*, 2007)). However, for a successful clinical application different strategies for transporting MSCs to their target destinations have to be evaluated regarding their applicability and efficiency.
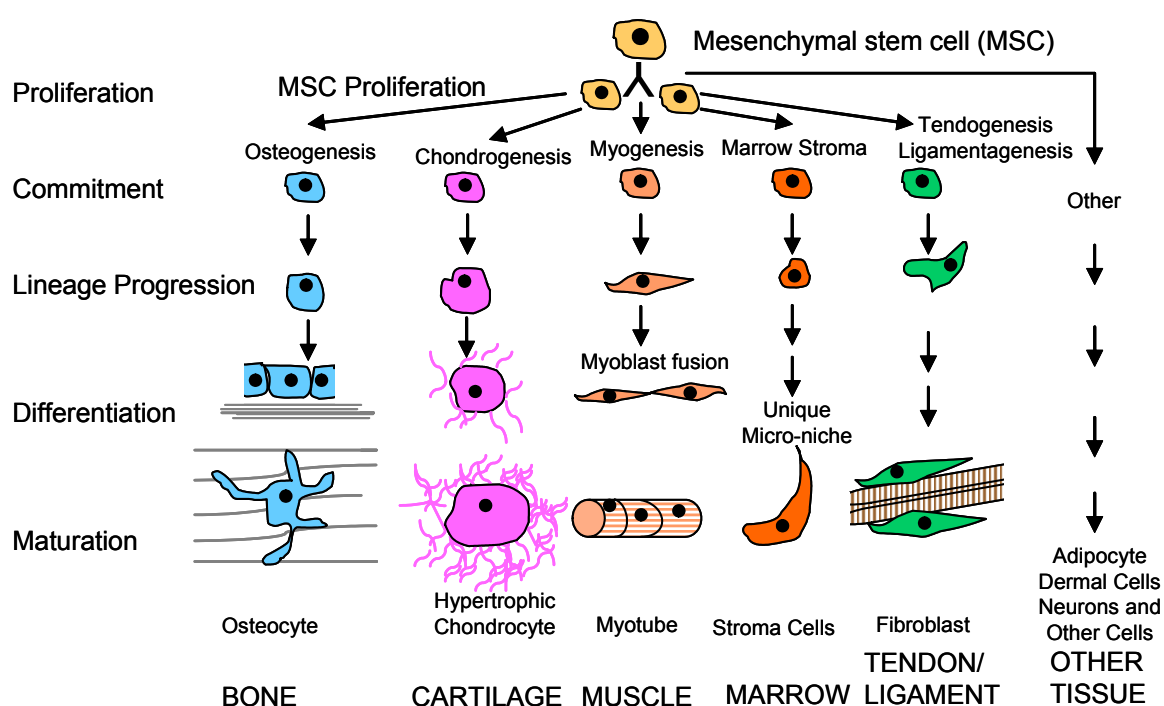
Figure 1: MSC multi-lineage differentiation potential

MSCs are able to undergo extensive proliferation prior to differentiation into a range of mesenchymal tissue and cell types, including bone, cartilage, muscle, stroma, tendon and adipose tissue. In addition, there is evidence that MSCs possess the ability to differentiate into non-mesenchymal tissues including skin and nervous tissues. Scheme adapted from Caplan and Bruder, 2001 (Caplan *et al.*, 2001).

Various routes of administration have been tested for delivering MSCs. For example, stem cells were applied during a heart catheter session (Wang *et al.*, 2001; Assmus *et al.*, 2002; Chen *et al.*, 2004; Kang *et al.*, 2004; Wollert *et al.*, 2004; Katritsis *et al.*, 2005; Chen *et al.*, 2006) or *via* an intramyocardial (Wang *et al.*, 2000; Kawamoto *et al.*, 2003; Li *et al.*, 2005a; Yoon *et al.*, 2005), intraventricular or intravenous injection (Barbash *et al.*, 2003).

However, as lately demonstrated by Breitbach and co-workers (Breitbach *et al.*, 2007), a direct intramyocardial transplantation of bone marrow cells into the infarcted heart carries a considerable risk since MSCs formed encapsulated structures in the infarcted myocardium containing ossifications. Apparently, systemic delivery of MSCs circumvents theses problems associated with site-specific delivery, such as risks of calcification and tissue damage (Fox *et al.*, 2007), because none of these complications have been reported after systemic administration (Saito *et al.*, 2002; Barbash *et al.*, 2003; Price *et al.*, 2006). Furthermore, systemic cell delivery allows the administration of multiple doses (Fox *et al.*, 2007). Indeed, MSCs have the ability to home to sites of myocardial injury when administered intravenously after acute infarction (Saito *et al.*, 2002; Price *et al.*, 2006). Therefore, for therapeutic purposes systemic infusion of MSCs is not only the most practicable way of administration, but also holds less risk due to its minimal-invasive character. However, during a systemic application MSCs must be attracted to the target tissue, come into contact with the endothelial barrier and subsequently open and transmigrate across the endothelium to exit the blood circulation and to invade their target tissue. To date, most of the underlying morphological and molecular mechanisms involved in transmigration and invasion of MSCs remain unelucidated. However, improving our knowledge on these core processes might help elevate the efficiency of stem cell therapy.

1.3   Open questions regarding transmigration and invasion of MSCs

1.3.1 Adhesion molecules involved

In order to elucidate key steps of transendothelial migration and invasion of MSCs, the diapedesis of leukocytes can serve as a model system. Leukocyte diapedesis is well characterized and divided into four steps: (1) margination, (2) rolling, (3) adherence and finally (4) transmigration (Seely *et al.*, 2003). This multi-step process involves several types of adhesion molecules, proteases and cytokines (De Becker *et*

al., 2007). Most of the leukocyte adhesion molecules like β$_2$ integrin linked molecules are not expressed on the surface of MSCs (Pittenger and Martin, 2004; Ruster *et al.*, 2006; Docheva *et al.*, 2007). However, very late antigen-4 (VLA-4, α4β1 integrin) and its most important ligand, vascular cell adhesion molecule-1 (VCAM-1), are expressed in MSCs (Minguell *et al.*, 2001; Ruster *et al.*, 2006; Segers *et al.*, 2006). A recent study reported that anti-VCAM-1 antibodies, but not anti-ICAM-1 (intercellular adhesion molecule-1) antibodies, reduce the adhesion of rat MSCs to microvascular endothelial cells (Segers *et al.*, 2006). In addition, it has been shown that β1 integrins are crucial for the rolling and adhesion of human MSCs to endothelial cells (Ruster *et al.*, 2006). Thus far, adhesion molecules involved in the transmigration of MSCs – the final step of exiting the blood circulation – remain to be identified.

1.3.2 Role of proteases for the invasion of MSCs

The second key barrier within vascular walls is the basement membrane. It is composed of a complex network of several extracellular matrix proteins, such as laminins (Sorokin *et al.*, 1994), collagen type IV (Timpl, 1996) and gelatine (Nagase *et al.*, 1999). The vascular basement membrane serves as a significant structural support for endothelial cells, but also provides a distinct and effective barrier to macromolecules and infiltrating cells, such as leukocytes. Leukocytes navigate toward their target sites by adhering to extracellular matrix glycoproteins and secreting degradative enzymes (Vaday *et al.*, 2001). This proteolytic cleavage of the basement membrane is a commonly proposed mode of leukocyte penetration of basement membrane barriers (Wang *et al.*, 2006). Such degradation of the basement membrane *via* proteolytic enzymes is also a prerequisite for the invasion of MSCs. Matrix metalloproteinases (MMPs) are candidate proteolytic enzymes which could be involved in this process. MMPs depend on binding a Zn^{2+} ion for their catalytic activity. They are synthesized as pre-pro-enzymes and most are secreted as inactive pro-enzymes or zymogens that are activated by cleavage of the pro-domain (Sternlicht *et al.*, 2001). Based on substrate specificity and structure they are divided into several subgroups: gelatinases, collagenases, stromelysins, matrilysins and membrane-type MMPs. The gelatinases, MMP-2 and MMP-9, have the same basic structure as the other MMPs, but their catalytic domain contains three repeats of the fibronectin type II domain. These repeats interact with major constituents of the basement membrane, gelatine, laminin and collagen type IV (Nagase and Woessner,

1999). Gelatinases are not only involved in cancer cell migration, but also in leukocyte homing (Leppert *et al.*, 1995; Faveeuw *et al.*, 2001). Furthermore, De Becker *et al.* recently demonstrated a functional involvement of MMP-2 in MSC homing through bone marrow endothelium (De Becker *et al.*, 2007). However, involvement of MMPs in transmigration and invasion of MSCs outside the bone marrow has not been verified, yet.

1.3.3 Role of endothelial phenotype and cytokines

For successful and efficient systemic delivery of MSCs it might be important to identify target vessels, which enable the most effective transmigration of MSCs. It is known that in various regions of the vascular tree, the endothelium is functionally different and its barrier function varies accordingly (Dejana *et al.*, 1995). For example, variances in the amount of intercellular tight junctions exist at different points along the vascular tree and thereby cause differences in the endothelial permeability. For instance, intercellular junctions are well-organized and numerous in large arteries or in the blood vessels of the brain where the control of permeability must be restricted, whereas they are very primitive and almost disappear in the postcapillary venules where cell extravasation needs to be particularly efficient (Simionescu *et al.*, 1991). For the extravasation of leukocytes it is discussed that endothelial cells not only play an important role in regulating leukocyte attachment, but also actively modulate their extravasation. For example, differences comparing the modalities of leukocyte extravasation exist for different types of vessels such as lymphatic versus large vessels (Dejana *et al.*, 1996). Similar differences depending on the endothelial phenotype could also play a key role for the transmigration of MSCs.

During extravasation leukocytes constantly orientate themselves in response to specific signals in their surroundings. Cytokines and chemokines are key biological mediators that provide such signals for cell navigation (Vaday *et al.*, 2001). Lately, Schmidt *et al.* (Schmidt *et al.*, 2006a) validated that cytokines, in particular basic fibroblastic growth factor (bFGF), increase the migratory activity of MSCs. Because cytokines such as bFGF (Kuwabara *et al.*, 1995; Stavri *et al.*, 1995), vascular endothelial growth factor (VEGF) (Sasaki *et al.*, 2001), interleukin-6 (IL-6) (Imaizumi *et al.*, 2007), interleukin-1 beta (IL-1β) (Mitchell *et al.*, 2007) and tumor necrosis factor alpha (TNF-α) (Pasqui *et al.*, 2006) are released after a myocardial infarction

they may play an important role in recruiting MSCs to infarcted myocardium and in facilitating or increasing transmigration.

Recently, Segers and co-workers demonstrated an increase of cardiac infiltration of MSCs after activation with TNF-α or IL-1β before cell interaction (Segers *et al.*, 2006). In addition, rolling and adhesion of MSCs was found to be increased after pre-stimulation of endothelial cells with TNF-α (Ruster *et al.*, 2006). Therefore, the question arises whether cytokines not only improve the migratory capacity as well as rolling and adhesion, but also the transmigration of MSCs. Till date, no study has clarified the involvement of cytokines in the transmigration of MSCs.

1.3.4 Involvement of nitric oxide and reactive oxygen species

Nitric oxide (NO), the classic vasorelaxing factor discovered by Furchgott in 1980 (Furchgott *et al.*, 1980), is a short-lived ubiquitous second messenger that has been linked to events in the MSC lifecycle like proliferation, differentiation or apoptosis (Klinz *et al.*, 2005). NO is produced by nitric oxide synthases (NOS), namely the neuronal nNOS, the inducible iNOS and the endothelial nitric oxide synthase eNOS (Alderton *et al.*, 2001). In the vascular system a continuous production of NO by eNOS helps to maintain the endothelium in an anti-atherogenic state, in part by preventing the activation of transcription factors that determine the expression of proatherogenic adhesion molecules required for the attachment and sequestration of monocytes through the endothelial cell monolayer (Fleming *et al.*, 2003). It is known that NO can modulate the permeability of endothelial cell monolayers to mononuclear cells (Isenberg, 2003; Isenberg *et al.*, 2005). Klinz *et al.* showed that the NO-producing enzyme eNOS is not only expressed by endothelial cells, but also by MSCs (Klinz *et al.*, 2005). In a recent study implantation of MSCs overexpressing eNOS improved right ventricular impairments caused by pulmonary hypertension (Kanki-Horimoto *et al.*, 2006). Whether this is at least partly the result of an increase in MSC engraftment has not been assessed, though. Moreover, Kaminski and co-workers recently demonstrated that the firm adhesion of c-kit[+] bone marrow stem cells to the endothelium was entirely abrogated in eNOS-kockout mice (Kaminski *et al.*, 2007). Thus, the presence of eNOS appears to be crucial for the firm adhesion of c-kit^{+} cells (Kaminski *et al.*, 2007). However, only little information is available about the involvement of NO during the contact of MSCs and the endothelial barrier, while NO released by MSCs might also play a key role during the transmigration of MSCs.

Beside NO, reactive oxygen species (ROS) function as important intracellular and intercellular second messengers to modulate many downstream signaling molecules in endothelium and vascular smooth muscle (Paravicini *et al.*, 2006). ROS also have distinct physiological and pathophysiological impacts on vascular cells. Herein, ROS contribute to vascular dysfunction and remodeling through oxidative damage, for example by stimulating cell migration, activating adhesion molecules and inflammatory reaction (Yung *et al.*, 2006) as well as modifying the extracellular matrix (Paravicini and Touyz, 2006). In addition, Fischer and colleagues revealed that H_2O_2 induces an increased endothelial permeability (Fischer *et al.*, 2005). Therefore, it might be interesting to examine whether MSCs release ROS to modulate the permeability of the endothelial barrier.

1.4 Approaches to enhance the transmigration of MSCs

Therapeutic success of stem cell therapy essentially depends on an efficient cell delivery to the required site. Based on experimental and clinical data best functional recovery of infarcted myocardial tissue was obtained in the peri-infarction myocardial borderzone tissue (Schachinger *et al.*, 2004; Hofmann *et al.*, 2005; Ghanem *et al.*, 2007). Therefore, the peri-infarction borderzone, but not the myocardial scar itself seems to be the adequate target tissue for regenerative stem cell therapy. Moreover, transplantation efficacy improved significantly after a direct application of MSCs into the left-ventricular cavity (Barbash *et al.*, 2003). This improvement was due to less entrapment of the stem cells in the pulmonary circulation as it has been described for the intravenous transfusion of MSCs (Barbash *et al.*, 2003). However, even after intracoronary cardiomyoplasty the actual number of MSCs delivered to the myocardium is very low, whereas cell uptake in liver and spleen is very high (Barbash *et al.*, 2003). Targeted cell delivery, for example to the borderzone of myocardium is possible *via* intramyocardial cell injection, but this strategy is limited because of its invasive character resulting in tissue damage, the difficulty of delivering multiple doses and risks for calcification (Breitbach *et al.*, 2007). Due to a markedly lower expression of chemoattractant factors, recruitment and transmigration of a reasonable number of stem cells into non-ischemic myocardium is a rare event. Therefore, since stem cell therapy should be aimed at vital myocardium, for example to the peri-infarction borderzone, improvements in non-invasive transplantation efficacy is of major interest.

1.4.1 Genetic modification of MSCs

One way to augment the efficiency of cardiomyoplasty is to genetically modify MSCs by transgene expression before transplantation. Such a targeted modification of MSCs could trigger an enhancement of stem cell transplantation. Successful genetic modification of MSCs *via* retroviral transduction has been reported (Mangi *et al.*, 2003; Bhakta *et al.*, 2006; Gnecchi *et al.*, 2006). Mangi and co-workers discovered that intramyocardial injection of MSCs overexpressing the prosurvival gene Akt remarkably prevented ventricular remodeling and improved cardiac function after myocardial infarction compared with the administration of control MSCs (Mangi *et al.*, 2003). Therefore, genetic modification of MSCs might help to elevate the efficiency of stem cell therapy.

The chemokine stromal-derived-factor-1 (SDF-1) and its G-protein-coupled receptor CXCR4 play an important role in the homing and engraftment of hematopoietic stem cells in the bone marrow. For example, an overexpression of CXCR4 in mobilized peripheral blood hematopoietic stem cells improves their marrow engraftment (Brenner *et al.*, 2004). Lately, Schmidt *et al.* evidenced that the CXCR4-ligand SDF-1 significantly enhances the migratory activity of MSCs (Schmidt *et al.*, 2006a). Furthermore, a study using MSCs transduced with a retroviral vector containing CXCR4 showed a significantly increased migration toward SDF-1 (Bhakta *et al.*, 2006). To summarize, a genetic modification of the CXCR4-expression in MSCs could be an approach to improve the transmigratory capacity of MSCs.

1.4.2 Ultrasound-mediated microbubble stimulation

A second approach to possibly improve targeted cell delivery makes use of a novel non-invasive strategy: the focussed ultrasound-mediated microbubble stimulation (UMS) (Imada *et al.*, 2005; Zen *et al.*, 2006). The focussed effect of this technique is based on intravascular oscillation and possibly implosion of gas-filled lipid-coated microbubbles after their activation *via* targeted ultrasound (Imada *et al.*, 2005; Zen *et al.*, 2006; Caskey *et al.*, 2007). The ultrasound-mediated oscillation of microbubbles results in a transient alteration of the endothelium. UMS was reported to cause at high emission power an acute inflammatory action on the cell surface by the transient formation of small holes (less than 5 µm) in the cell surface that revert to normal appearance (Taniyama *et al.*, 2002b). Those local small transient pores were induced

immediately after regional insonication and allowed targeted gene and cell delivery over the endothelial barrier. This technique has been used recently for targeted delivery of unfractionated bone marrow-derived mononuclear cells into chronic ischemic skeletal muscle (Imada *et al.*, 2005) and myocardium (Zen *et al.*, 2006). In skeletal muscle ultrasound-mediated microbubble oscillation activated platelet-derived proinflammatory factors, which induced *in vitro* expression of the adhesion molecules P-selectin and ICAM-1 1 hour after UMS (Imada *et al.*, 2005). These UMS-mediated effects resulted in an increased attachment of transplanted bone marrow-derived mononuclear cells on the endothelium (Imada *et al.*, 2005). Zen *et al.* reported that stimulation *via* UMS induced the expression of the adhesion molecules VCAM-1 and ICAM-1 in capillaries. Furthermore, the UMS-mediated supply of bone marrow-derived mononuclear cells in the myocardium of a hamster cardiomyopathy model increased the myocardial content of VEGF and improved cardiac function 12 weeks after UMS application (Zen *et al.*, 2006). Additionally, low-frequency contrast microbubble-enhanced ultrasound was reported to increase the vascular permeability (Stieger *et al.*, 2007). To summarize, UMS alters the functionality of the endothelial barrier over a longer period of time after the insonication by up-regulating the secretion of cytokines, inducing the expression of adhesion molecules, enhancing the attachment of bone marrow-derived mononuclear cells on the endothelium and increasing the vascular permeability (Taniyama *et al.*, 2002b; Imada *et al.*, 2005; Zen *et al.*, 2006; Stieger *et al.*, 2007). Therefore, UMS might be a powerful and non-invasive tool to locally improve the transmigration of MSCs.

1.5 Aims and experimental design of this study

For a successful systemic therapy, mesenchymal stem cells must come into contact with the endothelium and subsequently open and transmigrate across the endothelial barrier to exit the blood circulation and to invade their target tissue. To date, most of the underlying mechanisms of transmigration and invasion remain unelucidated. Improving our knowledge on these core processes might elevate the efficiency of stem cell therapy. The aims of the study were (1) to characterize key mechanisms involved in transmigration and invasion of MSCs and (2) to identify strategies to enhance the efficiency of myocardial MSC engraftment. Hence, this study comprises two major parts, the second of which concentrates on possible applications.

(1) Characterization of the transmigration and invasion of MSCs

(a)   Interaction of MSCs with the endothelial barrier

Several model systems were established to visualize and morphologically characterize the interaction of MSCs with the endothelial barrier. Furthermore, *in vivo* experiments were conducted to validate that transmigration of MSCs is a physiologically occurring process. Although, MSCs home to infarcted myocardium after systemic administration (Barbash *et al.*, 2003) and transmigrating MSCs were observed *ex vivo* (Schmidt *et al.*, 2006b), thus far, no direct evidence about transmigration of MSCs *in vivo* exists.

(b)   Mechanisms involved in the transmigration and invasion of MSCs

To investigate the mechanisms involved in the transendothelial migration and invasion of MSCs, the diapedesis of leukocytes served as a model system. Consequently, experiments were designed to (a) identify adhesion molecules involved in transmigration by investigating the effect of blocking VCAM-1 and VLA-4; (b) to monitor the involvement of matrix metalloproteinases during the invasion of MSCs into cardiac tissue; (c) to determine the role of the endothelial phenotype for the transmigration and finally (d) to elucidate the influence of cytokines on the transmigration of MSCs.

(c)   Possible role of NO and ROS for the transmigration of MSCs

This section deals with nitric oxide and reactive oxygen species, because it is known that NO as well as ROS can modulate the permeability of the endothelium (Isenberg, 2003; Fischer *et al.*, 2005; Isenberg *et al.*, 2005). Therefore, the contribution of NO- and ROS-release during the contact of MSCs and the endothelial barrier was investigated.

(2)   Strategies to enhance the transmigration of MSCs

(a)   Possible improvement of transmigration by genetic modification of MSCs

MSCs were genetically manipulated by infecting them with a CXCR4-expressing adenovirus to study whether CXCR4 overexpression of MSCs improves their transmigratory activity.

(b)   Influence of ultrasound-mediated microbubble stimulation

A novel strategy, the ultrasound-mediated microbubble stimulation (UMS), was employed, which allows a non-invasive focussed alteration of myocardial endothelium. Such focussed pretreatment of endothelium by UMS could influence the targeted myocardial engraftment of MSCs. Therefore, the distinct effects of UMS on the endothelium as well as the impact of focussed UMS on the cell attraction and the transmigration of MSCs into non-ischemic and ischemic myocardium were characterized *in vivo*.

2. Material and Methods

2.1 Cell Culture

2.1.1 Mesenchymal stem cells (MSCs)

2.1.1.1 Isolation of human MSCs

MSCs were isolated from the bone marrow of hip heads of 48 patients (average age 73 ± 7 years; 72% of patients were female, 28% male) undergoing hip prosthesis surgery in the Dreifaltigkeits Hospital Cologne by Professor Dr. Joachim Schmidt. Samples were obtained following procedures as approved by the local ethics committee.

MSCs were prepared as previously described (Klinz *et al.*, 2005; Schmidt *et al.*, 2006a; Schmidt *et al.*, 2006b). Bone marrow samples were diluted with 35 ml Ca^{2+}- and Mg^{2+}-free phosphate-buffered saline (0.1 M PBS: 81 mM di-sodiumhydrogenphosphate-di-hydrate, 19 mM sodium-di-hydrogenphosphate monohydrate, 150 mM sodium chloride, pH 7.4, Gibco BRL, Karlsruhe, Germany) and filtered through a 70-µm nylon mesh (Cell strainer, Falcon, Becton Dickinson, Franklin Lakes, USA). The cell suspension was laid over 15 ml Ficoll-Paque™ Plus (Amersham Pharmacia Biotech, Uppsala, Sweden) and centrifuged at 800 g for 30 minutes at room temperature (Multifuge 3, Heraeus, Hanau, Germany).

The layer containing mononuclear cells was isolated and washed with 50 ml PBS. After centrifugation at 1200 rpm for 10 minutes the washed cells were resuspended in 1 ml growth medium: Minimum Essential Medium Alpha Modification (α-MEM) supplemented with 2 mg/ml L-glutamine, 50 U/ml penicillin, 50 µg/ml streptomycin and 20% (v/v) of a selected batch of non-heat-inactivated fetal calf serum (all chemicals and media were obtained from Gibco). The MSC growth medium is referred to as 20% α-MEM throughout this work. Figure 2 schematically depicts the isolation procedure. Cells were maintained as monolayers in 100-mm culture dishes (Falcon, Becton Dickinson Labware) in 10 ml 20% α-MEM. Non-adherent cells were removed after 1 day at 37°C in a humidified 5% CO_2 atmosphere (Binder GmbH, Tuttlingen, Germany).
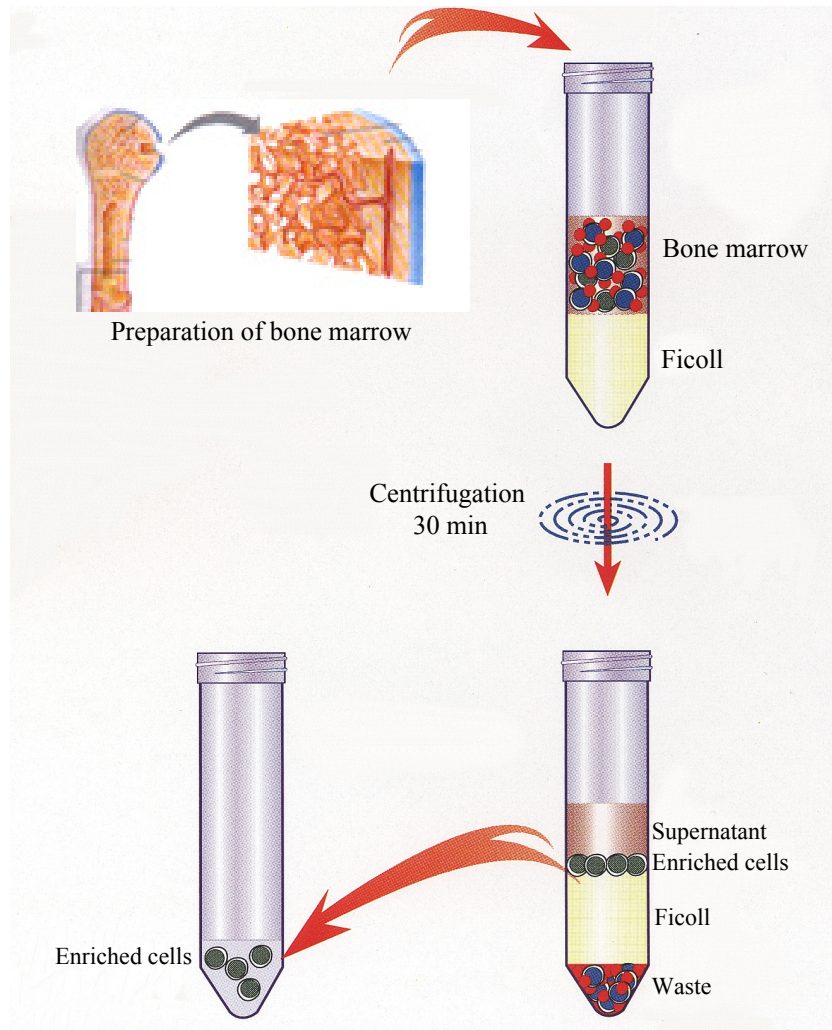
Figure 2: Scheme of the isolation procedure of mononuclear cells *via* density gradient centrifugation

Scheme adapted from Dynal Biotech GmbH, Hamburg, Germany.

2.1.1.2 Culture of human MSCs

MSCs were supplemented with fresh pre-warmed 20% α-MEM twice a week. For each passage confluent MSCs were washed with 10 ml PBS and detached from the culture dish with 2 ml pre-warmed Accutase™ (PAA Laboratories, Cölbe, Germany) for 3 minutes at 37°C. Accutase is a synthetic enzyme, which comprises both activities of collagenase and trypsin, but in a mild manner. Detached cells were diluted in 9 ml 20% α-MEM and centrifuged at 150 g for 5 minutes. MSCs were resuspended in 1 ml 20% α-MEM, counted in a "Neubauer counting chamber" and re-plated at a density of 2000 cells/cm^2 onto 100-mm culture dishes with 10 ml 20%

α-MEM. The MSCs thus maintained within passages 1 to 4 were utilized for the experiments.

2.1.2 Feeder cells

A layer of feeder cells (fibroblasts) constitutes the basis for embryonic stem cell growth as it enables embryonic stem cells to attach. Furthermore, the feeder cells produce leukaemia inhibition factor (LIF), which prevents the differentiation of embryonic stem cells. Feeder cells isolated from mouse embryos were kindly provided by Professor Dr. Jürgen Hescheler (Institute for Neurophysiology, University of Cologne).

2.1.2.1   Culture of feeder cells

Feeder cells were passaged as described for MSCs in section 2.1.1.2. Because of their lower metabolism rate, feeder cells were passaged and supplemented with fresh medium only once a week. Feeder cells were cultured in D-MEM-medium high glucose (Dublecco`s Modified Eagle Medium, Gibco) supplemented with 2 mg/ml L-glutamine, 25 U/ml penicillin, 25 µg/ml streptomycin, 1% (v/v) MEM non-essential amino acids solution, 100 µM β-mercaptoethanol and 15% (v/v) of a selected batch of fetal calf serum (all chemicals were obtained from Gibco). This growth medium is referred to as 15% D-MEM throughout this work.

2.1.2.2   Inactivation of feeder cells

Before cultivation of embryonic stem cells on a feeder cell layer, feeder cells were inactivated using the cell toxin mitomycin C, which inhibits mitosis acitvity, to prevent their proliferation. Adherent cells were treated with 10 µg/ml mitomycin C (Serva, Electrophoresis GmbH, Heidelberg, Germany) for 2-3 hours at 37°C. After inactivation cells were washed thrice with PBS and detached with Accutase. Cells were centrifuged for 5 minutes at 150 g and resuspended in 15% D-MEM. After counting, 10^6 feeder cells were seeded onto 60-mm culture dishes (Falcon).

2.1.3 Embryonic stem cells

Mouse blastocyst-derived embryonic stem cells of the D3 cell line were kindly provided by Professor Dr. Jürgen Hescheler (Institute for Neurophysiology, University of Cologne).

2.1.3.1 Culture of embryonic stem cells

Cells were maintained and cultured on feeder layers as described by Doetschman *et al.* (Doetschman *et al.*, 1985). Adherent cells were passaged thrice a week to prevent induction of differentiation of the pluripotent embryonic stem cells. For passaging cells were washed with PBS and detached using Accutase. The suspension was centrifuged for 5 minutes at 150 g and cells were resuspended in 15% D-MEM. After counting, $5x10^4$ cells were plated onto 60-mm culture dishes containing an inactivated feeder layer. Medium was changed the day after the passage.

2.1.3.2 Preparation of hanging drops

To stimulate the formation of embryoid bodies (EBs) embryonic stem cells were grown in hanging drops (Fassler *et al.*, 1996). Therefore, cells were detached as described in section 2.1.3.1, centrifuged and counted. A hanging drop should contain 1000 cells in a total volume of 20 µl. After dilution of the cell suspension in an appropriate manner in 15% D-MEM 50-60 drops were placed onto the inside of the lid of non-adhesive bacteriological dishes (Greiner, Frickenhausen, Germany). The lid was inverted and the dish was filled with 10 ml PBS to prevent drying out of hanging drops. Within 2 days the single cells formed EBs.

2.1.3.3 Culturing of aggregates in suspension

Two days after preparing hanging drops, EBs were rinsed with 10 ml 15% D-MEM and cultured in suspension (10 ml 15% D-MEM) in non-adhesive bacteriological dishes for 3 days. During this cultivation period cells proliferated without differentiating.

2.1.3.4 Gelatine coating and plating of embryoid bodies

Differentiation of EBs was induced by plating them on gelatine-coated cover slips. Cover slips (12 mm diameter) were placed in each well of a 24-multi well plate (Falcon), covered with gelatine (0.1% in PBS; gelatine from porcine skin, Sigma-Aldrich, Steinheim, Germany) and incubated overnight at 37°C. Before plating EBs, the gelatine solution was removed, cover slips were air-dried for 2 minutes and each well was filled with 1 ml 15% D-MEM. One to three embryoid bodies were isolated out of suspension and placed onto a gelatine-coated cover slip. EBs were supplemented with fresh medium every 3-4 days. Figure 3 schematically depicts the preparation of embryoid bodies.

2.1.4 Endothelial cells

2.1.4.1 Isolation of murine microvascular endothelial cells *via* Magnet associated cell sorting (MACS) and culture

Magnet associated cell sorting (MACS)-sorted microvascular endothelial cells were isolated as previously described (Schmidt *et al.*, 2004a; Schmidt *et al.*, 2004b; Muller-Ehmsen *et al.*, 2006).

After a period of 5+7 days EBs were dissociated by treatment with Accutase. For immunomagnetic selection a single cell solution of 10^6 cells in 1 ml 15% D-MEM was stained with the endothelial-specific marker PECAM-1 (rat anti-mouse-PECAM-1/CD31, 1:800, mAb, Pharmingen, San Diego, USA) for 30 minutes under growth conditions. Cells were washed twice with 2 ml MACS buffer (0.5% BSA and 2 mM EDTA in 0.1 M PBS). Cells were incubated with secondary antibody goat anti-rat IgG-conjugated micro beads (1:4 in MACS buffer, Miltenyi Biotec GmbH, Bergisch Gladbach, Germany) for 15 minutes at 4°C. After washing in MACS buffer, up to 10^8 cells were resuspended in 500 µl MACS-buffer. The mini-MACS system with MS separation columns (Miltenyi Biotec GmbH) was equilibrated using 500 µl MACS buffer and loaded with the cell suspension. After washing thrice with MACS buffer the MS separation column was removed from the magnetic holding device. The endothelial cell fraction was removed into a reaction cup (Eppendorf, Wesseling, Germany). Cells were centrifuged (5 minutes, 800 rpm) and resuspended in 1 ml 15% D-MEM. The isolated endothelial cell fraction was cultured on gelatine-coated

dishes. After 2 to 3 weeks, the murine microvascular MACS-sorted endothelial cells were passaged the first time, afterwards twice a week. The purity of cells was tested by Dr. Annette Schmidt, German Sport University Cologne, with dil-Ac-LDL (Paesel + Lorei GmbH & Co, Hanau, Germany) and different endothelial specific markers (e.g. PECAM-1, VE-Cadherin, flk-1, flt-1, VEGF, Lectin and eNOS) and was amounted to 89% (Schmidt, 2003). Murine microvascular MACS-sorted endothelial cells are referred to as MACS cells throughout this work.

Time schedule
[days]

0 — Embryonic stem cells D3 (cultivated on feeder layer)

Suspension with 1000 embryonic stem cells/20 µl medium in hanging drops

Formation of embryo-like aggregates (embryoid bodies, EBs) in hanging drops

2 — Collection of EBs and further cultivation in suspension

5 — Plating of EBs on gelantine-coated cover slips in 24-well tissue plates

5+7 — Appearing of first vessel-like structures in D3-EBs

Figure 3: Scheme of the preparation of embryoid bodies

Scheme adapted from Schmidt, 2003 (Schmidt, 2003).

2.1.4.2 Culture of human umbilical vein, coronary artery and aortic endothelial cells

Human umbilical vein endothelial cells (HUVEC), human coronary artery endothelial cells (HCAEC) and human aortic endothelial cells (HuAoEC) were obtained from PromoCell (Heidelberg, Germany). HUVEC were cultured in ECG-medium (PromoCell), HCAEC and HuAoEC in ECG-MV-medium (PromoCell) (Schmidt *et al.*, 2004a). All three types of cells were incubated until confluence at 37°C, 95% humidity and 5% CO_2. The cells were detached upon treatment with Accutase, centrifuged and resuspended in medium. For every passage, cells were distributed to 25-cm^2 cell culture flasks (200.000 cells/flask) and were supplemented with fresh medium twice a week. The cells were utilized within passages 3 to 4.

2.2 Quality control of MSCs

The quality of MSCs was ensured by microscopic observations for their characteristic spindle-shaped morphology, flow cytometry, colony forming unit-fibroblast assays and differentiation assays.

2.2.1 Flow cytometry (FACS)

For flow cytometric analysis, MSCs were detached with Accutase, centrifuged at 1300 rpm for 3 minutes, washed with PBS and stained in 100 µl PBS with CD106-Fluorescein isothiocyanate (FITC) (1:20, Becton Dickinson), CD105-Phycoerythrin (PE) (1:50, Ancell, Bayport, USA), CD45-energy-coupled dye (ECD) (1:20, Beckman Coulter, Krefeld, Germany), CD34- Phycoerythrin-Cyanine 5 (PC5) (1:20, Beckman Coulter) and CD14-PC5 (1:20, Beckman Coulter) at room temperature in dark for 15 minutes. The excess dye was removed by washing with PBS and cells were resuspended in 200 µl PBS. FACS analyses were performed by means of a Beckman Coulter Epics XL/MCL with Expo 32 software (Beckman Coulter) (Klinz *et al.*, 2005; Schmidt *et al.*, 2006a). According to published data, human MSCs were defined to be CD14, CD34 and CD45 triple-negative and CD105, CD106 double-positive (Pittenger *et al.*, 1999).

2.2.2 Colony forming unit-fibroblast (CFU-F) assay

To determine the proliferative potential of cultured MSCs, CFU-F assays were performed as described before (Shur *et al.*, 2004). Immediately after isolation (passage P_0) 100.000 MSCs were seeded onto a 60-mm culture dish. Cells were cultured for 14 days without changing the media. MSC colonies were washed with PBS and stained with cresyl-violett (Merck, Darmstadt, Germany) for 10 minutes. After repeated washing steps, blue colonies were macroscopically counted.

2.2.3 Differentiation assays

The differentiative potential of MSCs was evaluated by growing the cells under conditions favorable for adipogenic, osteogenic and chondrogenic differentiation (Pittenger *et al.*, 1999; Arnhold *et al.*, 2006).

2.2.3.1   Adipogenic differentiation

For adipogenic differentiation 1000 MSCs/cm^2 were seeded onto 4-well plates (Nunc GmbH, Wiesbaden, Germany) and cultured under adipogenic-specific culture conditions in growth medium α-MEM supplemented with 2 mM L-glutamine, 0.5% antibiotic-antimycotic solution (Fungizone, Gibco), 1 µM dexamethasone (Sigma-Aldrich), 5 µg/ml insulin (ITS Liquid Media supplement 100x, Sigma-Aldrich) and 15% (v/v) of a selected batch of non heat-inactivated fetal calf serum (Gibco). Additionally 60 µM indomethacin (Sigma-Aldrich) was added shortly before use. Cells growing in 20% α-MEM served as control. Cells were cultured at 37°C in a humidified 5% CO_2 atmosphere for 2 weeks and were supplemented with fresh pre-warmed medium thrice a week.

Adipose differentiation was analyzed by Oil Red O-staining. To prepare the working solution a stock solution of 0.17% Oil Red O (Merck) in 60% isopropanol (Merck) was diluted 3+2 with distilled water. After shaking for 5 minutes the working solution was filtered. Unfixed cells were incubated with fresh Oil Red O working solution for 15 minutes at room temperature. Cells were washed thrice with distilled water and counterstained for 4 minutes using Mayer`s hematoxylin stain. Cells were mounted with Kaiser`s glycerol gelatine (Merck). Staining resulted in red lipid drops and blue nuclei. Staining was analyzed using a Zeiss Axiophot microscope (Oberkochem, Germany).

2.2.3.2 Osteogenic differentiation

For Osteogenic differentiation 1000 MSCs/cm^2 were seeded onto 32-mm culture dishes (Falcon) and cultured under osteogenic-specific culture conditions in growth medium α-MEM supplemented with 2 mM L-glutamine, 0.5% antibiotic-antimycotic solution, 60 µM ascorbic acid (Sigma-Aldrich), 10 mM β-glycerophosphate (Sigma-Aldrich), 0.1 µM dexamethasone and 15% (v/v) of a selected batch of non heat-inactivated fetal calf serum. Cells growing in 20% α-MEM served as control. Cells were cultured at 37°C in a humidified 5% CO_2 atmosphere for 2 weeks and were supplemented with fresh pre-warmed medium thrice a week.

Osteogenic differentiation was analyzed by von Kossa staining to visualize deposits of calcium. Cells were fixed for 5 minutes in a solution containing equal volumes of methanol and acetone and washed in distilled water for 5 minutes. Samples were incubated with 5% aqueous silver nitrate solution (Sigma-Aldrich) in the dark and washed thrice with distilled water. After incubating with 5% sodium carbonate (Merck) in formaldehyde, cells were rinsed several times in distilled water. Nuclei were counterstained for 10 minutes using a 0.1% nuclear fast red solution (2-methyl-4-chlorobenzenediazonium tetrachlorozincate, Roche Diagnostics, Mannheim, Germany) containing 5% ammonium sulfate (Sigma-Aldrich). After washing, cells were dehydrated through graded EtOH (Hoffmann, Germany) and xylol (Alfred Quadflieg, Germany) and mounted in Entellan (Merck). Staining resulted in black calcifications and red nuclei. Staining was analyzed using a Zeiss axiophot.

2.2.3.3 Chondrogenic differentiation

To promote chondrogenic differentiation 500.000 MSCs were centrifuged for 5 minutes at 800 g to form a pelleted micromass which was cultured under chondrogenic-specific culture conditions in growth medium D-MEM supplemented with 2 mM L-glutamine, 0.5% antibiotic-antimycotic solution, 10 ng/ml transforming growth factor-β1 (Sigma-Aldrich), 50 µM ascorbic acid, 0.5 µg/ml insulin (Sigma-Aldrich) and 1% (v/v) of a selected batch of non heat-inactivated fetal calf serum (Gibco). Cells growing in 20% α-MEM served as control. Micromasses were cultured at 37°C in a humidified 5% CO_2 atmosphere and were supplemented with fresh pre-warmed medium thrice a week. After 3 weeks the probes were rapidly frozen in liquid nitrogen and stored at -80°C.

2.2.3.3.1 RNA isolation

To analyze the chondrogenic differentiation potential of MSCs total RNA of samples under differentiation conditions or control conditions was extracted using peq-Gold TriFast™ Reagent (Peqlab, Erlangen, Germany). This reagent allows single step RNA isolation. Frozen micromasses were lysed in 1 ml TriFast and homogenized by applying ultrasound (Vibracell, Bioblock, Illkirch, France) for 20 seconds followed by incubation for 5 minutes at room temperature. After addition of 200 µl chloroform samples were agitated and incubated for 5 minutes. Centrifugation for 5 minutes at 12000 g and room temperature separated the solution into an upper aqueous phase containing the RNA and an organic phase. After transfer of the aqueous phase RNA was recovered by precipitation with 500 µl isopropyl alcohol. After agitation samples were incubated for 10 minutes at room temperature and centrifuged at 12000 g for 10 minutes at 4°C. The supernatant was removed, precipitated RNA was washed twice with 70% EtOH and air dried for 30 minutes. RNA was dissolved in 10 µl DEPC-treated H_2O (0.1% DEPC in 100 ml distilled H_2O, agitated overnight and autoclaved, Sigma-Aldrich) and its concentration was measured photometrically at 260 nm; A_{260nm} of 1 corresponds to a concentration of 40 ng/µl RNA. Afterwards RNA was treated with DNAse for 15 minutes at room temperature to eliminate DNA contaminations. The reaction was performed in the following mixture:

2 µg RNA

2 U DNAse (Invitrogen GmbH, Karlsruhe, Germany)

2 µl DNAse-buffer (10x, Invitrogen)

ad 20 µl DEPC-H_2O

The DNAse digest was terminated by addition of 2 µl 25 mM EDTA (Invitrogen). Samples were heated for 10 minutes to 65°C followed by 2 minutes incubation on ice.

2.2.3.3.2 Semi-quantitative RT-PCR

2 µg of total RNA was reverse transcribed using M-MLV reverse transcriptase. The reverse transcription (RT) reaction was performed in the following mixture:

2 µg RNA (from DNAse digest)

10 µl First-Strand-buffer (5x, Invitrogen)

2.5 µl dNTP-Mix (10 mM, Invitrogen)

1 µl Oligo dT (0.5 µg/µl, Invitrogen)

2 µl DTT (100 mM, Invitrogen)

1 µl M-MLV RT (Invitrogen)

ad 50 µl DEPC-H_2O

RT-reaction was performed for 60 minutes at 37°C followed by 5 minutes at 90°C. Afterwards, a hotstart PCR was performed (94°C for 10 minutes, followed by 40 cycles of 94°C for 1 minute, 59°C for 45 seconds and 72°C for 90 seconds, followed by 72°C for 10 minutes) using 2 µg of cDNA as template and specific primers (MWG-Biotech, Ebersberg, Germany) for collagen II to amplify a 388 bp fragment of collagen II mRNA. As reference for the quantification the mRNA of the housekeeping gene β-actin was employed (amplified fragment size 698 bp). The reaction was performed in the following mixture:

4 µl cDNA (from the RT-mixture)

5 µl PCR-buffer (10x, Genecraft, Lüdinghausen, Germany)

1.5 µl dNTP-Mix (10 mM)

1 µl of each antisense and sense specific primer (25 pmol/µl, MWG-Biotech)

2.5 U BioTherm DNA polymerase (Genecraft)

ad 50 µl DEPC-H_2O

The following pimers were used:

Primer		Sequence (5´-3)	GeneBank	Position	Fragment
ß- Actin- F	sense	ACC TTC AAC ACC CCA GCC ATG TAC G	NM_001101	449- 473	698 bp
ß- Actin- R	antisense	CTG ATC CAC ATC TGC TGG AAG GTG G		1122-1146	
Collagen II- F	sense	GAA CAT CAC CTA CCA CTG CAA G	BC116449.1	4163-4184	388 bp
Collagen II- R	antisense	GCA GAG TCC TAG AGT GAC TGA G		4550-4529	

PCR products were analyzed by agarose gel electrophoresis. 15 µl PCR-products and 3 µl 6x DNA-sample buffer (Fermentas, St. Leon-Rot, Germany) were transferred onto a 2% agarose gel (Biozym, Oldendorf, Germany) with 1x TAE-buffer

(90 mM Tris pH 7.4, 2 mM EDTA pH 8, 90 mM acetic acid) and separated in an electrical field (5 V/cm). To visualize the DNA, agarose-solution contained 1 µg/ml ethidium bromide (Sigma-Aldrich). After electrophoresis gels were analyzed with UV light (302 nm, MWG-Biotech).

2.3 Vital staining of cells

2.3.1 PKH26 and PKH67 staining

MSCs and ECs were vital stained using a MINI-67 or MINI-26 staining kit (Sigma-Aldrich) according to the manufacturer's instructions. A uniform single cell suspension was incubated with 2 µl/ml PKH67 dye (green fluorescence) or PKH26 dye (red fluorescence) in Diluent C for 5 minutes in the dark. After terminating the reaction by washing with medium, cells were centrifuged for 5 minutes at 150 g, resuspended in medium and counted.

2.3.2 CellTracker staining

Prior to co-cultivation, adherent endothelial cells and MSCs were stained with CellTracker™ Green CMFDA or Red CMTPX (Molecular Probes, Eugene, USA). The medium was removed and cells were washed with PBS. A pre-warmed staining solution, containing 0.5 µM CellTracker in serum-free medium was added and cells were incubated for 30 minutes under growth conditions. The excess staining solution was removed by washing the cells with PBS following incubation for 30 minutes in fresh, pre-warmed serum-free medium.

2.4 Monolayer co-cultivation experiments

For co-cultivation experiments, endothelial cells were seeded onto 12-mm glass cover slips at a density sufficient to become a confluent monolayer overnight. The confluence of the endothelial monolayers was randomly checked by immunostaining with anti-VE-cadherin (see section 2.8).

2.4.1 Co-cultivation

For co-cultivation, MSCs stained with CellTracker Red were detached and seeded on endothelial monolayers stained with CellTracker Green at a density of 10.000 MSCs per cm^2. MSCs seeded on cover slips without an endothelial monolayer served as control. Co-cultivations were conducted for 15, 30, 60, 120, 180 and 240 minutes and were performed independently of the endothelial phenotype in 20% α-MEM. Cells were fixed with 4% paraformaldehyde (PFA, Merck) in 0.1 M PBS for 20 minutes, washed 3 times with PBS and embedded in Entellan. During fixation the NH$_2$-groups of cellular and membrane proteins were connected by aldehyde bindings. The duration of fixation procedure depended on tissue size. Experiments were carried out on 4 to 6 samples and analyzed as described in section 2.16.2.

2.4.2 Cytokines and additive substances

Cytokines/chemokines were used in the following concentrations: 20 ng/ml bFGF (Cell Concepts, Umkirch, Germany), 20 ng/ml VEGF (PAN Biotech, Nürnberg, Germany), 0.5 U/ml EPO (Roche), 10 ng/ml IL-6 (Boehringer, Mannheim, Germany) and 50 ng/ml SDF-1β (Acris Antibodies, Hiddenhausen, Germany).

Additive substances were used in the following concentrations: 0.05 mM H$_2$O$_2$ (Merck), 10 mM N-Acetylcysteine (Sigma-Aldrich), DETA (Diethylenetriamine) NONOate 10 µM (Alexis Biochemicals, Lörrach, Germany), 100 µM L-NAME (N-Nitro-L-Arginine Methyl Ester, Sigma-Aldrich).

2.4.3 Blocking experiment

For blocking experiments, the monoclonal blocking antibodies against CD49d (integrin alpha4 chain of VLA-4 complex), CD106 (VCAM-1) and isotypic control IgG1 (Beckman Coulter) were used at 20 times the saturating dilution as determined by the manufacturer to conduct immunohistochemistry experiments. HUVEC monolayers were pre-incubated with anti-VCAM-1, IgG1 or in absence of antibodies for 30 minutes under growth conditions. Co-cultivation was performed for 120 minutes in the presence of anti-VLA-4, IgG1 or as a control in the absence of antibodies and analyzed as described in section 2.16.2.

2.5 Three-dimensional model systems for transmigration

2.5.1 Collagen invasion assay

For collagen invasion assays collagen gels were prepared (Bauer *et al.*, 2007). A solution containing equal volumes of 1 M sodium hydroxide and 1 M HEPES buffer was equally mixed with 10x Minimum Essential Medium Eagle (Sigma-Aldrich). 2 ml of this solution was mixed with 4 ml of Collagen R solution from rat tail (Serva) and 4 ml of Collagen G from calf skin (Biochrom AG, Berlin, Germany). 500 µL of the resulting solution was applied for each 12-mm well and incubated at 37°C for 24 hours in order for it to solidify into a thin collagen gel matrix. HUVEC were seeded on the gel, grown to confluence, stained with CellTracker Green CMFDA and co-cultivated with MSCs (CellTracker Red CMTPX, see section 2.3.2) for 2 to 24 hours. Collagen constructs were fixed with 4% PFA for 1 hour, washed with PBS and were either transferred onto a glass slide and embedded in AquaPolyMount (Polysciences, Warrington, USA) or cryo-embedded in Tissue-Tek® (Sakura Fintek, Zoeterwoude, Netherlands) and sliced in 7 µm (Leica CM1900, Wetzlar, Germany). Specimens were analyzed by confocal microscopy (section 2.16.1).

2.5.2 Endothelial spheroid model

Endothelial spheroids of random size were generated using MACS cells as described previously (Korff *et al.*, 1998). Briefly, MACS cells were detached, suspended in culture medium containing 20% carboxymethyl cellulose (Sigma-Aldrich), seeded into non-adhesive bacteriological dishes (Greiner) and cultured overnight at 37°C. Spheroids were harvested by centrifugation for 1 minute at 200 g, stained with CellTracker Green CMFDA and co-cultivated with MSCs (CellTracker Red CMTPX, see section 2.3.2) in 20% α-MEM containing 20% carboxymethyl cellulose for 2, 4 and 6 hours. After fixation with 4% PFA the spheroids were transferred onto a glass slide, embedded in AquaPolyMount and analyzed by confocal microscopy (section 2.16.1).

2.5.3 Perfusion of isolated mouse hearts

Wild-type mice (C57BL/6, both genders, aged 3-18 months) were obtained from the animal care facility of the Institute for Physiology, University of Cologne. They were

housed and fed according to federal guidelines, and all procedures were approved by local authorities. Mice were killed by cervical dislocation and the hearts were quickly removed. The aorta was cannulated for the initiation of an antegrade perfusion. Either PKH67/26 vital stained MSCs (section 2.3.1) or MSCs after adenoviral transfection (section 2.6) were used. A uniform single cell suspension of 5×10^5 MSCs in 50 ml 20% α-MEM aerated with 100% O_2 at 37°C was perfused into the heart for 60 or 90 minutes with constant flow velocity and at a pressure of 60 cm H_2O.

The isolated heart samples were prepared for microtome sectioning by fixing the tissue immediately with 4% PFA for 4 to 6 hours at 4°C. The fixed heart samples were washed thrice in PBS followed by incubation of the tissue in 18% sucrose solution for 6 to 8 hours to prevent further tissue damage during the freezing process. The heart samples were frozen at -80°C in Tissue-Tek and 7 µm slices were prepared by cryo-slicing.

The endothelium was stained with a selective endothelial marker Rhodamine-*Griffonia (Bandeiraea) simplicifolia* Lectin I (10 µg/ml in 10 mM HEPES, 0.15 M NaCl, pH 7.5, Vector Laboratories, Buringame, USA) (Laitinen, 1987; Porter *et al*., 1990) for 30 minutes, washed with PBS and embedded in AquaPolyMount. Experiments were carried out on 4 samples and analyzed as described in section 2.16.3.

2.6   Adenoviral infection of MSCs

For overexpression of CXCR4 stem cells were infected with a CXCR4-expressing adenovirus (Ad.CXCR4.GFP). The recombinant adenovirus was constructed and kindly provided by Dr. Birgit Boelck, German Sport University Cologne, and Professor Roger Hajjar, Department of Gene and Cell Medicine, The Mount Sinai School of Medicine, New York. The generation of a recombinant (E1 deficient) adenovirus (serotype 5) carrying the reporter gene green fluorescent protein (GFP) and the human CXCR4 (kindly provided by Dr. Alison Schecter, The Mount Sinai School of Medicine, New York) was performed with the overall strategy developed by He *et al.* (He *et al.*, 1998). Briefly, human CXCR4 cDNA was cloned into the shuttle vector pAdTrack-CMV under the control of the cytomegalovirus promoter (see Figure 4). The resulting construct was cleaved with the restriction endonuclease *Pme*I to linearize it. This was then cotransformed with the supercoiled backbone adenoviral vector pAdEasy-1 into *Escherichia coli* strain BJ5183. Recombinants were selected with kanamycin and screened by restriction endonuclease digestion. The

recombinant adenoviral construct was cleaved with *Pac*I to expose its inverted terminal repeats and transfected into the packing cell line, subconfluent HEK-293 cells, by using a modified calcium phosphate coprecipitation method (Lieber *et al.*, 1993). The process of viral production could be directly and conveniently followed in HEK-293 cells by visualization of the GFP reporter, which was incorporated into the viral backbone. After 8-10 days, the virus was harvested and then amplified by infecting increasing numbers of packing cells each time, with a final round using a total of 50 145-cm^2 dishes. After 2-3 days, the resultant virus (Ad.CXCR4.GFP) was purified by CsCl banding, with the final yield at 3.5 x 10^{12} particles/ml. A reporter virus producing GFP alone, but also under the control of the cytomegalovirus promoter was generated (Ad.GFP) at 1.58 x 10^{12} particles/ml and served as control. Viral titers were determined to be 3.5 x 10^{10} plaque-forming units (pfu)/ml for Ad.CXCR4.GFP and 4.72 x 10^9 pfu/ml for Ad.GFP (He *et al.*, 1998).

For infection MSCs were washed with PBS and incubated with Ad.CXCR4 at a multiplicity of infection (MOI) between 20-80 in 20% α-MEM at 37°C in a humidified 5% CO$_2$ atmosphere. The MOI is the number of viral particles per cell that is desired during the infection reaction. The excess viruses were removed by washing with 20% α-MEM after 24 hours. Experiments using CXCR4-infected MSCs were performed 48 hours after infection. To study the efficiency of adenoviral infection MSCs were assessed by fluorescent microscopy at increasing concentrations (MOI). Reactivity to SDF-1β was studied by performing migration assays (2.9). Western blots were conducted to evaluate the amount of overexpession on protein level (2.12).
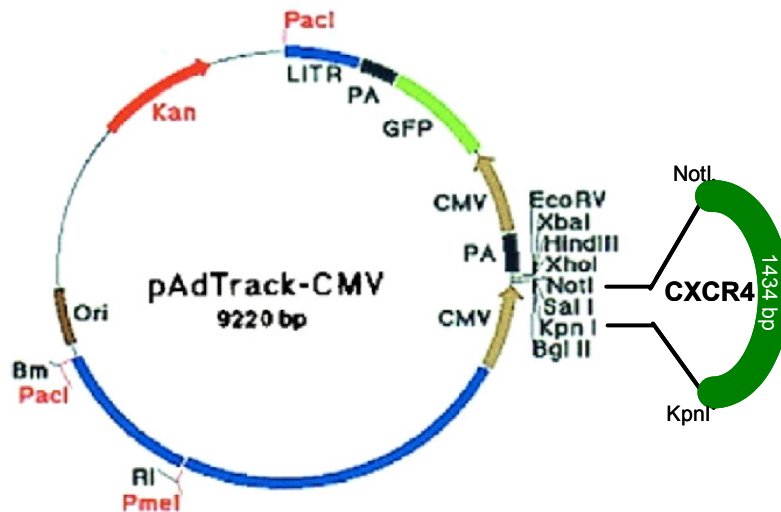
Figure 4:   Scheme of the adenoviral shuttle vector pAdTrack-CMV

Cytomegalovirus (CMV) long-terminal repeats served as promoters. The vector contained green fluorescent protein (GFP) under the control of a separate CMV promoter and the subcloned CXCR4-cDNA. Scheme adapted from http://www.coloncancer.org/adeasy/pAdTrack-CMV%20vector%20map.htm

2.7   *In vivo* experiments

The *in vivo* experiments were designed by Dr. Alexander Ghanem, Department of Medicine/Cardiology, University of Bonn, and were performed in the laboratories of Dr. Klaus Tiemann, Department of Medicine/Cardiology, University of Bonn. Surgical interventions were conducted by the technical assistant Pascal Pachenda and ultrasound techniques by Dr. Ghanem.

2.7.1 Experimental protocol

All experimental protocols were approved by the animal care committee at the University of Bonn and by the local government authorities and conformed to the guidelines of the American Heart Association for use of animals in research. All animals were housed at constant room temperature of 24°C and 12 hours light-dark cycle and maintained on an *ad libitum* diet (Altromin 1324, Altromin, Lage, Germany) with free access to water. Female WISTAR rats (200-250 g; Charles River, Kisslegg, Germany) were used for all experiments. All procedures were performed in inhalative anaesthesia with isoflorane (3% for induction and 1.0-1.5% for maintenance) in 50%

nitrous oxide and 50% oxygen. For continuous ECG-recording a 2 lead ECG was connected using an established ECG-analysis system (PowerLab™ System, AD Instruments, Milford, USA). Chest-walls were carefully shaved and remaining fur was removed by means of depilation crème. Intrathoracic instrumentation was performed in all animals eleven days ahead of the transfusion experiments to avoid influence of post-traumatic cytokine expression (Nossuli *et al.*, 2000). The effect of focussed ultrasound-mediated microbubble stimulation (UMS) was investigated in native, non-ischemic and ischemic myocardium *in vivo* resulting in 4 groups (n=24). Figure 5 summarizes the experimental protocol. *Groups C* and *D* received 1 hour of anterolateral myocardial ischemia (Nossuli *et al.*, 2000). Therefore, rats were intubated and ventilated with a tidal volume of 200 µl and respiratory rate of 80/min (Hugo-Sachs, Type Small Animal Ventilator KTR4, Harvard Apparatus). After left thoracotomy in the fourth intercostal space, the pericardial sac was opened and a 6-0 monofilament polypropylene suture was passed under the left anterior descending coronary artery (LAD) 2 mm distal of the atrioventricular grove avoiding affection of septal branches. After forming a loose snare around the LAD, each end of the suture was then exteriorized through each side of the chest wall and placed subcutaneously. Four days before cell transplantation left anterior descending coronary artery was ligated for 60 minutes. Anterolateral myocardial ischemia and reperfusion were controlled by means of electro- (ST-segment analysis) and echocardiography (wall motion abnormality, wall thinning) as described previously (Kim *et al.*, 2007).

For application of microbubbles a femoral vein was cannulated with a Polyethylene (PE)-50 tube (0.4 mm inner diameter) for continuous echocontrast application. SonoVue™ (Bracco Inc., Milano, Italy) was infused during constant agitation at approximately 130 µl/minute (Lohmaier *et al.*, 2004). Flow rate was adapted to achieve good left-ventricular opacification without shadowing, steady state conditions were achieved approximately 2 minutes after infusion start. Centrifuged ultrasound gel was placed on top of the depilated chest wall to ensure optimal acoustic coupling with the ultrasound system.

For cell application the aorta was additionally cannulated for cell delivery *via* right common carotid artery by means of a PE-40 tube (Templin *et al.*, 2006). Positioning of the catheter in the aortic root approximately 2 mm distal of the aortic valve was

guided sonographically; coronary delivery was proved by means of myocardial contrast enhancement.

	Group			
	A	**B**	**C**	**D**
I / R	**-**	**-**	**+**	**+**
UMS	**-**	**+**	**-**	**+**
	Ultrasound-guided cell application *in vivo*			
	Organ harvesting & Organ fixation			

Figure 5:   Scheme of experimental protocol of *in vivo* experiments

> Impact of focussed ultrasound-mediated microbubble stimulation (UMS) on myocardial stem cell attraction and transendothelial migratory capacity was evaluated in native (*groups A, B*) and ischemic (*groups C, D*) myocardium. *Groups C* and *D* received 1 hour of anterolateral myocardial ischemia (I) followed by reperfusion (R) 4 days before MSC transfusion. *Groups B* and *D* were treated with UMS. Cell application was conducted *in vivo via* percutaneous PE-catheter placement in the aortic root.

2.7.2 Focussed ultrasound-mediated microbubble stimulation (UMS)

For UMS a hybrid ultrasound device (Philips Research North America, Briarcliff, USA) provided a) b-mode high-resolution ultrasound imaging of anatomical structures (15 MHz) electronically and mechanically coupled with b) low-frequency / high-energy focussed ultrasound application (see Figure 6a). The simultaneous use of both technologies allowed positioning of the focus point within the b-mode window. For aiming at cardiac structures, e. g. the vital borderzone of myocardial infarction, the focus point of the system was positioned in regions of interest guided by the high frequency transducer. Borders of the UMS zone (approximately 3x10 mm) were identified in b-mode, coordinates were stored and insonication was programmed within these borders (see Figure 6b). Focus was set on the anterior left-ventricular wall in native myocardium (*group B*). In ischemic hearts (*group D*) UMS was aimed at the anteroseptal peri-infarction borderzone. The ultrasound system was attached to a

stepper-motor driven tripod which allowed movements in three dimensions within a stereotactic grid. The movements of the tripod system and the application of UMS were synchronized with a time trigger to ensure a) delivery of identical ultrasound-pulses to dedicated target zones phase of the cardiac cycle resulting in optimum interindividual reproducibility as well as b) to ensure a distinct replenishment time for fresh contrast microbubbles in the left ventricle following UMS. Each therapeutic pulse (frequency of pulse 0.2 Hz) resulted in the oscillation and the destruction of myocardial microbubbles and was followed by a programmed movement of the scanhead. In total every heart received the sequence of 30 pulses twice.
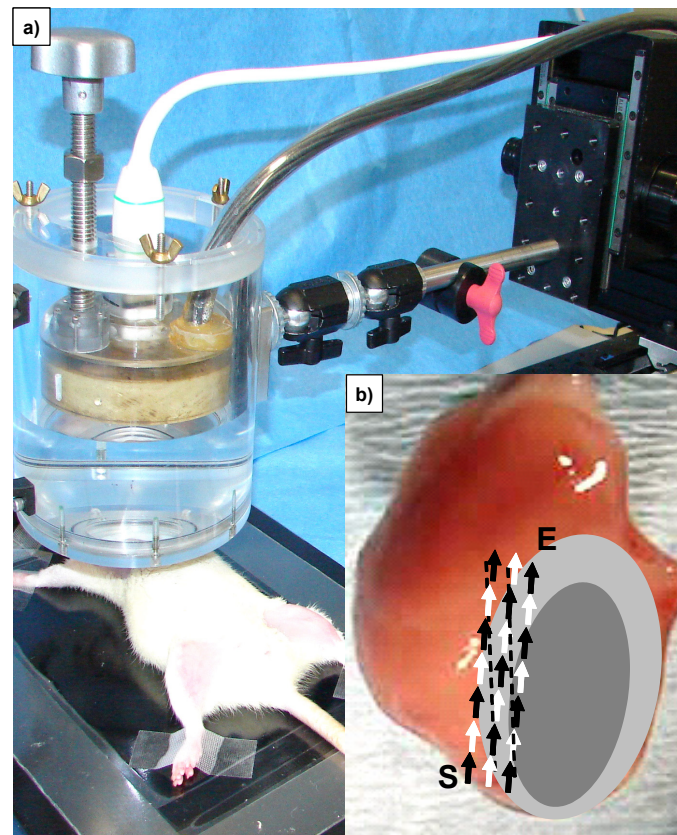
Figure 6:   Focussed ultrasound-mediated microbubble stimulation (UMS)

a) Hybrid ultrasound device allows simultaneous high-resolution imaging (for aiming) and focussed ultrasound at high-emission power (for UMS).

b) Sequential UMS-pulses were synchronized with an automated stepper motor and allowed application to a standardized volume. Arrows indicate UMS-pulse-movement-sequences on the left-ventricular anterior wall in native myocardium from start (S) to end (E). In case of anterolateral ischemia UMS was targeted on anteroseptal borderzone tissue (light grey). Myocardial scar is depicted dark grey.

Photographs were kindly provided by Dr. Alexander Ghanem, Department of Medicine/Cardiology, University of Bonn.

2.7.3 Transplantation of MSCs *via* aortic root catheter

MSCs were PKH67 vital-stained, washed and counted in a 'Neubauer counting chamber'. For each experiment 1.5×10^5 MSCs were resuspended and homogenized in 1 ml of 20% α-MEM. The homogenized cell suspensions were administered slowly (1 ml during constant agitation over 90 seconds) *via* a catheter placed in the aortic root within 5-10 minutes after UMS. To rule out microembolisms resulting in further acute myocardial ischemia left-ventricular function was investigated during cardiomyoplasty with two-dimensional echocardiography for new wall motion abnormalities. Rats were kept in inhalative anaesthesia before organs were harvested after 30, 60 and 120 minutes and fixated as described above (section 2.5.3).

2.8   Immunohistochemistry

Fixed co-cultures were washed thrice with 0.05 M Tris-buffered saline (TBS: 50 mM Tris, 150 mM NaCl, pH 7.6) and were permeabilized using TBS containing 0.5 M ammonium chloride (Sigma-Aldrich) and 0.25% Triton-X-100 (Serva). The detergent Triton-X-100 permeabilizes the cell membrane while ammonium chloride reacts with free aldehyde groups to prevent unspecific binding of the antibody. Non-specific binding sites were blocked using 5% bovine serum albumin (BSA, PAA) in TBS (1 hour, room temperature). Primary antibodies CD29 mouse IGg1 integrin β1 chain of VLA-4 (Becton Dickinson) and VE-cadherin (F-8) mouse IgG1 (Santa Cruz Biotechnology, Santa Cruz, USA) were diluted in 1:500 and 1:400 ratios in 0.8% BSA and incubated overnight at 4°C. Specimens were washed three times with TBS. Cy5- and Cy2-conjugated goat anti-mouse IgG (1:400 in TBS, Jackson Immuno Research Laboratories, Suffolk, UK) served as secondary antibodies and were incubated for 1 hour at room temperature. Non-specific staining was assessed by omission of the primary antibody and examination of the samples in the presence of the secondary antibody alone. The coverslips were washed three times with TBS. Afterwards cells were dehydrated for 2 minutes in each of the following alcohols: 70% EtOH, 96% EtOH, 100% EtOH and Xylol. The coverlips were mounted onto glass slides using Entellan.

To examine the integrity of the basement membrane immunohistochemical staining for laminin was carried out. Frozen sections were blocked with 5% BSA. Anti-laminin

rabbit IgG (Sigma-Aldrich) was diluted 1:200. Cy5-conjugated goat anti-rabbit IgG (1:400; Jackson Immuno Research Laboratories, Suffolk, UK) served as secondary antibodies.

2.9 Migration assay

To evaluate the migratory capacity of MSCs a modified Boyden chamber assay was conducted by using a 24-well HTS Fluoro Blok TM insert system (Falcon) as shown in Figure 7. Each insert consists of a polyethylene membrane with 8.0 µm pores which blocks >99% of the light transmission in a wavelength region from 490-700 nm. 10.000 MSCs in 20% α-MEM were seeded into each insert. For testing the migratory reactivity to SDF-1β 50 ng/ml SDF-1β was added. After 6 hours incubation at 37°C in a humidified 5% CO_2 atmosphere, cells were fixed with 4% PFA for 20 minutes, washed 3 times with PBS. Filters were excised and mounted with DAPI mounting medium (4´,6-diamidino-2-phenyl-indole, Vectashield, Vector Laboratories, absorption 360 nm, emission 460 nm). The total number of migrated cells was counted using a LSM 510 Meta microscope (Zeiss). Assays were performed in 4 setups.
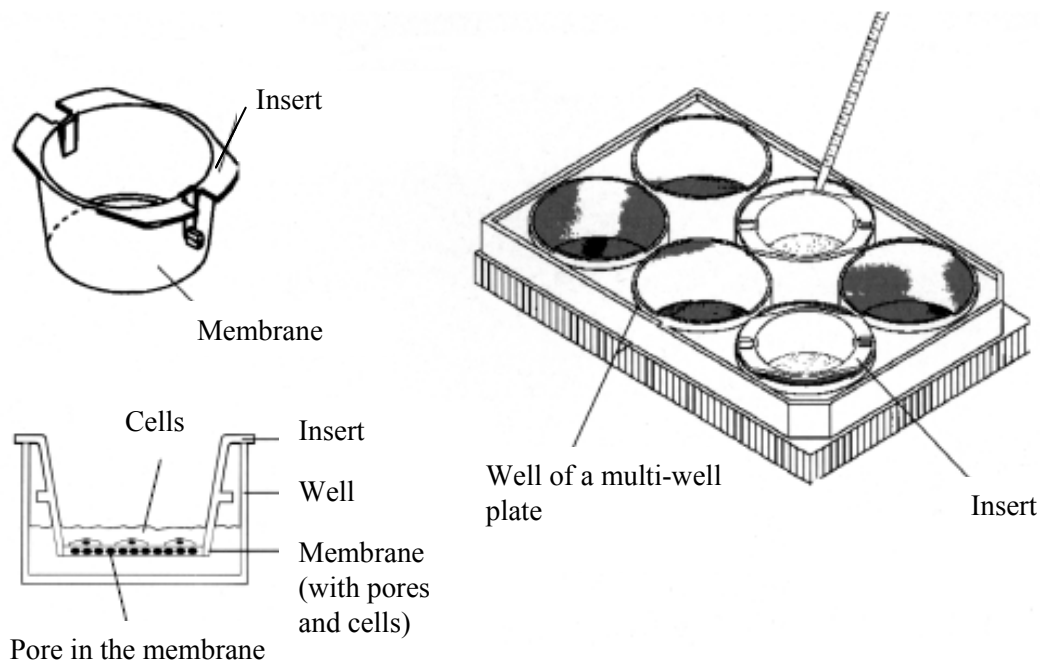
Figure 7:   Scheme of a modified Boyden Chamber migration assay

Scheme adapted from Schmidt, 2003 (Schmidt, 2003).

2.10 DAF and APF fluorometry

To detect changes in NO and ROS levels upon contact of MSCs with endothelial cells (ECs), adherent MACS were co-cultivated with PKH26 stained MSCs for 30 minutes. NO and ROS levels were measured on MSCs and ECs which were in contact with each other as well as on MSCs and ECs cultivated solitarily.

For NO measurements 4-Amino-5-methylamino-2`,7`-difluorofluorescein diacetate (DAF-FM DA, Alexis) was used. DAF is converted *via* an NO-specific mechanism to an intensely fluorescent triazole derivative (Kojima *et al.*, 1998). Cells were equilibrated in tyrode (1.8 mM $CaCl_2$, 1.1 $MgCl_2$, 5.4 mM KCl, 140 mM NaCl, 4.2 mM NaH_2PO_4, 10 mM glucose, 23 mM $NaHCO_3$ and 1 mM L-arginine) for 2 minutes and subsequently incubated with DAF (1:1000 in tyrode) for 2 minutes at 37°C. For negative controls the nitric oxide synthase (NOS) inhibitor L-NAME (100 µM) was used.

For the measurement of reactive oxygen species 3'-(p-aminophenyl) fluorescein (APF, Alexis) was used. APF is an aromatic amino-fluorescein derivative that has little intrinsic fluorescence. It immediately reacts with ROS such as hydroxyl radical, peroxynitrite and hypochlorite ion and certain peroxidase intermediates, but is inert to NO, H_2O_2, superoxide and other oxidants. Upon oxidation, APF is converted to the highly fluorescent molecule fluorescein, allowing the simple direct detection of highly reactive biological radicals. Cells were incubated with APF (1:1000 in PBS) for 30 minutes at 37°C. For negative control 10 mM of the free radical scavenger N-acetylcysteine was used.

The intensity of DAF and APF fluorescence was measured every 50 seconds for 15 minutes using a LSM 510 Meta microscope.

2.11 TUNEL assay

For quantification of apoptotic cells terminal uridine deoxynucleotidyl transferase dUTP nick end labeling (TUNEL) assay using *In Situ* Cell Death Detection Kit AP (Roche) was performed. 7 µm thick sections were prepared on Poly-L-Lysin coated slides (Menzel, Braunschweig, Germany) and incubated with Proteinkinase K (diluted 1:1000 in 5 mM TBS pH 7.4) for 30 minutes at 37°C in a humidified 5% CO_2 atmosphere. Sections were washed twice with PBS. Positive controls were treated with 1 µg/ml DNAse (Qiagen, Hilden, Germany) in 25 mM Tris pH 7.6 for 10 minutes

at 37°C. Sections were incubated with FCS (1:25 diluted in PBS) for 30 minutes at room temperature and afterwards with 50 µl TUNEL-reagent per slide for 10 minutes at room temperature. Negative controls were incubated in the absence of the terminal desoxynucleotidyl-transferase. Sections were washed twice with PBS and 50 µl Converter-AP (2:1 diluted with 0.1 M Tris containing 1% milk powder) was added and incubated for 30 minutes at 37°C. One tablet of nuclear fast red (Roche) was suspended in 2 ml 0.1 M Tris pH 8.2 and filtered. After washing 50 µl fast red solution was added to each section and incubated for 30 minutes at room temperature in the dark. Sections were washed twice with distilled water and finally counterstained with Mayer`s hematoxylin stain. Sections were embedded in AquaPolyMount. Apoptotic signals appeared in pink. Sections were examined using a Zeiss Axiophot microscope.

2.12 Immuno blot (SDS-Page)

2.12.1 Preparation of cell and tissue lysates

For cell lysates cells were washed with PBS (4°C) and detached from the culture dish with 500 µl of RIPA lysis buffer (25mM Tris/HCl pH 8, 150mM NaCl, 0.1% SDS, 0.1% Natriumdesoxycholat, 1% Nonidet P-40 (IGEPAL), 10% Glycerol, 2 mM EDTA) containing protease inhibitor complete (Roche) using a cell scraper. Cells were incubated on ice for 30 minutes and lysed by repetitive freezing and thawing cycles. After centrifugation at 10000 g, 4°C (table centrifuge 5417R, Eppendorf), cell debris was separated from cell lysate. Cell lysates were stored at -80°C until usage.

For tissue lysates frozen heart tissue was homogenized in liquid nitrogen. The frozen state of the tissue facilitated to smash bigger tissue pieces to small ones using a crucible. Subsequently the small tissue fragments were crushed with a wolfram carbide bead (5 mm) in a Teflon container by using a micro-dismembranator (1600 beats/minute) for 1 minute. During this procedure the tissue pieces were crushed to powder. Pulverized tissue was resuspended in 1 ml of cell lysis buffer (RayBiotech, Norcross, USA) containing protease inhibitor and homogenized. Probes were centrifuged 10 minutes at 10000 rpm (4°C, Eppendorf).

2.12.2 Measurement of protein content

The protein content of the supernatant was measured by the method of Lowry (Lowry *et al.*, 1951) using the DC protein ASSAY (BIO-RAD, München, Germany). According to the manufacturer's instructions 5 µl of each lysate was transferred twice into a 96-well plate. 25 µl of reagent A and 200 µl of reagent B were added. Additionally, to calculate the protein content a calibration dilution line with bovine serum albumin (BSA) was added. After 15 minutes absorption was measured at 650 nm using a Molecular Devices kinetic microplate reader (Sunnyvale, USA) and the mean value of protein content was calculated as µg/µl.

2.12.3 Separation of proteins *via* SDS-Polyacrylamid-gelelectrophoresis (PAGE)

For SDS-PAGE 40 µg of tissue or cell lysates were used. The required volume of 5x SDS-loading buffer (300 mM Tris pH 6.8, 5% SDS, 50% glycerol, 25% mercaptoethanol, 0.02% bromphenolblue) was added. Samples were denatured for 5 minutes at 95°C. After quick centrifugation proteins were submitted to commercial SDS-PAGE (Criterion™ XT Precast Gel, 4-12% Tris-HCl gel, BIO-RAD) inside the Criterion™ electrophoresis chamber (BIO-RAD). After addition of running buffer (1x XT MOPS Running Buffer, BIO-RAD) proteins were separated at 200 V, 90 mA and 200 W per SDS-gel. Precision Plus (BIO-RAD) served as molecular weight standard.

2.12.4 Western blot

The transfer of electrophoretically separated proteins on a PVDF (polyvinylidene fluoride)-membrane (BioTrace™ PVDF Transfer Membrane, BIO-RAD) was carried out in a semi-dry-procedure using a Biometra blotter (Göttingen, Germany). The SDS-gel, filter papers and sponges were equilibrated in transfer buffer (25 mM Tris, 150 mM glycine, 10% methanol) for 5 minutes. The PVDF-membrane was activated in methanol and equilibrated in transfer buffer. Afterwards the following transfer unity was built up between the two electrodes:

cathode

sponge

2 layers filter paper

SDS-gel

PVDF-membrane

2 layers filter paper

sponge

anode

For blotting an electrical current of 160 mA per gel was applied for 1 hour. The quality of protein transfer was checked by staining the membrane for 10-20 minutes in Ponceau S-solution (0.1% Ponceau S, 1% glacial acetic acid). After washing the membrane in distilled water, bands became visible.

2.12.5 Immunological Detection

After the transfer of proteins, non-specific binding sites were blocked for 1 hour at room temperature in TBST (50 mM Tris, 50 mM NaCl, 0.05% Tween 20, pH 7.5) containing 1% non-fat dry milk (BIO-RAD). After washing in TBST the membrane was incubated overnight at 4°C with the primary antibody in TBST. After washing 6 times for 5 minutes with TBST at room temperature the membrane was incubated with the HRP (horseradish peroxidase)-conjugated secondary antibody in TBST for 1 hour at room temperature. The membrane was then washed 6 times for 5 minutes. Specific immunoreactive proteins were detected by chemiluminescent reaction. After a short incubation in chemiluminescence substrate (SuperSignal™ West Dura, Pierce, Rockford, USA) the membrane was wrapped inside a foil followed by exposure of the membrane to x-ray film (BioMac Light Film, Kodak) for 1 second to 2 hours. Signals were detected using film developer and fixer (Adefo, Dietzenbach, Germany). Quantifications were performed by densitometry with ImageJ 1.38 (http://rsb.info.nih.gov/ij). The ratio of the protein of interest to actin was calculated.

Primary antibodies:

Rabbit anti-laminin (1:1.000; Sigma-Aldrich)
Rabbit anti-CXCR4 (1:2500; Chemicon, Millipore GmbH, Schwalbach, Germany)
Mouse anti-actin (1:4.000; Chemicon)

Secondary antibodies:

ImmunoPure® Peroxidase conjugated Goat anti-rabibt (1:4000; Pierce)

ImmunoPure® Peroxidase conjugated Goat anti-mouse (1:1500; Pierce)

2.13 Cytokine Antibody Array

Non-ischemic rat hearts (n=4) were removed within 5-10 minutes after UMS. Hearts without UMS insonication (n=4) served as control. After isolation the anterior and posterior walls were separated and the tissues were immediately frozen in liquid nitrogen. Tissue lysates were prepared in Cell Lysis Buffer (RayBiotech) as described in section 2.12.1. Rat Cytokine Antibody Arrays (RayBiotech) were performed with 100 µg of lysates according to the manufacturer's instructions. All chemicals and buffers were obtained from RayBio. All incubation steps were performed under gentle rotation. Briefly, membranes were incubated with Blocking Buffer for 20 minutes. 100 µg tissue lysate was diluted in Blocking Buffer to obtain a final volume of 1 ml. Membranes were incubated with samples for 2 hours at room temperature. Membranes were washed 3 times with Wash Buffer I and 2 times with Wash Buffer II and were incubated with Biotin-conjugated Anti-Cytokines at 4°C overnight. Membranes were washed as described and incubated with HRP-conjugated streptavidin for 2 hours at room temperature. Membranes were washed, incubated with Detection Buffer for 2 minutes and exposed to x-ray film. Signals were detected using film developer and fixer. The intensity of signals was quantified by densitometry with ImageJ 1.38. The amount of cytokines in anterior walls was normalized to the level of cytokines detected in the posterior wall.

2.14 Enzyme-linked immunosorbent assay (ELISA)

The amounts of matrix metalloproteinase (MMP)-2 and MMP-9 secreted by MSCs were determined using enzyme-linked immunosorbent assays (ELISA) (Quantikine, R&D Systems, Minneapolis, USA). Conditioned medium was collected after growing MSCs in α-MEM without FCS in the presence or absence of gelatine coating for 2, 4, 6, 24, 48 and 96 hours. Supernatants plus protease inhibitors were centrifuged to remove particulates and stored at -20°C. ELISA was performed according to the manufacturer's instructions. All chemicals and buffers were obtained from R&D Systems. Briefly, 100 µl Assay Diluent was added to each microplate well as well as

50 to 100 µl of MMP-standard or sample and incubated for 2 hours at room temperature. The microplate was washed 4 times with Wash Buffer and 200 µl of MMP-2 or MMP-9 Conjugate was added. After 2 hours of incubation the microplate was washed and 200 µl of Substrate Solution was added to each well. The assay was incubated for 30 minutes in the dark and subsequently 50 µl Stop Solution was added. Optical density was determined at 650 nm and 450 nm with the Molecular Devices kinetic microplate reader. The readings at 650 nm were subtracted from the readings at 450 nm to correct for optical imperfections of the plate. The results were related to the total protein concentration of the cells (section 2.12.2).

2.15 *In situ* zymography

To localize active MMPs during transmigration isolated mouse heart perfusions were performed with PKH26 (Sigma-Aldrich) labeled MSCs for 120 minutes as described above (2.5.3).

To evaluate active MMPs after UMS application non-ischemic rat hearts (n=4) were removed within 5-10 minutes after UMS. After isolation the tissue was immediately frozen in liquid nitrogen. MMP activity was identified in anteroseptal and posterolateral myocardium of 7 µm heart slides using a modified method of Agrawal *et al.* and Oh *et al.* (Oh *et al.*, 1999; Agrawal *et al.*, 2006). Slides were placed on 10 µg/ml DQ-gelatin (EnzCheck; Invitrogen) in 50 mM Tris-HCl, pH 7.4, plus 1 mM CaCl$_2$ in the presence or absence of 0.5 mM 1,10-phenanthroline (Sigma-Aldrich) and incubated for 24 hours in a humid chamber at 37°C. Slides were washed and embedded in AquaPolyMount. Digestion of DQ-gelatin resulted in unquenching of fluorochrome, which was detected with excitation at 488 nm and emission at 512-542 nm.

2.16 Microscopy

2.16.1 Confocal laser scanning microscopy

Confocal microscopy was performed using a LSM 510 Meta microscope (Zeiss). Images at a resolution of 512x512 or 1024x1024 pixels were acquired in the multi-track mode. CellTracker Green, digested DQ-gelatin, GFP, PKH67, DAF, APF and Cy2 were excited at 488 nm (AI laser), CellTracker Red and PKH26 at 543 nm (HeNe

laser) and Cy5 at 633nm (HeNe laser). After the main dichroic beam splitter (HFT 488/543) the fluorescence signal was divided by a secondary dichroic beam splitter (NFT 543) and detected in the separate channels using the appropriate filters: BP 505-530 (for CellTracker Green, DQ-gelatin, GFP, PKH67, DAF, APF and Cy2) LP 560 (for CellTracker Red and PKH26), and LP 650 (for Cy5). In this set-up, no cross-talk between the green and red channels was observed.

2.16.2 Calculation of MSC integration

For calculating the percentage of MSCs integrated into endothelial monolayer, slides were microscopically analyzed. Confocal images of 20 randomly selected MSCs per slide were classified as (1) MSC adherent on the endothelial monolayer, but still possessing their initial round shape, (2) start of flattening phase, or (3) MSC completely flattened and integrated into the monolayer. Additionally, the formation of plasmic podia of the MSCs was evaluated as (1) no plasmic podia, (2) short (< 25 µm) or (3) long plasmic podia (≥ 25 µm).

2.16.3 Quantification of transmigration

All cell interactions were graded after three-dimensional visualization of confocal z-stacks. Therefore eight representative short-axis slides of each left-ventricular level were analysed. For UMS experiments slides were placed within the UMS grid. Overall a minimum of 20 fluorescently labeled cells were randomly selected in each heart and evaluated with regards to adhesive properties. MSCs were counted as within the process of transendothelial migration if both of the following criteria applied: (1) a distinct plasmic podium connected to the MSC cell body was localized outside the endothelial cell layer and if (2) the staining of the endothelial barrier was regionally interrupted at the site of the penetrating plasmic podia (Schmidt *et al.*, 2006b). Results are expressed as percentage of the analysed cells. For absolute cell count in UMS experiments, all labeled MSCs observed in the standardized slides were counted and normalized to 100.000 transplanted MSCs. Transmigration was additionally evaluated in anteroseptal and posterolateral myocardium as well as in peri-infarction borderzone of ischemic myocardium.

2.16.4 Electron microscopy

Embedding and microscopy was performed at the Institute I for Anatomy, University of Cologne (Professor Dr. Klaus Addicks). Ultrathin sections were prepared by the technical assistant Mojgan Ghilav. For electron microscopy of co-culture MACS cells were cultured on gelatine-coated foil (Plano, Wetzlar, Germany) to confluence. MSCs were gold labeled with 10 nm colloid gold (Sigma-Aldrich) for 7 days as described before (Christensen *et al.*, 1992). In each change of medium 20% α-MEM was supplemented with 25 µl colloid gold solution per ml medium. Accuracy of gold labeling was checked *via* a Silver enhancement kit (Sigma-Aldrich). On addition of the kit, precipitation of metallic silver occurs, which enlarges colloidal gold labels normally visible only at the electron microscope level, yielding high-contrast signals visible by light microscopy. Therefore, MSCs were fixed with 4% PFA, rinsed with distilled H_2O, incubated with a solution containing equal volumes of solution A (silver salt) and solution B (initiator) for 10 minutes at room temperature in the dark. After washing cells, were incubated with aqueous 2.5% sodium thiosulfate for 2 minutes, rinsed, dehydrated and embedded in Entellan. Gold particles were examined using a Zeiss Axiophot microscope.

Co-culture samples were fixed in 2% glutaraldehyde and 0.2% picric acid (Merck) in 0.1 M cacodylate buffer pH 7.4 for 45 minutes at room temperature.

For electron microscopy of hearts the tissue was immediately fixed with 2% glutaraldehyde and 2% PFA in 0.1 M cacodylate buffer pH 7.4 for 6 hours at room temperature. The following steps were performed on ice or at 4°C. After washing three times in cacodylate buffer for 7 minutes, samples were treated with 1% OsO_4 in cacodylate buffer for 30 minutes, washed three times in cacodylate buffer for 7 minutes, treated with 50% EtOH for 7 minutes and 70% EtOH for 7 minutes. Afterwards samples were incubated with 1.5% uranyl acetate (Plano) in 70% EtOH for 1 hour. Incubation with uranyl acetate contrasted the nuclei. After dehydration in a series of graded ethanol (90% EtOH for 7 minutes, thrice in 100% EtOH for 7 minutes, 7 minutes in a solution containing equal volumes of 100% EtOH and propylenoxide and 7 minutes in propylenoxide) specimens were embedded in Epon-araldite (Sigma-Aldrich) (Schmidt *et al.*, 2006b). The Epon solution contained (w/v): 11.56 g epoxy-embedding medium, 7.13 g expoxy-embedding medium hardener DDSA, 6.28 g epoxy-embedding medium hardener MNA and 0.38 g epoxy-embedding medium accelerator. First samples were incubated in Epon/1.2-

epoxypropan in a 1:1 ratio for 30 minutes, second in a 3:1 ratio for 30 minutes and finally overnight at 60°C in pure Epon. For final polymerization samples were placed in rubber forms containing fresh Epon and incubated for 3 days at 60°C and 1 day at room temperature.

After trimming (TM60, Reichert, Bensheim, Germany) thin sections (500-1000 nm) of embedded tissue were cut with a glass knife on an ultramicrotome (Reichert) and stained with methylene-azure-blue II solution (1:1 of 1% methylene blue in 1% borax and 1% azure-II in H_2O). After localization of adequate position of the sample, ultra thin sections (70-80 nm) were processed on the same microtome with a diamond knife and placed on copper grids (Plano). For contrasting samples were incubated for 20 minutes with aqueous 1.5% uranyl acetate at room temperature in the dark. After washing several times with H_2O samples were contrasted in leadcitrate (800 µl H_2O, 155 µl 1.3 M tri-sodiumcitrate-2-hydrate-solution, 100 µl 1 M lead(II)-nitrate-solution, 200 µl 1 M NaOH) for 5 minutes. After washing, grids were dried. Ultra thin sections were examined using a Zeiss 902A transmission electron microscope with TEM Imaging Platform iTEM software (Soft Imaging Systems, Münster, Germany). Pictures were taken using the cooled digital camera Megaview II (Soft Imaging Systems).

2.17 Statistical analysis

All experiments were carried out 4 to 6 times. All data are represented in mean ± standard deviation. The mean value and the standard deviation were calculated using Microsoft Excel. Statistical significance of differences was determined using the two-tailed unpaired Student`s *t*-test (2-sided) or One-way Analysis of Variance (ANOVA) with post-test Bonferroni using GraphPad InStat v. 3.01 (GraphPad Software, San Diego, USA). A *p*-value of less than 0.05 was considered statistically significant.

3. Results

3.1 Characterization of human mesenchymal stem cells

Before experiments the quality of cultivated MSCs was routinely ensured by microscopic observations, flow cytometry, colony forming unit-fibroblast assays and differentiation assays. Figure 8 shows a light microscopic picture of a confluent monolayer of MSCs with their characteristic spindle-shaped morphology (Pittenger *et al.*, 1999). Flow cytometric analyses were performed to characterize the expression of MSC surface antigens. Figure 9 summarizes the results of a representative FACS analysis of MSCs in passage 2 derived from a male 67 years old patient. In this example, 84.0% of the analyzed cells were negative for the leukocyte common antigen CD45. 77.7% of these CD45-negative cells were additionally double-negative for the hematopoietic markers CD14 (lipopolysaccharide receptor) and CD34 (marker of human hematopoietic stem and progenitor cells). 98.9% of the $CD45^-/CD34^-/CD14^-$ triple negative population of cells were double positive for CD105 (endoglin or TGF β1/3-receptor, highly expressed on vascular endothelial cells) and CD106 (VCAM-1). According to Pittenger *et al.* (Pittenger *et al.*, 1999), this population of cells ($CD45^-$ $/CD34^-/CD14^-/CD105^+/CD106^+$) was defined as human MSCs. Thus, in the presented example 64.5% (0.84·0.777·0.989) of all cells were $CD45^-/CD34^-/CD14^-$ and $CD105^+/CD106^+$. A purity of MSCs yielding a comparable range was considered to be a homogeneous phenotypic population (Pittenger *et al.*, 1999; Klinz *et al.*, 2005; Schmidt *et al.*, 2006a).
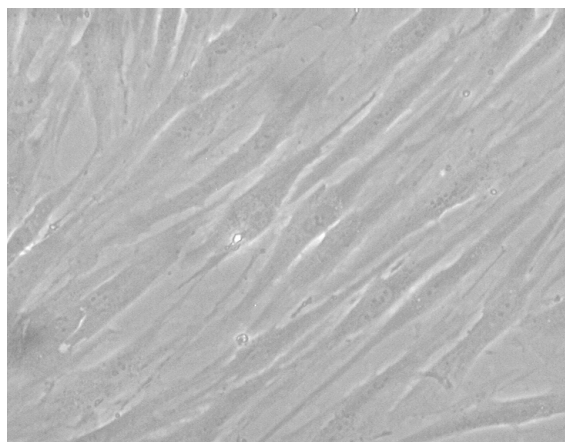
Figure 8: Light microscopic picture of a confluent monolayer of MSCs

In culture MSCs displayed a characteristic fibroblast-like and spindle-shaped morphology. Magnification: 100x.

All cells

CD45⁻

CD45⁻/CD34⁻/CD14⁻
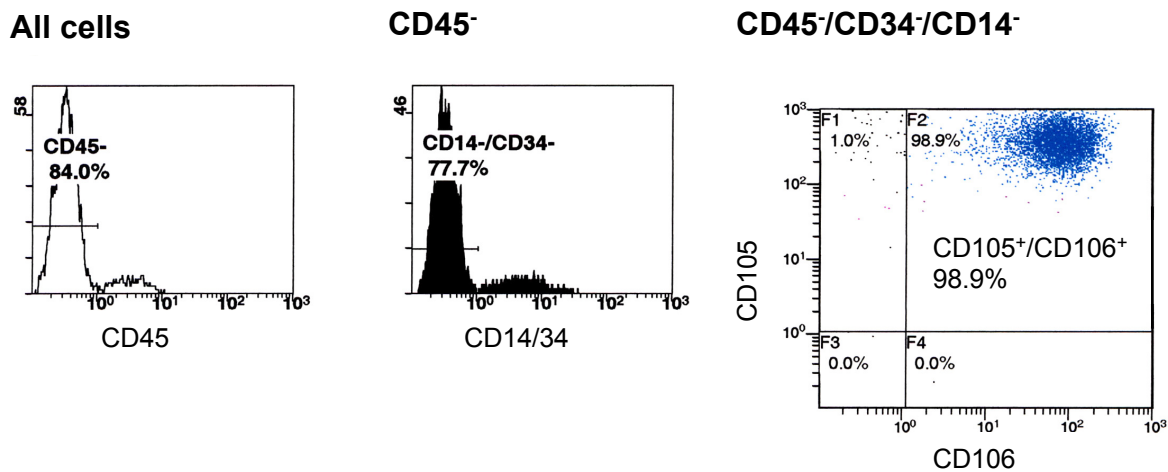
Figure 9: Flow cytometric analysis of expressed surface antigens of MSCs

Representative FACS analysis of MSCs in passage 2 derived from a male 67 years old patient. 84.0% of all cells were $CD45^-$. 77.7% of this $CD45^-$-population were additionally CD14 and CD34 double-negative. 98.9% of all $CD45^-$/$CD34^-$/$CD14^-$ cells were double positive for $CD105^+$/$CD106^+$.

MSCs did not differentiate spontaneously during culture expansion. Thus, to evaluate their multilineage differentiation potential MSCs were cultured under conditions favourable for adipogenic, osteogenic and chondrogenic differentiation. After 2 to 3 weeks in the lineage specific culture conditions, the expanded MSCs differentiated. As Figure 10a illustrates, induction of an adipogenic phenotype of MSCs grown under conditions favourable for adipogenic differentiation was apparent by the accumulation of lipid-rich vacuoles within the cells. Differentiation to the osteogenic lineage accompanied by an increase in calcium depositions is shown in Figure 10b. Chondrogenesis was validated by semi-quantitative analysis of collagen II mRNA expression. Figure 10c summarizes that only MSCs grown under conditions favourable for chondrogenic differentiation expressed collagen II, but not MSCs grown under control conditions.

a)

b)

c)
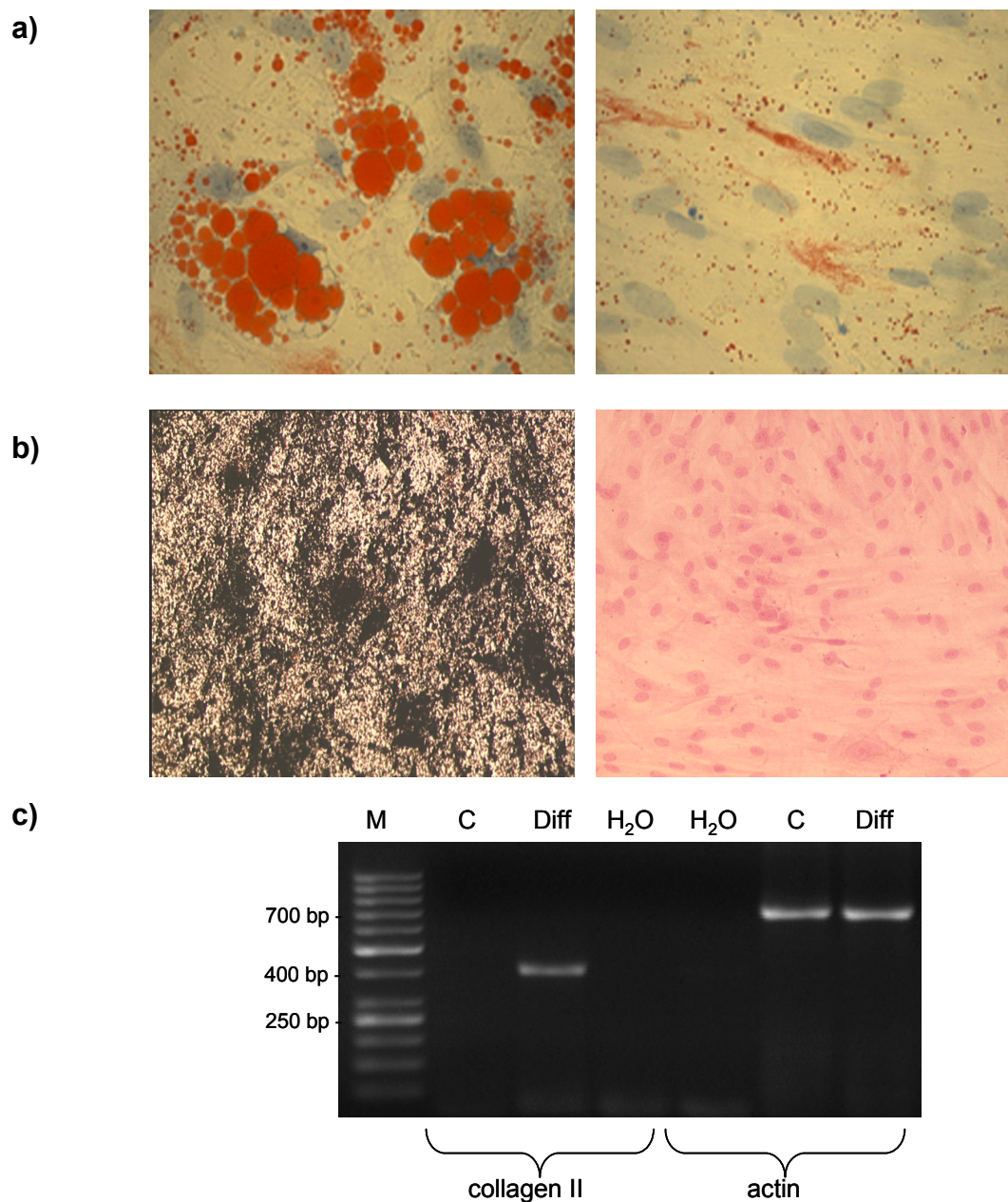
Figure 10:   MSCs differentiate to mesenchymal lineages

a) Adipogenesis of MSCs grown under conditions favourable for adipogenic differentiation (left panel) was indicated by the accumulation of neutral lipid droplets in vacuoles which stain with Oil Red O. MSCs under control conditions did not accumulate lipids (right panel). Nuclei were counterstained by Mayer`s hematoxylin. Magnification: 100x.

b) Osteogenesis of MSCs grown under conditions favourable for osteogenic differentiation (left panel) was indicated by formation of calcium depots stained with von Kossa staining. MSCs under control conditions did not accumulate calcium (right panel). Nuclei were counterstained by nuclear fast red. Magnification: 40x.

Legend to Figure 10, continued:

> c) Chondrogenesis was demonstrated by semi-quantitative RT-PCR analysis. Only MSCs grown under conditions favourable for chondrogenic differentiation expressed collagen II (388 bp). Expression of actin (698 bp) served as internal standard.
>
> M: 50bp DNA ladder (Fermentas), C: MSCs grown under control conditions, Diff: MSCs grown under conditions favourable for chondrogenic differentiation, H_2O: water control.

3.2 Characterization of transmigration and invasion: different model systems

3.2.1 Co-cultivation

To examine the morphology and time course of the interaction of MSCs with the endothelial barrier, an *in vitro* co-cultivation approach was established. Representative pictures of red-labeled MSCs co-cultivated with green-labeled MACS endothelial monolayers illustrate that MSCs flattened and integrated into the endothelial monolayer (Figure 11a). In addition, further morphological changes of the MSC cell shape including the formation of long plasmic podia occurred. The first contact and adhesion of MSCs was observed within 15 minutes as shown in Figure 11b. Here, MSCs still possessed a spherical shape. Later, MSCs integrated into the monolayer and endothelial cells started to grow on top of the MSCs to seal the monolayer. VE-cadherin staining revealed the integrity of the endothelial monolayer prior to co-cultivation experiments (Figure 12).

In a different approach, ultrastructural analysis by electron microscopy of co-cultivation supplements demonstrated as well that MSCs integrated into the endothelial cell monolayer *in vitro* (Figure 13). Here, MSCs still exhibited a spherical shape after 30 minutes, while a thin plasmic edge of endothelium was visible underneath the stem cell. The 240 minutes sample confirmed that the MSCs flattened and integrated into the endothelial monolayer.
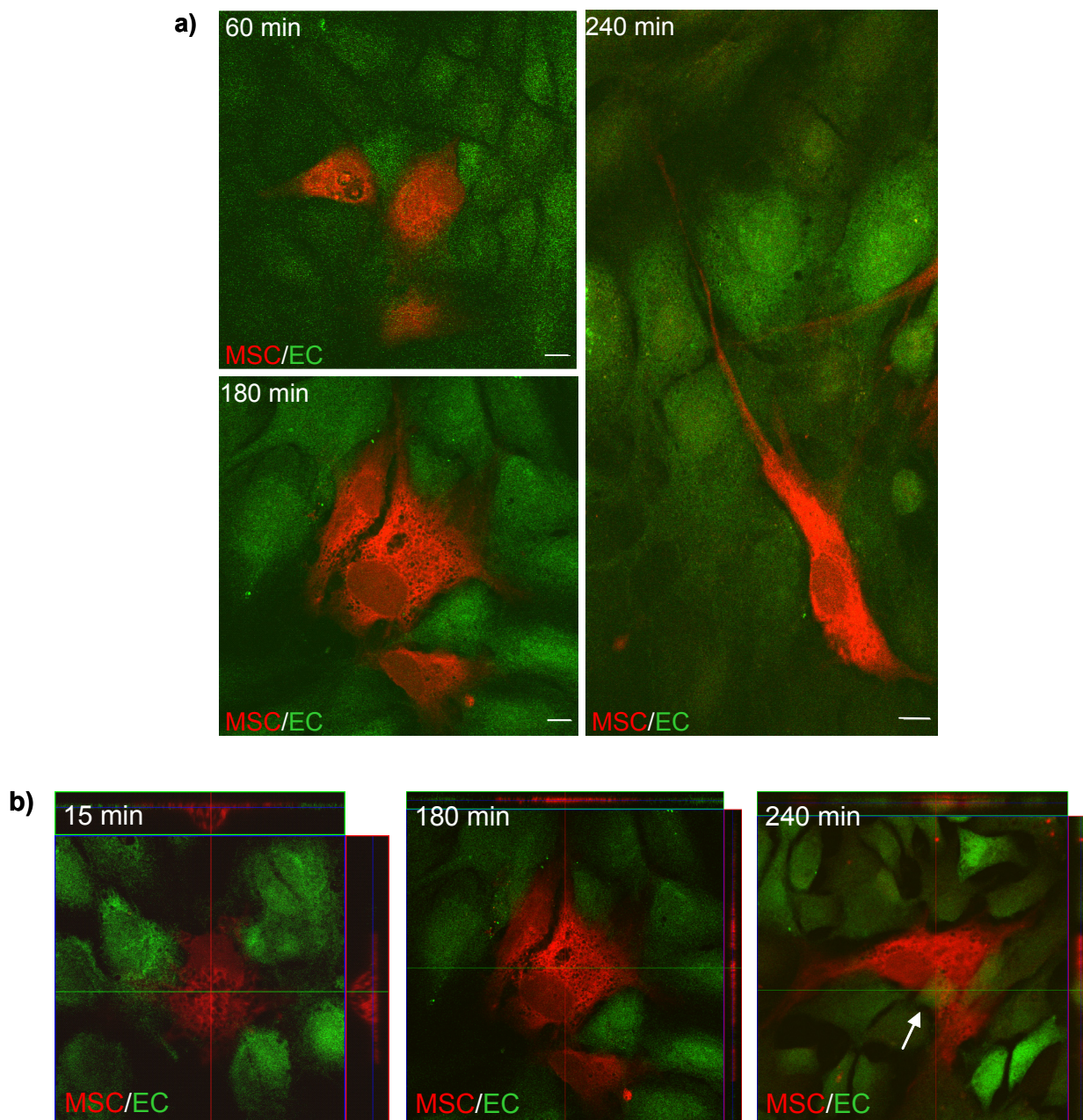
Figure 11:   MSCs integrate into endothelial monolayer *in vitro*

MSCs co-cultivated with MACS endothelial monolayer (EC) for 15 to 240 minutes (MSCs: CellTracker Red, EC: CellTracker Green).

a) MSCs quickly interacted with endothelial cells, flattened and integrated into the monolayer. Morphological changes of MSC cell shape occurred *via* formation of podia. Scale bar: 10 µm.

b) Orthogonal projections illustrate that MSCs quickly attached within 15 minutes (left panel) and integrated into the monolayer (center panel, after 180 minutes). In some cases, endothelial cells (arrow) grew on top of MSCs (right panel, after 240 minutes). Horizontal bar: section of the XZ plane through a confocal image stack; vertical bar: section of the YZ plane through a confocal image stack.
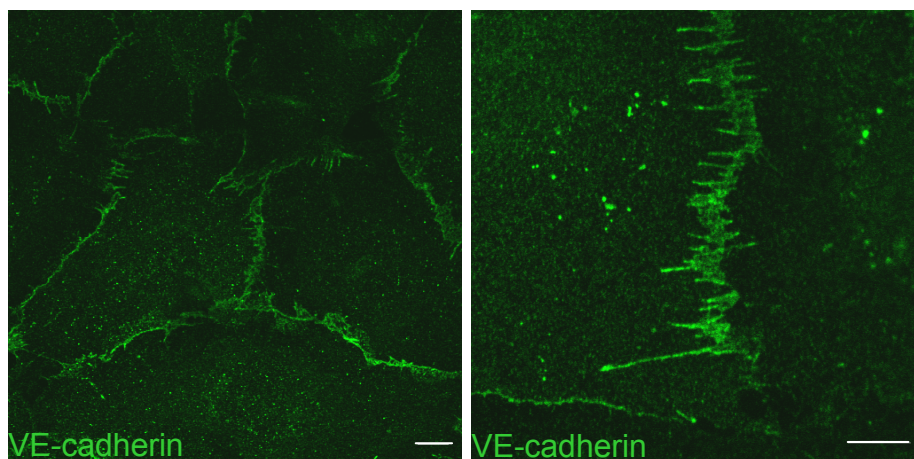
Figure 12:   Integrity of endothelial monolayer

The integrity of the endothelial monolayer was checked *via* immunohistochemical VE-cadherin distribution. Cy2 served as secondary antibody. Representative pictures of a HUVEC monolayer with tight cell-to-cell-contacts. Scale bar: 10 µm.
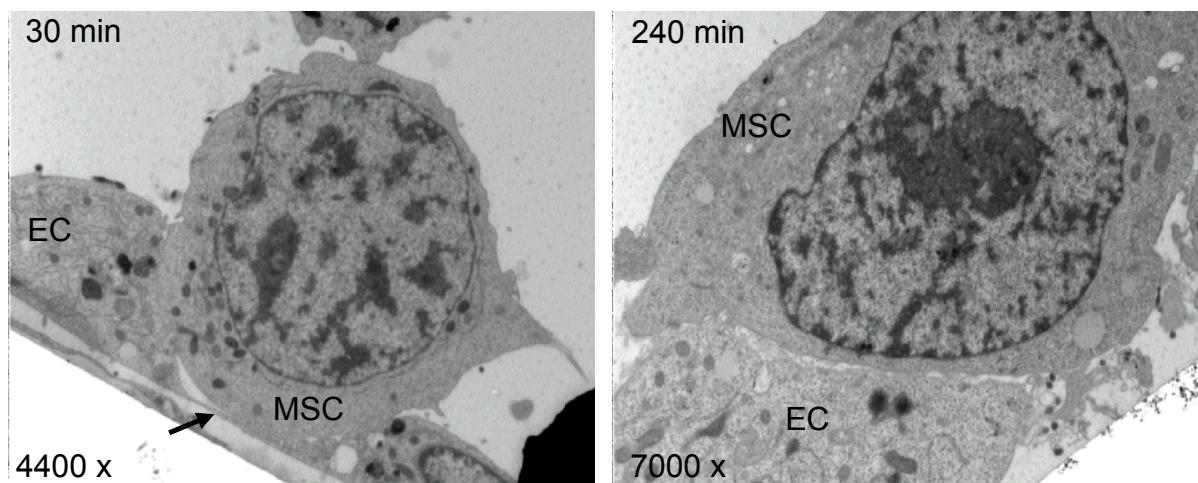
Figure 13:   Electron micrographs of *in vitro* co-cultivation

Ultrastructure of MSCs co-cultivated with endothelial MACS cell monolayer. After 30 minutes, MSCs exhibited a spherical shape. A thin plasmic edge of endothelial cells (EC) was visible underneath the MSC (arrow). After 240 minutes, MSCs flattened and integrated into the endothelial monolayer. Magnification: 4400x/7000x.

3.2.2 Three-dimensional model systems for transmigration

To visualize not only the transmigration and opening of the endothelial barrier, but also the invasion of MSCs into the surrounding tissue, three different three-dimensional approaches have been established. Taken together, the three-dimensional model systems enabled the visualization of both the transmigration and the invasion process of MSCs. Both processes were accompanied by the formation of plasmic podia.

3.2.2.1 Collagen invasion assay

First, growing endothelial monolayers on collagen gels allowed observing MSCs penetrating the endothelial monolayer and invading the matrix *in vitro* (Figure 14). After 2 hours, MSCs came into contact with the HUVEC monolayer, but retained a spherical shape. After 4 hours the MSCs had integrated into the monolayer and started to penetrate it by means of plasmic podia. After 6 to 24 hours MSCs transmigrated across the endothelial monolayer, invaded the collagen gel and remained underneath the endothelial cells.

3.2.2.2 Endothelial spheroids

Second, multi-cellular endothelial spheroids were generated and co-cultivated with MSCs (Figure 15). After 2 hours MSCs possessed a spherical shape and were in contact with the surface monolayer of the spheroid. After 4 hours MSCs started to invade the inner mass of the spheroids. The invasion was accompanied by the formation of plasmic podia.

3.2.2.3 Isolated mouse heart perfusions

Third, MSCs stained with the green-fluorescent dye PKH67 were perfused through isolated mouse hearts. The endothelium was stained using Rhodamine-*Griffonia simplicifolia* Lectin I. Figure 16a illustrates two MSCs in one vessel in close contact with the endothelium after 60 minutes of perfusion. Confocal microscopy facilitated a three-dimensional visualization of MSCs at an early phase of penetrating the endothelium and invading the cardiac tissue after 90 minutes (Figure 16b). Overall,

after 90 minutes perfusion 38 ± 11% of the MSCs which had been retained in the heart transmigrated across the endothelium and started to invade the heart muscle.
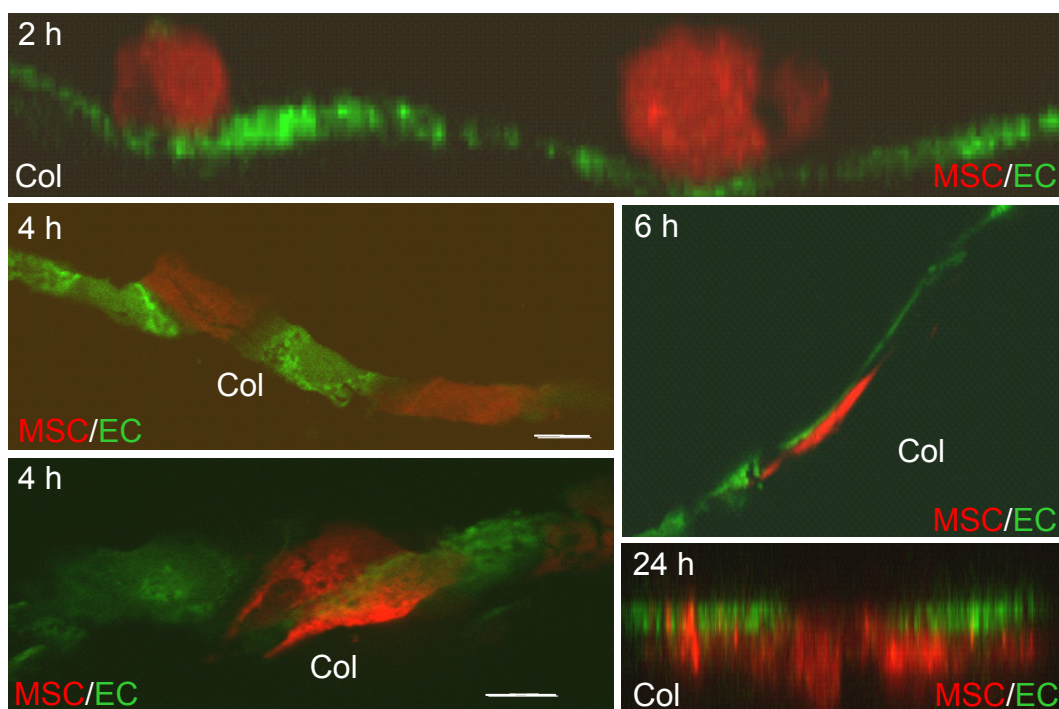
Figure 14: Collagen gel invasion assay

Co-cultivation of HUVECs (CellTracker Green) grown on top of a collagen matrix (Col) with MSCs (CellTracker Red). After 2 hours MSCs possessed a spherical shape. After 4 hours MSCs integrated into the monolayer and penetrated the barrier *via* plasmic podia. After 6 and 24 hours MSCs moved underneath the endothelial monolayer and invaded the collagen gel. 2 and 24 hours: XZ planes of confocal image stacks; 4 and 6 hours: cryo slices of the collagen matrix. Scale bar: 10 µm.
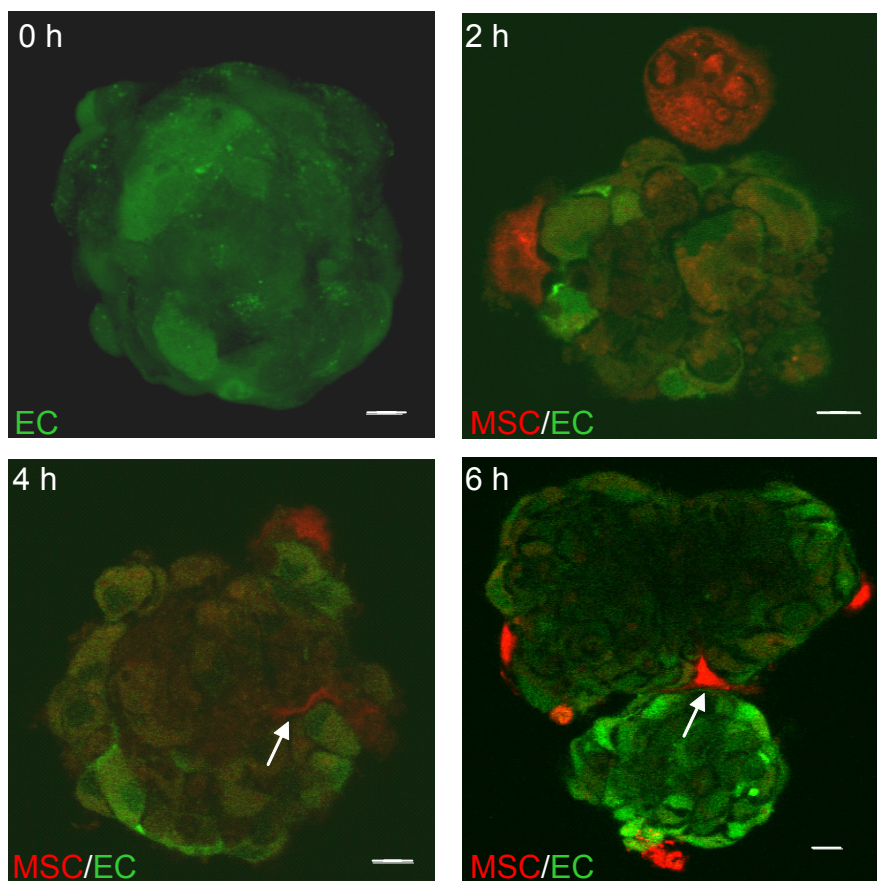
Figure 15: Co-cultivation of endothelial spheroids with MSCs

Spheroids were stained with CellTracker Green and were co-cultivated with MSCs (CellTracker Red). After 2 hours MSCs came into contact with the surface of the spheroids. After 4 and 6 hours MSCs had invaded the spheroids *via* plasmic podia (arrows). Scale bar: 10 µm.
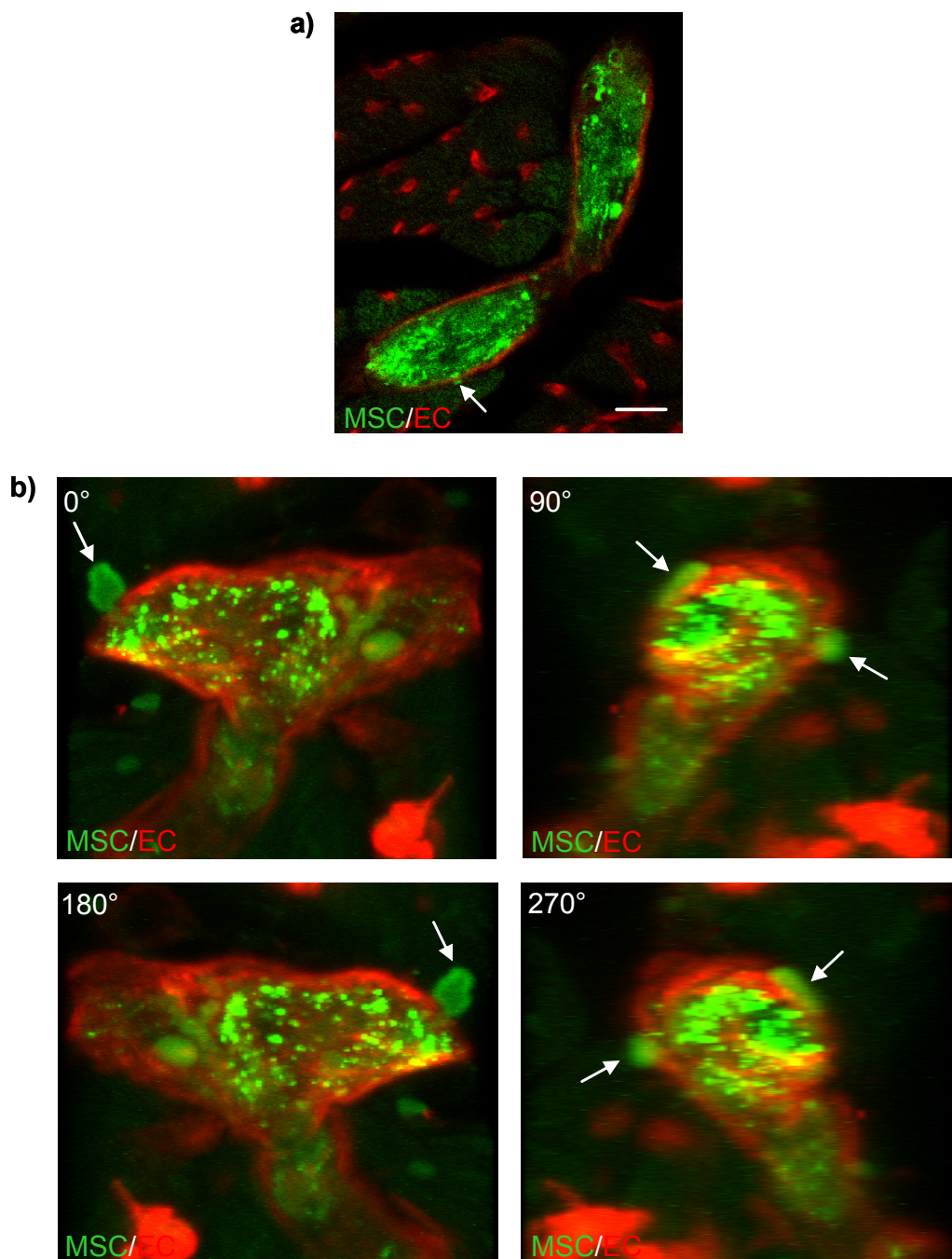
Figure 16: Isolated mouse heart perfusions visualize transmigration and invasion of MSCs *ex vivo*

Isolated mouse hearts were perfused with MSCs (PKH67-labeled, green); the endothelium was stained with Rhodamine-*Griffonia simplicifolia* Lectin I (red).

a) A vessel containing two MSCs which closely interacted and started to penetrate the capillary endothelial barrier (arrow) after 60 minutes of perfusion. Scale bar: 10 μm.

b) 3D-reconstruction of a confocal z-stack in an early phase of transmigration and invasion after 90 minutes of perfusion. The arrows point at plasmic podia of the MSC which penetrated the capillary endothelial barrier.

3.3   Observation of transmigrating MSCs *in vivo*

To evaluate whether the described transmigration and invasion phenomena also occur under physiological conditions, *in vivo* experiments were performed. Therefore, rat hearts were perfused with green fluorescent labeled (PHK67) MSCs *via* a catheter in the aortic root. Analyses of the hearts inferred that MSCs indeed transmigrate across the endothelium *in vivo* and that this transmigration shows the same morphological properties as observed in the *in vitro* and *ex vivo* experiments (section 3.2). Figure 17 illustrates a green-labeled MSC which transmigrated across the red-labeled endothelial barrier *in vivo*. Plasmic podia of the MSC penetrated the capillary endothelial barrier as it was observed in the previously described model systems (section 3.2). Initial experiments revealed endothelial adhesion of MSCs, but no signs of transmigration after 30 and 60 minutes (0% at both time points). Slow application of constantly homogenized 500.000 MSCs into the aortic root resulted in wall motion abnormalities and severe decrease of global systolic function, most likely as result of microembolisms and myocardial ischemia. Therefore, the *in vivo* protocol was modified to cardiomyoplasty of 150.000 MSCs. To achieve a comparable percentage of transmigrating MSCs as in isolated *ex vivo* mouse heart perfusions *in vivo* rat hearts were harvested 120 minutes after cardiomyoplasty.
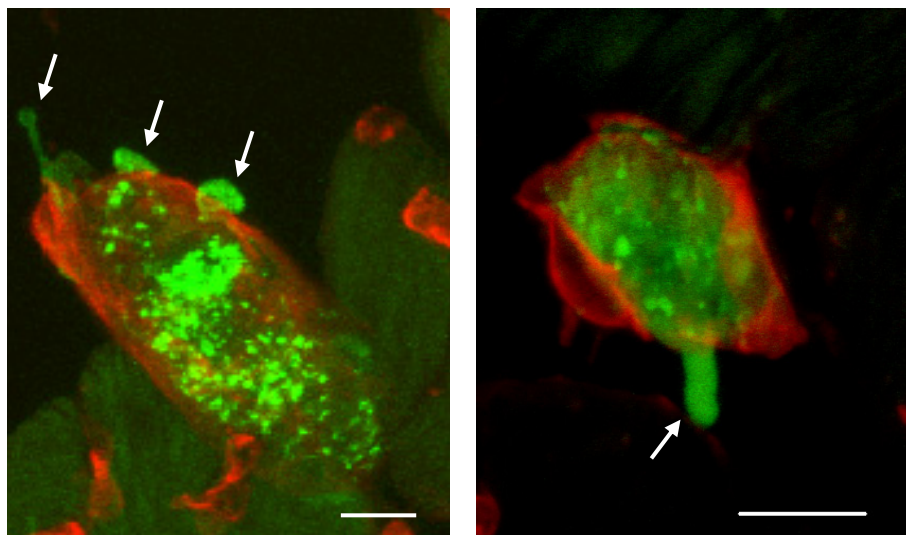
Figure 17:   MSCs transmigrate and invade *in vivo*

MSCs (PKH67-labeled, green) transmigrate *in vivo* across the endothelial border (stained with Rhodamine-*Griffonia Simplicifolia* Lectin I, red) in rat hearts. Note the plasmic podia (each marked with an arrow) of the MSCs which penetrated the capillary endothelial barrier. Scale bar: 10 µm

3.4 VCAM-1/VLA-4-interaction and β1 integrin clustering are crucial for transendothelial migration

In order to determine the role of VCAM-1 and VLA-4 for the transendothelial migration of human MSCs, blocking experiments were conducted. The use of blocking antibodies specific for CD106 (VCAM-1) and CD49d (integrin alpha4 chain of VLA-4 complex) resulted in a significant reduction of MSC integration into HUVEC monolayers compared to control experiments without antibodies or isotypic control IgG1 antibodies (percentage of integrated MSCs in the HUVEC monolayer: control: 71 ± 16%; anti VCAM-1: 25 ± 5%; anti VLA-4: 40 ± 7%; isotypic control: 59 ± 19%). Simultaneous blockade of VCAM-1 and VLA-4 did not lead to any further reduction of MSC integration (25 ± 5%, Figure 18).

In addition, from immunohistochemical staining of β1 integrin could be inferred that the interaction of MSCs with endothelial cells induced a distinct clustering of β1 integrins in MSCs (see Figure 19), which was not observed in MSCs cultivated without an endothelial monolayer.
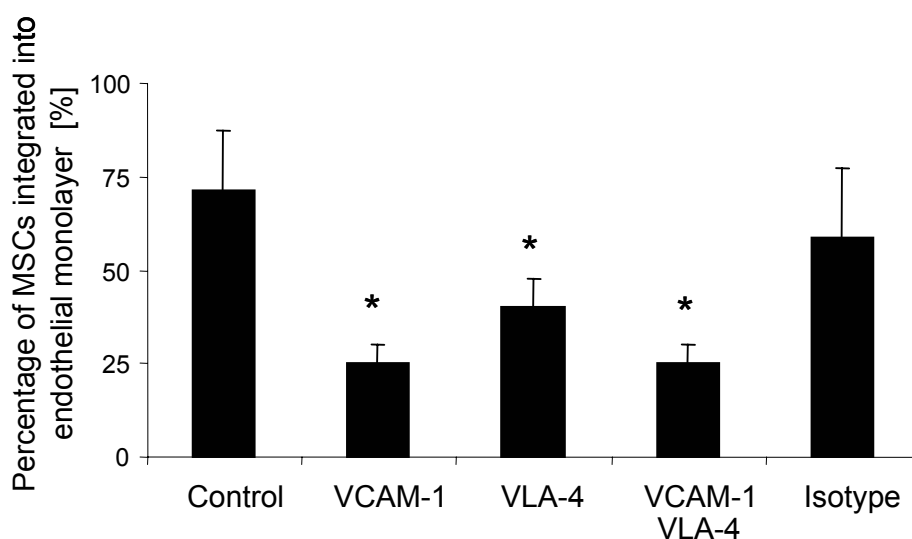
Figure 18: Transmigration requires VCAM-1/VLA-4

The usage of VCAM-1 and VLA-4 blocking antibodies during co-cultivation resulted in a significant reduction of MSC integration into HUVEC monolayers compared to control experiments. Combined blockade did not lead to a further decrease in MSC integration.

* significant difference compared to control ($p < 0.05$).
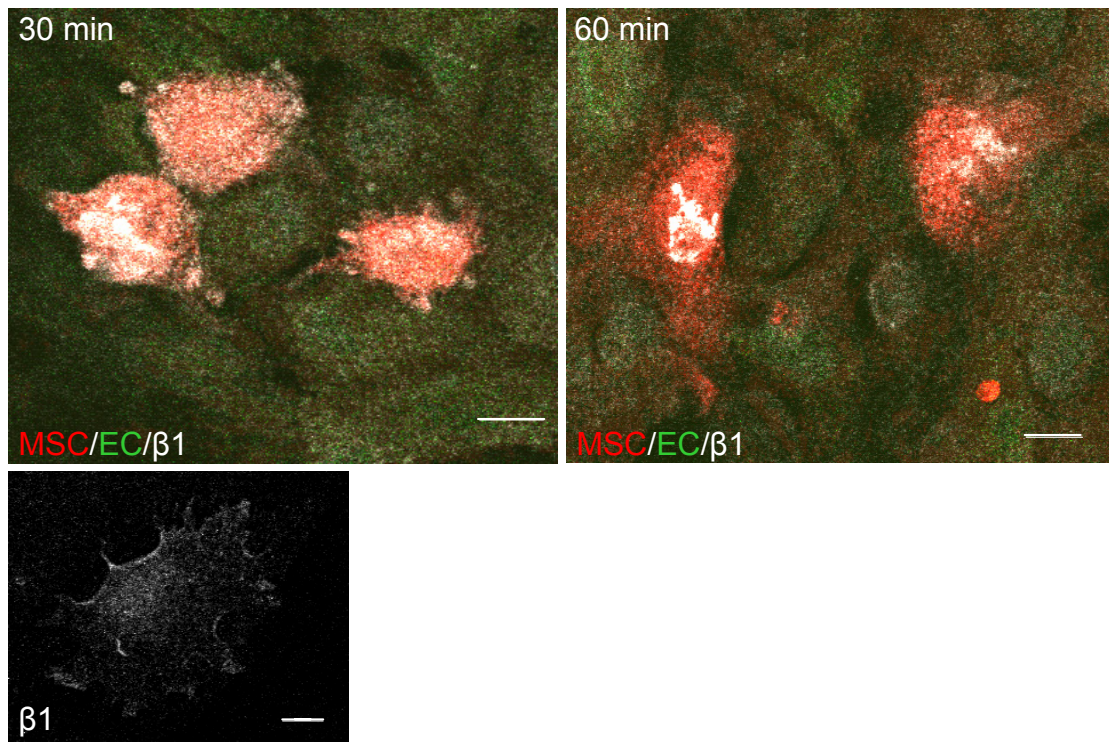
Figure 19: Transmigration triggers clustering of β1 integrins

Co-cultivated MSC on a MACS monolayer (EC) exhibited clusters of β1 integrins after 30 and 60 minutes which were not visible in MSCs cultivated without endothelial cells. MSCs: CellTracker Red, MACS: CellTracker Green, β1 integrin: Cy5 (white). Scale bar: 10 µm

3.5 MSCs secrete active MMPs at sites of invasion

ELISA for active gelatinases MMP-2 and MMP-9 using culture supernatant of MSCs revealed that *in vitro* MSCs secreted a high amount of active MMP-2 between 24 and 96 hours and that this secretion could be increased by pre-coating the culture dishes with gelatine (Figure 20; MMP-2 concentration after 96 hours: with gelatine 119.09 ng/ml·mg; without gelatine 83.59 ng/ml·mg). No detectable amount of active MMP-9 was secreted.

To define sites of gelatinase activity, *in situ* zymographies were performed on sections of mouse hearts that had been previously perfused with MSCs using a fluorescein-conjugated gelatine as substrate (Figure 21). This was combined with red-fluorescent labeling (PKH26) of MSCs to identify sites of MSC invasion. High gelatinase activity was restricted to heart vessels that contained invading MSCs (left panel). As a control cleavage of fluorescein-conjugated gelatine was prevented by the general MMP inhibitor 1,10-phenanthroline (right panel).
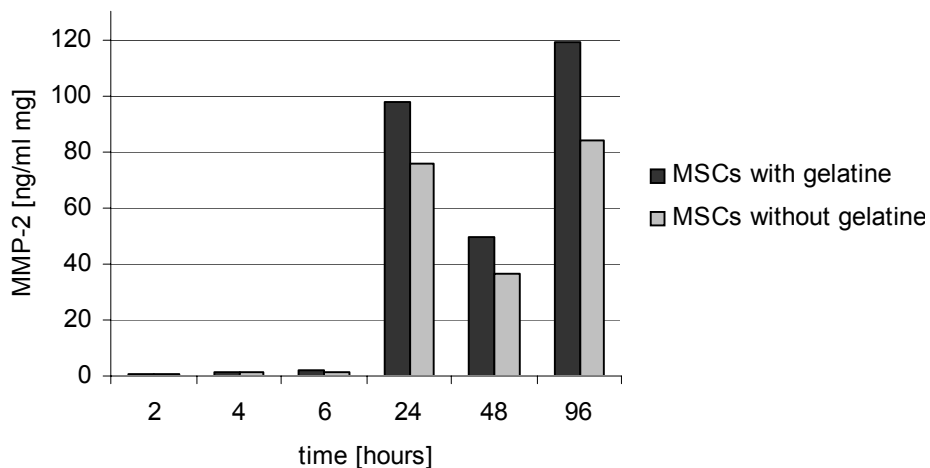
Figure 20: MSCs secrete MMP-2

ELISA with culture supernatants of MSCs grown in the presence or absence of gelatine pre-coating of culture dishes demonstrated that MSCs secreted active MMP-2, which was increased by gelatine coating of the culture dishes.
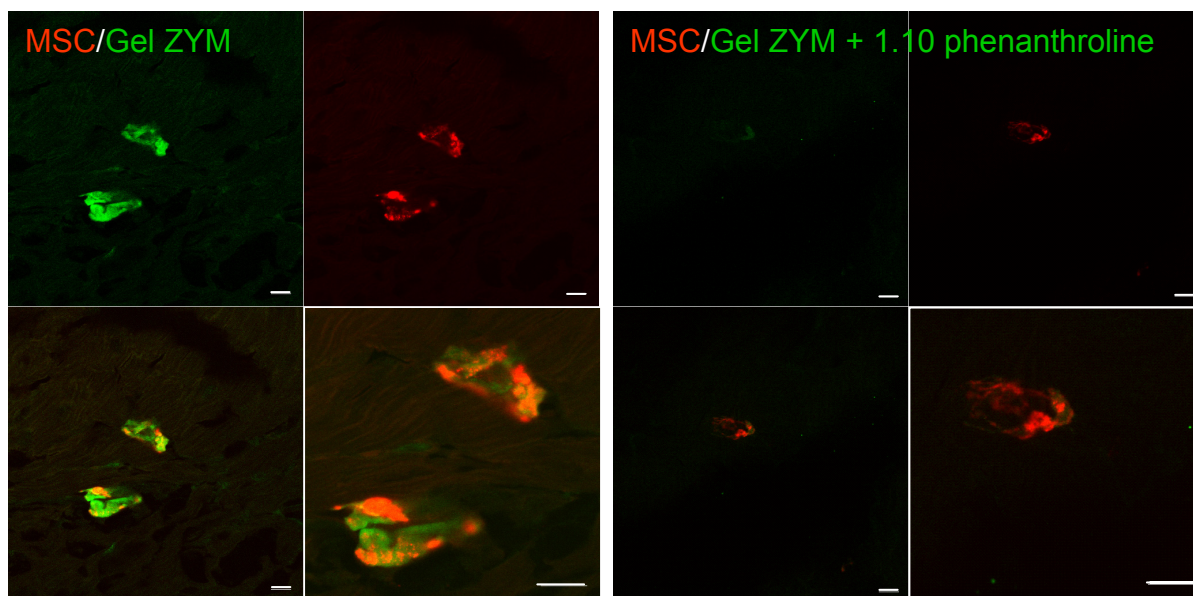
Figure 21: Active gelatinases are secreted at sites of MSC invasion

In situ zymography of murine cardiac tissue perfused with MSCs (PKH26, red) clearly showed the presence of active gelatinases (green fluorescence) which was restricted to sites of MSC invasion (left panel). 1,10-phenanthroline prevented gelatinase activity (right panel). DQ-gelantin was used as substrate. Scale bar: 10 µm.

3.6 Transmigration is dependent on the endothelial phenotype

To evaluate differences in the interaction between MSCs and the endothelium which depend on the endothelial phenotype, co-cultivation experiments with different endothelial monolayers were carried out. Major discrepancies were detected in the time course of integration (see Figure 22a) and alteration of MSC morphology depending on the endothelial phenotype (see Figure 22b). After 15 minutes, already 19 ± 4% of MSCs on HCAEC monolayer had completely integrated. In comparison, throughout the whole time-series, monolayers consisting of HUVEC enabled the most effective integration of MSCs (percentage of integrated MSCs in a HUVEC monolayer after 30 minutes: 59 ± 9%; 60 minutes: 93 ± 8%; 120 minutes: 96 ± 7%). The flattening of MSCs on HuAoEC monolayer was significantly slowed down compared to control experiments without endothelial monolayers (Figure 22a). In addition, morphological changes of MSCs quantified by the formation of plasmic podia (≥ 25 μm) were also dependent on the type of endothelial monolayer (Figure 22b). Co-cultivation on HCAEC monolayers resulted in the highest percentage of MSCs with long plasmic podia. In general, co-culture with any endothelial monolayers significantly increased the formation of plasmic podia compared to control experiments without endothelial monolayers.

3.7 Cytokines influence MSC transmigration

To elucidate the potential influence of cytokines on MSC transmigration, co-cultivation experiments in the presence of bFGF, VEGF, EPO and IL-6 were carried out. After 15 minutes all cytokines resulted in a significant increase of MSC integration compared to the control (Figure 23; 15 minutes: control: 5 ± 4%; bFGF: 16 ± 7%; VEGF: 23 ± 10%; EPO: 39 ± 9%; IL-6: 24 ± 14%). After 30 minutes, VEGF and EPO enhanced transmigration. After 60 minutes, only EPO showed any effect. After 120 minutes, VEGF and IL-6 enhanced the transmigration of MSCs, although the effect of IL-6 was small. Surprisingly, bFGF significantly decreased the transmigration of MSCs at the time point of 60 minutes (control: 66 ± 6%; VEGF: 74 ± 7%; EPO: 79 ± 2%; IL-6: 65 ± 8%; bFGF: 51 ± 10%).
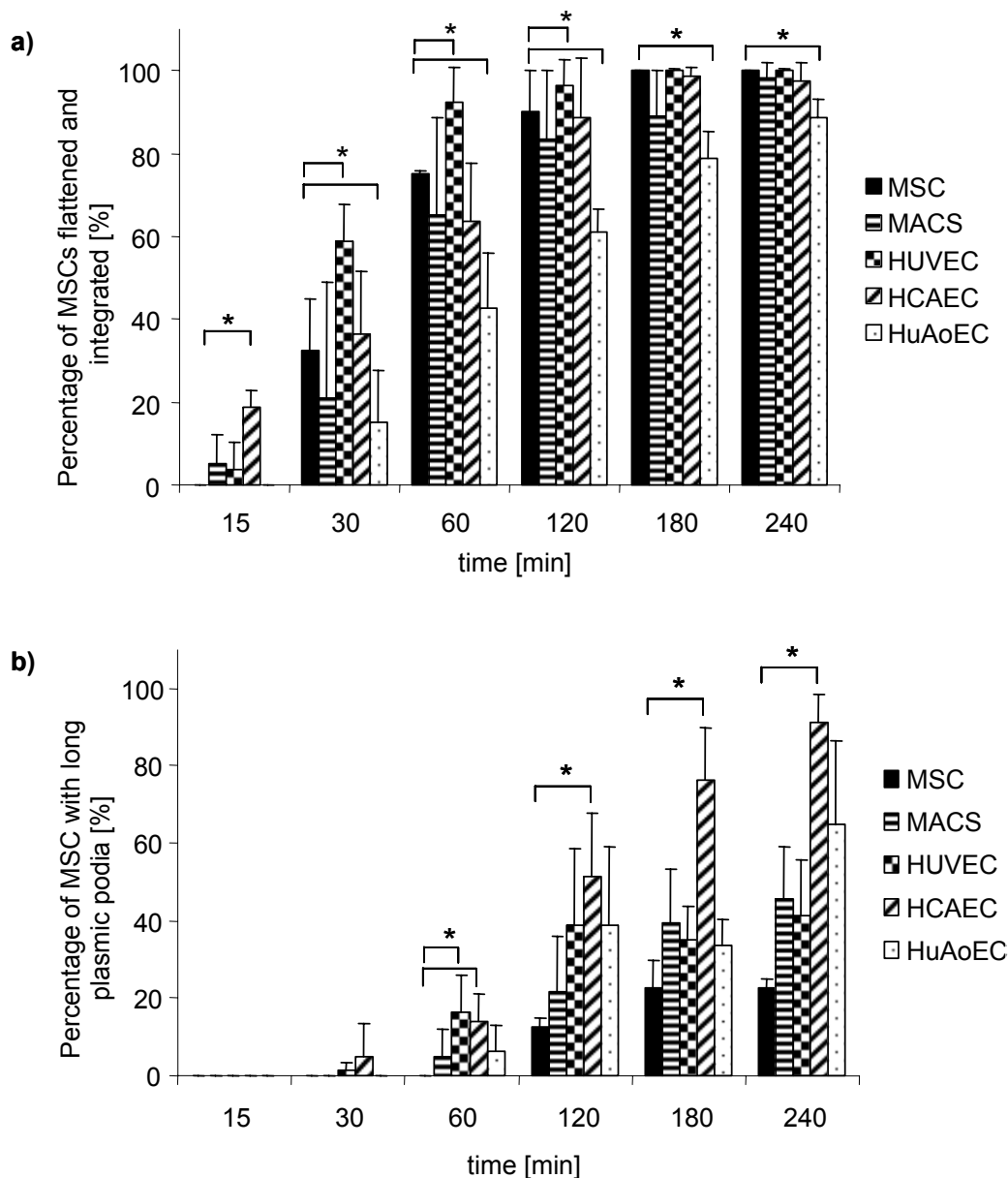
Figure 22: Differences in transmigration capacity depend on endothelial phenotype

a) MSC integration into different endothelial monolayer. The percentage of flattened and integrated MSCs was quantified. HCAEC monolayers enabled the fastest integration of MSCs. However, throughout the whole time-series, HUVEC monolayers were the most effective. The flattening of MSCs on HuAoEC monolayers was significantly slowed down compared to control experiments without endothelial monolayers (MSC).

b) Percentage of MSCs forming long plasmic podia (≥ 25 µm) on different endothelial monolayers. Co-cultivation on a HCAEC monolayer resulted in the highest amount of MSCs with long podia.

* significant difference compared to control experiments without endothelial monolayer (p < 0.05).
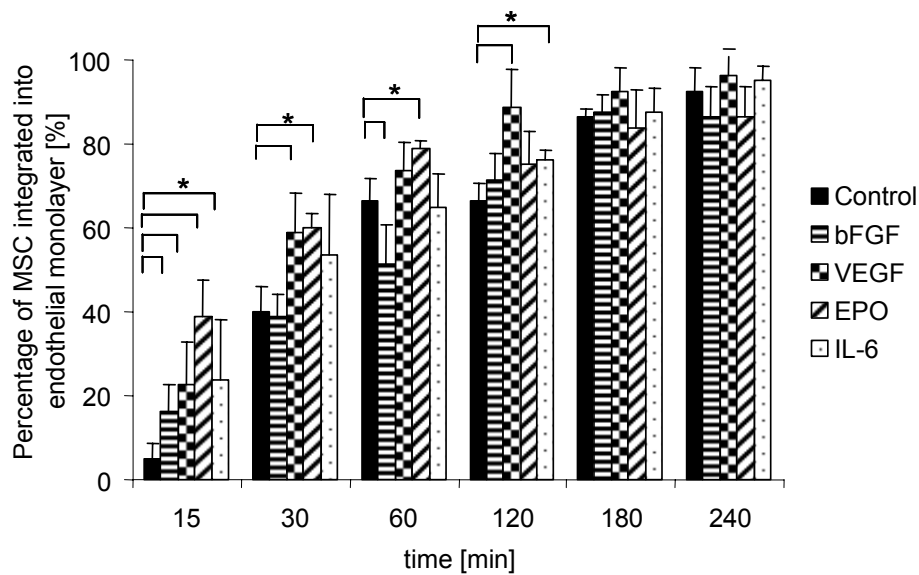
Figure 23: Cytokines influence the transmigration of MSCs at early time points

Influence of bFGF, VEGF, EPO and IL-6 on the integration of MSCs co-cultivated with MACS monolayer. After 15 minutes, all cytokines accelerated the integration of MSCs. VEGF significantly increased integration for up 120 minutes and EPO for up to 60 minutes. However, bFGF did not affect the integration of MSCs.

* significant difference compared to control (p < 0.05).

3.8 Role of nitric oxide for the transmigration of MSCs

To substantiate the role of nitric oxide synthase (NOS) and nitric oxide (NO) on the interaction of MSCs and endothelial cells, co-cultivations with the NO-donor DETA NONOate and the NOS-inhibitor L-NAME were conducted. Figure 24 summarizes the results of the co-cultures. DETA NONOate significantly increased the integration of MSCs into endothelial monolayers at the time points 15 and 30 minutes. Throughout the whole time series the addition of L-NAME slowed down the process of integration (Percentage of integrated MSCs after 15 minutes: control: 5 ± 3%; DETA NONOate: 38 ± 10%; L-NAME: 0 ± 0%; after 30 minutes: control: 21 ± 6%; DETA NONOate: 59 ± 11%; L-NAME: 1 ± 2%; after 60 minutes: control: 65 ± 5%; DETA NONOate: 64 ± 7%; L-NAME: 24 ± 9%).
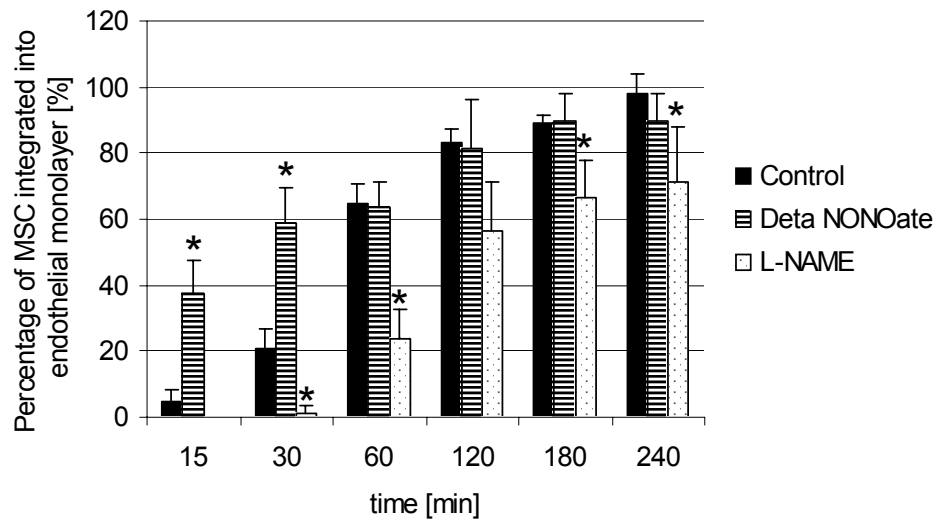
Figure 24: Co-cultivation under the influence of NO-donor and NOS-inhibitor

Influence of DETA NONOate and L-NAME on the integration of MSCs co-cultivated with a MACS monolayer. After 15 and 30 minutes, the NO-donor DETA NONOate accelerated the integration of MSCs. Throughout the whole time series the NO-inhibitor L-NAME reduced the integration.

* significant difference compared to control ($p < 0.05$).

Changes of NO-release were investigated by measurements using the fluorescent NO-indicator DAF. Therefore, red-labeled MSCs (PKH26) were cultivated solitarily or co-cultivated with MACS endothelial cells. NO-release was measured in MSCs cultivated solitarily, in MSCs which were in contact with endothelial cells, in endothelial cells cultivated solitarily and in endothelial cells which were in contact with MSCs. Experiments with the NO-inhibitor L-NAME served as controls. Figure 25 summarizes the results and Figure 26 shows representative pictures of the DAF-measurements. On the one hand, MSCs in contact with endothelial cells produced a significantly higher amount of NO as compared to MSCs cultivated solitarily. On the other hand, the NO-release of endothelial cells was not affected by co-cultivation with MSCs. In general, the NO-release of endothelial cells was higher than the NO-production of MSCs.
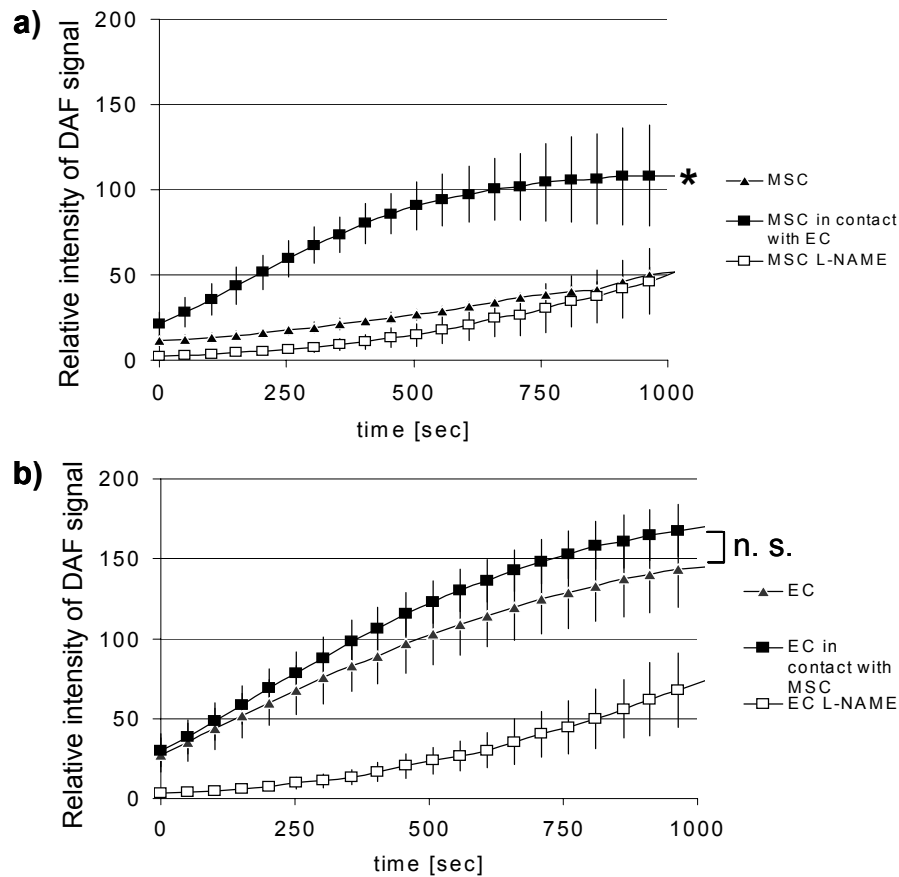
Figure 25: Changes in intracellular NO-levels caused by the co-culture of MSCs and endothelial cells

MSCs and endothelial cells (EC) were either cultured solitarily or in co-culture. The relative intensity of green fluorescence of intracellular DAF was measured over time. Experiments in the presence of L-NAME served as negative controls.

a) The relative intensity of DAF signal revealed a significant increase of the NO-release when MSCs were in contact with ECs as compared to experiments without ECs.

MSCs (▲), MSCs in contact with ECs (■), MSCs + L-NAME (□).

b) No significant difference in the NO-levels of ECs was measured when cells were in contact to MSCs or cultured solitarily.

ECs (▲), ECs in contact with MSCs (■), ECs + L-NAME (□).

* significant difference (p < 0.05), n. s.: no significant difference.
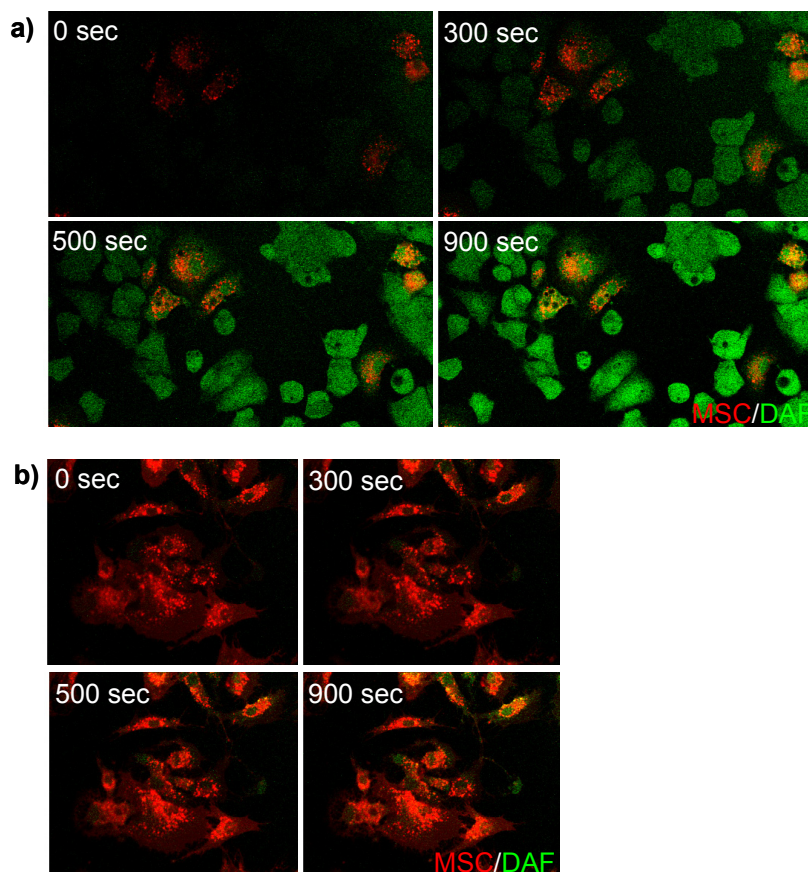
Figure 26: Representative pictures of DAF measurements

a) Pictures of red-labeled MSCs (PKH26) in contact with endothelial cells. High levels of NO-production indicated by green DAF signals were observed over time in MSCs contacting endothelial cells.

b) Pictures of red-labeled MSCs (PKH26) cultivated solitarily. The intensity of green DAF signal was significantly lower.

Magnification: 63x.

3.9 Influence of reactive oxygen species on transmigration of MSCs

To evaluate the role of reactive oxygen species (ROS) on the interaction of MSCs and endothelial cells, co-cultivations in presence of H_2O_2 and the ROS-scavenger N-acetylcysteine were conducted. Figure 27 summarizes the results of the co-cultures. Exposure to H_2O_2 tended to result in a decrease of integration whereas N-acetylcysteine tended to increase the integration of MSCs into endothelial monolayer (Percentage of integrated MSCs after 60 minutes: control: 60 ± 16%; H_2O_2: 41 ± 2%; N-acetylcyteine: 85 ± 10%).
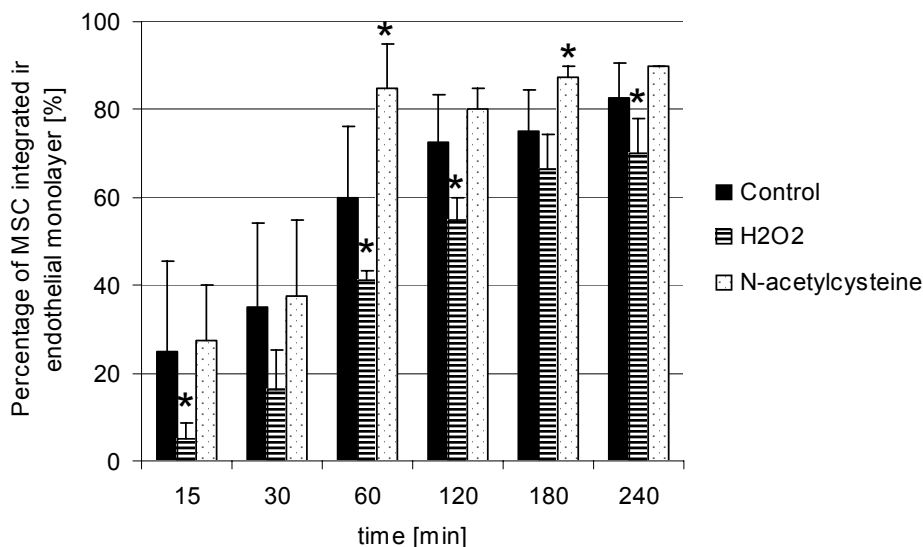
Figure 27: Co-cultivation under the influence of H_2O_2 and a radical scavenger

Influence of H_2O_2 and N-acetylcysteine on the integration of MSCs co-cultivated with MACS endothelial monolayer. After 15, 60, 120 and 240 minutes H_2O_2 reduced the integration of MSCs. N-acetylcysteine accelerated the integration after 60 and 180 minutes.

* significant difference compared to control ($p < 0.05$).

Changes of ROS-release, such as peroxynitrite, were investigated by measuring fluorescence of the ROS-indicator APF. Therefore, red-labeled MSCs (PKH26) were cultivated solitarily or co-cultivated with endothelial cells. ROS-release was measured in MSCs cultivated solitarily, in MSCs which were in contact with endothelial cells, in endothelial cells cultivated solitarily and in endothelial cells which were in contact with MSCs. Experiments with the ROS-scavenger N-acetylcysteine served as controls. Figure 28 summarizes the results and Figure 29 shows representative pictures of the APF-measurements. After a delay of 50 seconds, MSCs in contact with endothelial cells produced a significantly higher amount of ROS as compared to MSCs cultivated solitarily. The ROS-release of endothelial cells was also increased by co-cultivation with MSCs. In general, the production of ROS in MSCs was up to 4-times greater than in endothelial cells.
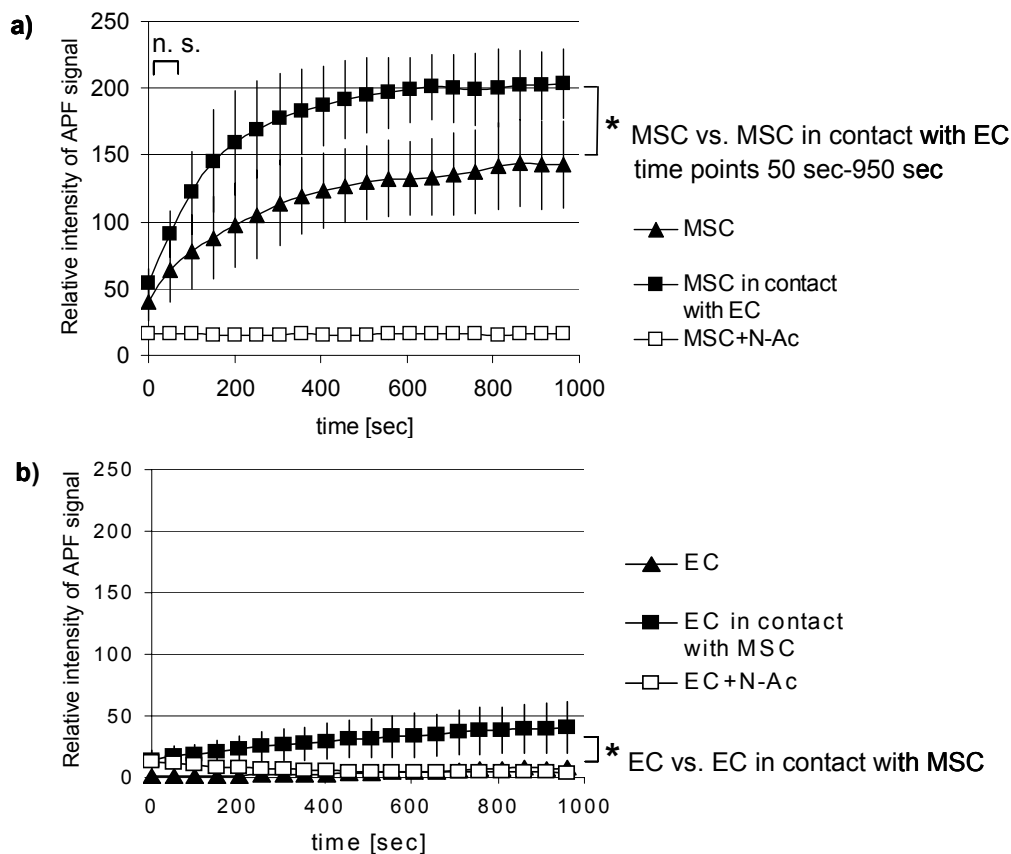
Figure 28: Changes in intracellular ROS-levels caused by co-culture of MSCs and endothelial cells

MSCs and endothelial cells (EC) were either cultured solitarily or in co-culture. The relative intensity of fluorescence of intracellular APF was measured over time. Experiments in the presence of N-acetylcysteine (N-Ac) served as negative controls.

a) The relative intensity of APF signal revealed a significant increase of ROS-release after a delay of 50 seconds when MSCs were in contact with ECs as compared to experiments without ECs.

MSCs (▲), MSCs in contact with ECs (■), MSCs + N-Ac (□).

b) A significant difference in ROS-levels of ECs was measured when cells were in contact to MSCs compared to ECs cultured solitarily. Note that ECs produce less ROS than MSCs.

ECs (▲), ECs in contact with MSCs (■), ECs + N-Ac (□).

* significant difference ($p < 0.05$), n. s.: no significant difference.
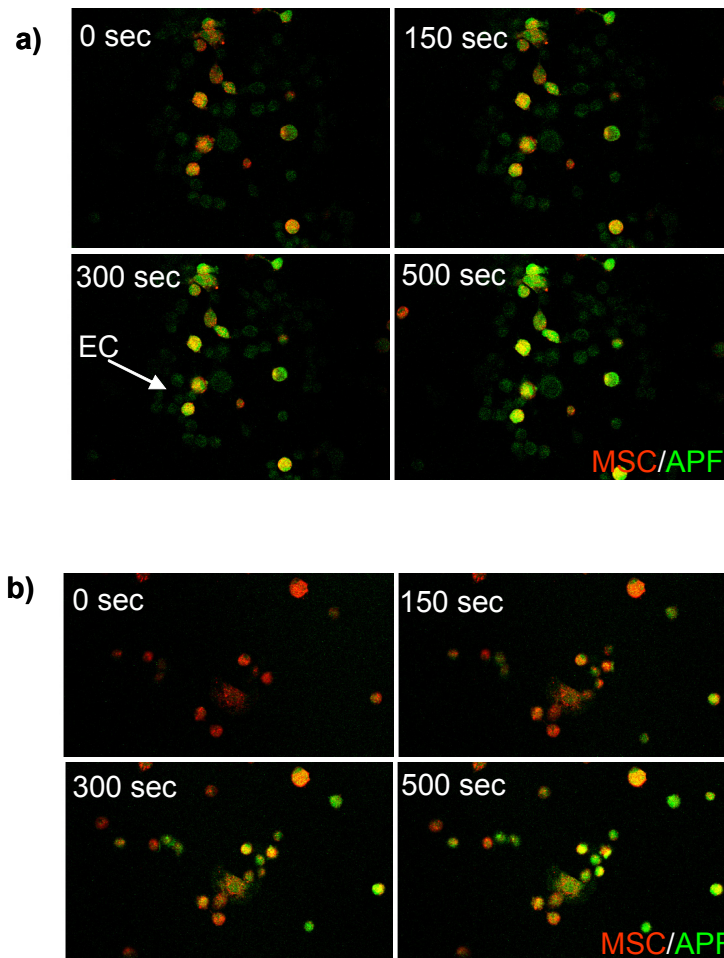
Figure 29: Representative pictures of APF measurements

a) Pictures of red-labeled MSCs (PKH26) in contact with endothelial cells (EC, arrow). A fast increase in ROS levels indicated by green APF signal was observed.

b) Pictures of red-labeled MSCs (PKH26) cultivated solitarily. The intensity of green APF signal was significantly lower.

Magnification: 63x.

3.10 Influence of adenoviral infection on the transmigration of MSCs

To study whether CXCR4 overexpression influences the transmigratory activity of MSCs an adenoviral gene transfer using the Ad.CXCR4.GFP adenovirus was performed.

3.10.1 Efficiency of MSC infection

To evaluate the efficacy of adenoviral infection on MSCs, MSCs were assessed by fluorescence microscopy 48 hours after infection. Figure 30 illustrates that with

increasing concentrations (MOI) of Ad.CXCR4.GFP significantly more infected MSCs were detected as indicated by their green fluorescence (Percentage of infected MSCs: MOI 0: 0%; MOI 20: 9 ± 3%; MOI 40: 27 ± 1%; MOI 60: 40 ± 1%; MOI 80: 55 ± 8%). Western blot analysis revealed that the expression of the CXCR4-protein was increased in a virus-concentration dependent manner.
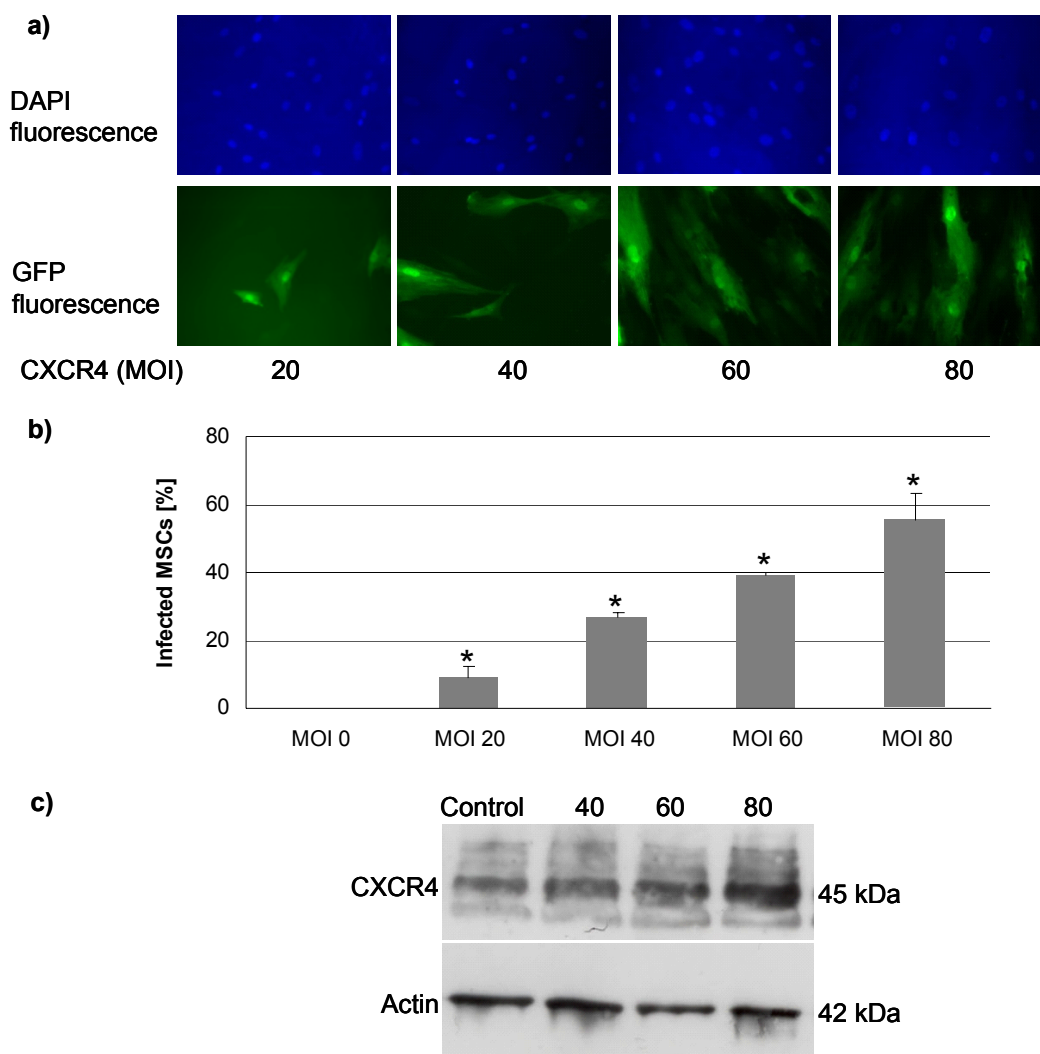
Figure 30:   Efficiency of adenoviral infection of MSCs

a) Adenoviral infection significantly increased the expression of CXCR4 on MSCs. GFP and DAPI fluorescence was visualized by fluorescence microscopy. The co-expression of GFP demonstrated visually that CXCR4 gene was expressed in the cells. Use of variable virus doses revealed significant increase in CXCR4-expressing MSCs with increased MOI. Magnification: 63x.

[continued on next page]

Legend to Figure 30, continued:

> b) The percentage of infected MSCs was determined as the number of GFP positive cells against the total number of cells counted by DAPI staining. The graph summarizes that there was a significant increase in CXCR4-infected MSCs even at the lowest MOI.
>
> * significant difference compared to MOI 0 ($p < 0.05$)
>
> c) Protein expression of CXCR4 in MSCs after adenoviral gene transfer with Ad.CXCR4.GFP demonstrated by western immunoblot analysis. Expression of CXCR4 in uninfected MSCs (control) versus MSCs infected with increasing virus doses (MOI 40, 60 and 80). The characteristic CXCR4 band of 45 kDa showed increasing intensities. The density of actin band (42 kDa) served as internal standard.

3.10.2 Decrease of migratory and transmigratory activity of MSCs by CXCR4-infection

The migratory activity of Ad.CXCR4.GFP infected MSCs was assessed in a migration Boyden Chamber assay in the presence of SDF-1β. Figure 31 summarizes the results. Interestingly, infection with Ad.CXCR4.GFP significantly decreased the migratory activity compared to control experiments using GFP-infected MSCs (number of migrated cells: CXCR4: 156.7 ± 25.6; GFP: 344.5 ± 92.0). SDF-1β significantly increased migration of GFP-MSCs (273.0 ± 71.0), but not of CXCR4-infected MSCs (204.3 ± 13.7).
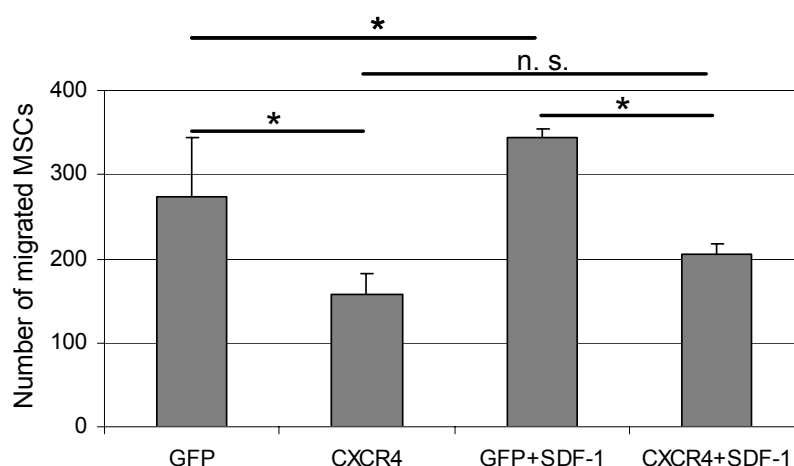
Figure 31:   Migratory activity of infected MSCs in the Boyden Chamber

> The number of migrated MSCs infected with Ad.CXCR4.GFP and as a control with Ad.GFP under the influence of SDF-1β. Infection with Ad.CXCR4.GFP significantly decreased the migratory activity compared to control experiments using GFP-infected MSCs. [continued on next page]

Legend to Figure 31, continued:

SDF-1β significantly increased migration of GFP-MSCs, but not of CXCR4-infected MSCs.

* significant difference (p < 0.05), n. s.: no significant difference.

To rule out the effect of CXCR4-overexpression on the transmigratory activity of MSCs isolated mouse heart perfusions were performed in the presence or absence of SDF-1β. Figure 32 illustrates that the rate of transmigration of MSCs infected with Ad.CXCR4.GFP was not increased by the addition of SDF-1β (Percentage of transmigrating MSCs: CXCR4: 33 ± 9%; CXCR4 + SDF-1β: 43 ± 4%; p>0.05). Also, the transmigratory activity of MSCs infected with the control adenovirus Ad.GFP was not significantly influenced by the addition of SDF-1β, but there was a higher tendency of enhancement (GFP: 31 ± 11%; GFP + SDF-1β: 47 ± 14%; p>0.05). Under standard conditions infection of MSCs either with Ad.GFP or with Ad.CXCR4.GFP did not significantly change the rate of transmigration as compared to uninfected wild-type MSCs (38 ± 11%).
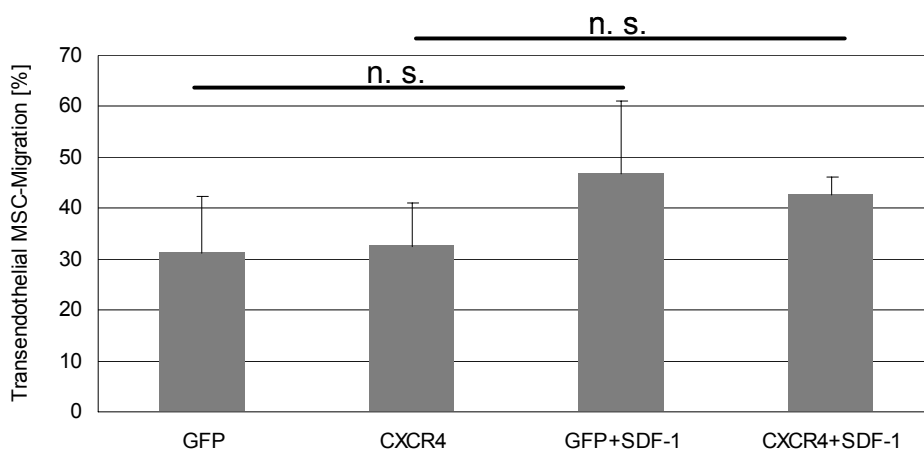
Figure 32: Transmigration of infected MSCs in isolated mouse heart perfusions

Transmigration of infected MSCs with Ad.CXCR4.GFP and as a control with Ad.GFP under the influence of SDF-1β. Perfusion of isolated mouse hearts in the presence of SDF-1β did not increase the transmigration of GFP-infected nor of CXCR4-infected MSCs.

n. s.: no significant difference.

3.11 Manipulation of MSC transmigration and attraction *via* focussed ultrasound-mediated microbubble stimulation (UMS)

To evaluate the impact of focussed ultrasound-mediated microbubble oscillation and destruction on the transmigratory activity of MSCs a series of *in vivo* experiments were conducted.

3.11.1 Placement of catheter

To characterize cell interactions with myocardial endothelium fluorescently labeled MSCs were transplanted into native and ischemic rat hearts *via* percutaneous delivery using an aortic root catheter. For optimal cell delivery into the left-ventricular myocardium the catheter tip was placed with ultrasound-guidance into the aortic root. Before cell transfusion the functionality of the catheter concerning coronary and microcirculatory delivery was confirmed with contrast echocardiography (see Figure 33).

3.11.2 Efficiency of focussed UMS

The efficiency of focussed ultrasound-mediated microbubble stimulation (UMS) was tested *via* ultrasound imaging. Figure 34 shows representative m-mode images which revealed complete left-ventricular contrast destruction and consecutive replenishment of contrast microbubbles.
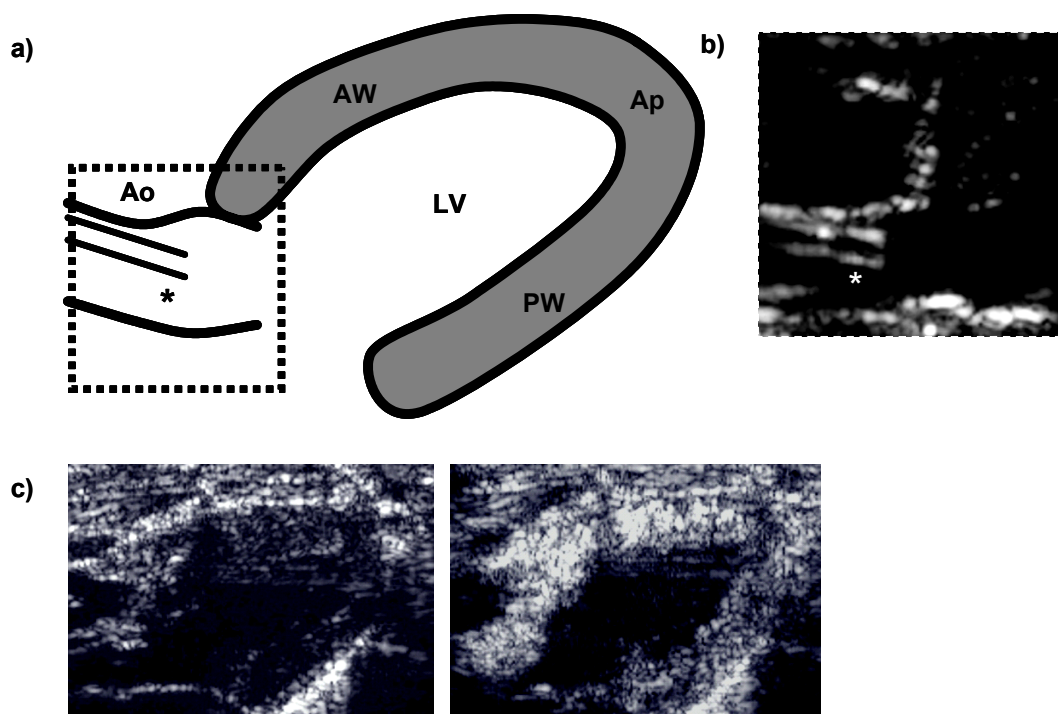
Figure 33: Percutaneous myocardial delivery *via* aortic root catheter

a) Scheme of echocardiographic parasternal long-axis view. AW - anterior wall, PW - posterior wall, Ap - apex, LV - left-ventricular cavity, * - catheter tip. For ultrasound-picture of the framed area see b).

b) For *in vivo* experiments the catheter tip (*) was placed with ultrasound-guidance into the aortic root.

c) Before cell transfusion the functionality of the catheter concerning coronary and microcirculatory delivery was confirmed with contrast echocardiography. Representative parasternal long axis view before (left panel) and after (right panel) application of a SonoVue-microbolus revealed good opacification of the left-ventricular myocardium.
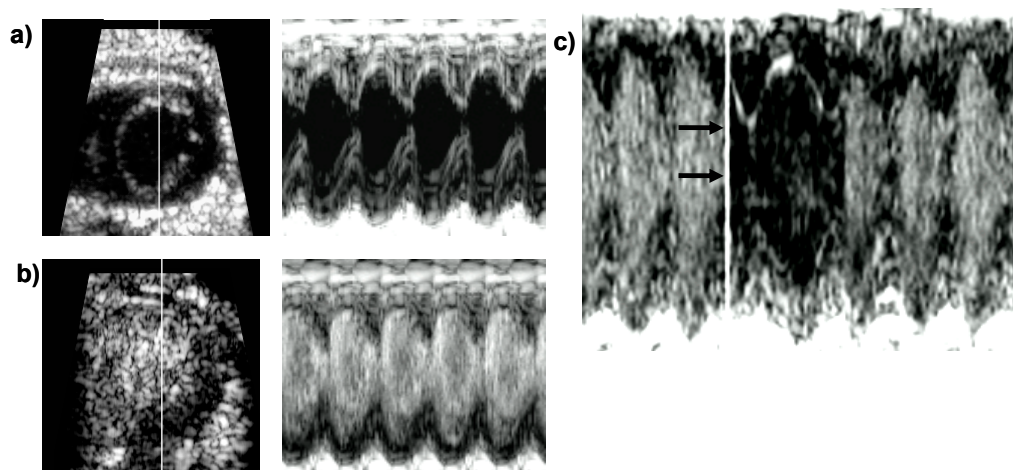
Figure 34: Focussed ultrasound-mediated microbubble stimulation (UMS)

a) and b) Target tissue was visualized in m- (right panel) and b-mode (left panel) before (a) and during (b) i.v. contrast enhancement. UMS-pulses were applied at contrast-opacified myocardium.

c) Arrows indicate UMS-induced sound-interference during high-resolution imaging, complete left-ventricular contrast destruction and consecutive replenishment of contrast microbubbles could be obtained during m-mode imaging.

3.11.3 Impact of UMS on MSC cell attraction

To evaluate the effect of UMS on the attraction of MSCs to myocardium the total number of MSCs per heart slide was quantified. Non-ischemic, native myocardium revealed the lowest cell infiltration (3.0 ± 1.1 MSCs/slide). UMS nearly doubled the total MSC cell count in non-ischemic myocardium (5.4 ± 2.2 MSCs/slide).

Moreover, regional analysis of the anterior wall in non-ischemic myocardium revealed an increase of MSC cell count in the anterior wall (focus of UMS) after UMS as compared to non-insonicated hearts reaching the level of significance (4.0 ± 1.2 vs. 2.2 ± 0.6 MSCs/slide, $p<0.05$). MSC cell count within the anteroseptal myocardial borderzone was significantly higher after myocardial ischemia as compared to non-ischemic myocardium (9.5 ± 3.7 MSCs/slide, $p<0.05$). Similar to native myocardium UMS induced a significant increase of MSC infiltration in the anteroseptal myocardial borderzone (focus of UMS) in ischemic tissue (13.1 ± 4.6 MSCs/slide, $p<0.05$). Furthermore, the anteroseptal myocardial borderzone (focus of UMS) revealed significantly higher absolute MSC count as compared to the posterolateral borderzone of insonicated rat hearts. Figure 35 and Figure 36 summarize the results.

For approximation of myocardial transplantation efficacy the absolute MSC amount per rat heart can be estimated as follows: the average length of a rat's left ventricle is 12 mm, in conclusion approximately 480-times wider than an average MSC (approximately 25 µm). To calculate correct volumetric measurements the area-length method is validated for estimation of left-ventricular volumes (Ghanem *et al.*, 2006). Therefore, multiplication of area and length of the cylindrical shape of the left ventricle needs to be multiplied by 5/6. For example, 9.5±3.7 MSCs were counted per representative slide in ischemic, non-insonicated myocardium (group C), resulting in approximately 5/6 * 9.5 * 480 = 3.800 MSCs counted per left-ventricle normalized to 100.000 transplanted MSCs. The corresponding results for the other groups are: for non-ischemic, non-insonicated myocardium (group A) 880 MSCs, for non-ischemic, insonicated myocardium (group B) 1.600 MSCs and for ischemic, insonicated myocardium (group D) 5.240 MSCs.
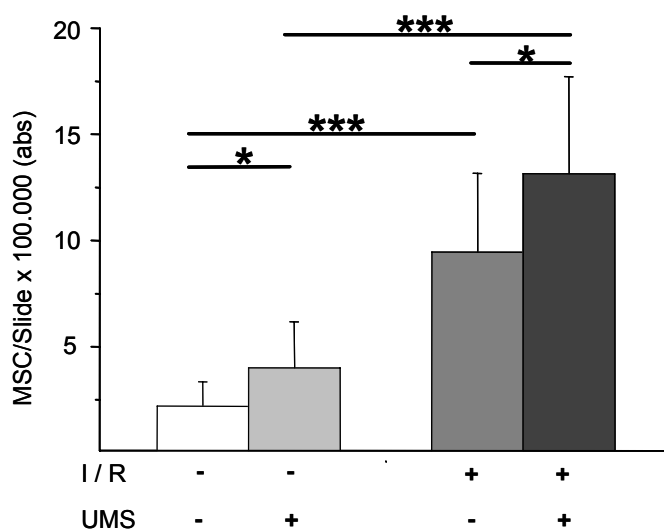
Figure 35: Focussed UMS enhanced cell attraction

The graph summarizes the regional (anterior wall) analyses of MSC cell counts per heart slide. Compared to native tissue, baseline cell attraction was higher in the anteroseptal myocardial borderzone of ischemic myocardium. Myocardial MSC count of the target tissue was significantly increased after UMS in non-ischemic and ischemic myocardium (I/R). Significant differences: * $p < 0.05$, ** $p < 0.01$, *** $p < 0.001$
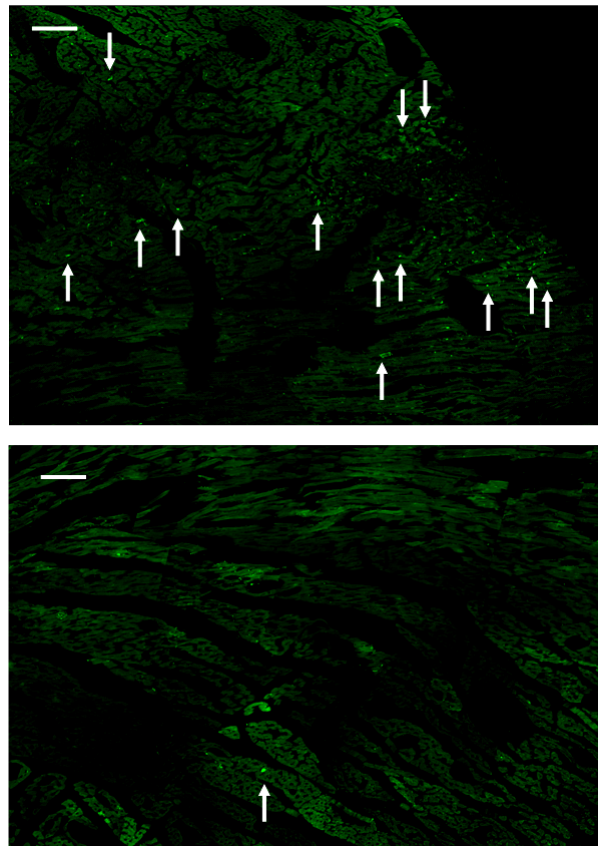
Figure 36:   UMS preconditioning increased MSC cell attraction

Representative collages of high-resolution fluorescence micrographs demonstrated significantly higher myocardial MSC count in the anterior wall after preconditioning with UMS (upper panel) in comparison to control tissue without UMS (lower panel). Arrows highlight green labeled MSCs. Original magnification: 20x. Scale bar: 100 μm

3.11.4 Transmigration

As second part of the engraftment cascade transendothelial migration was quantified *in vivo* in native as well as in ischemic rat hearts with and without UMS insonication. Initial results revealed endothelial adhesion of MSCs, but no signs of transmigration after 30 and 60 minutes (0% each). Therefore, the perfusion time was extended to 120 minutes. Figure 37 illustrates that after 120 minutes transendothelial migration of MSCs was significantly enhanced by UMS in native and ischemic myocardium. 41 ± 3% of the MSCs demonstrated migration across the endothelial barrier of native myocardium. Ischemic myocardium revealed a significantly higher level of transendothelial migration (53 ± 6%, p<0.01). The rate of transmigrating MSCs was facilitated significantly after focussed preconditioning with UMS in non-ischemic

myocardium (50 ± 6%, p<0.05). UMS revealed significant enhancement of transmigration of MSCs in ischemic myocardium as well (64 ± 9%, p<0.01; see Figure 37).
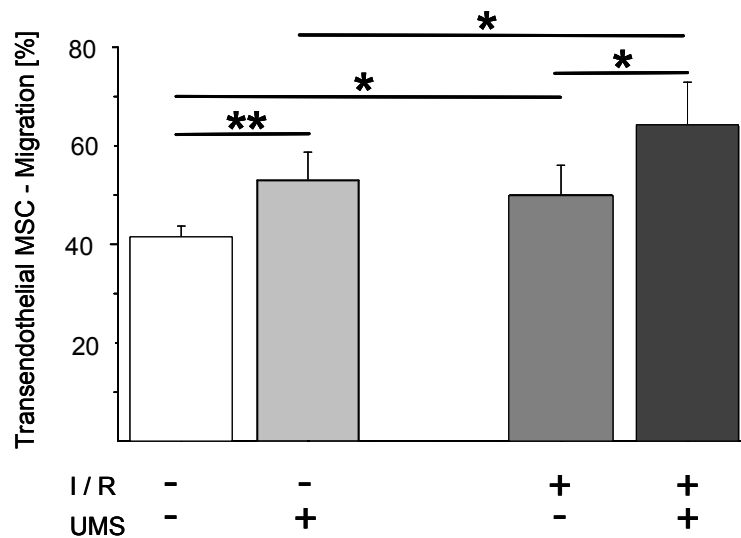
Figure 37:   Focussed UMS enhanced transendothelial migration

> The graph summarizes the percentage of transmigrated MSCs after 120 minutes. Transmigration of MSCs was significantly enhanced by UMS in native as well as in ischemic myocardium (I/R). Significant differences: * p < 0.05, ** p < 0.01

3.11.5 Influence of UMS on endothelial structure, basal lamina, cytokines and apoptosis

The impact of UMS on the basement membrane was further assessed, due to the fact that its invasion represents the final step of cell engraftment. Laminin distribution demonstrated an inhomogeneous pattern in insonicated myocardium (see Figure 38b). Moreover, the total content of laminin in non-ischemic myocardium receiving UMS was decreased in immunofluorescent stainings. This finding was confirmed by western blot (Figure 38c). Here, tissue lysates of anterior walls after UMS treatment contained less immunoreactive laminin than untreated probes. However, myocardial endothelium of insonicated regions remained intact. Interestingly, in some cases its surface looked increased in fluorescence microscopy (see Figure 39b). Ultrastructural analysis, however, revealed no alteration of endothelial cell-to-cell contacts and no destruction with respect to the basement membrane (see Figure 39c-k).
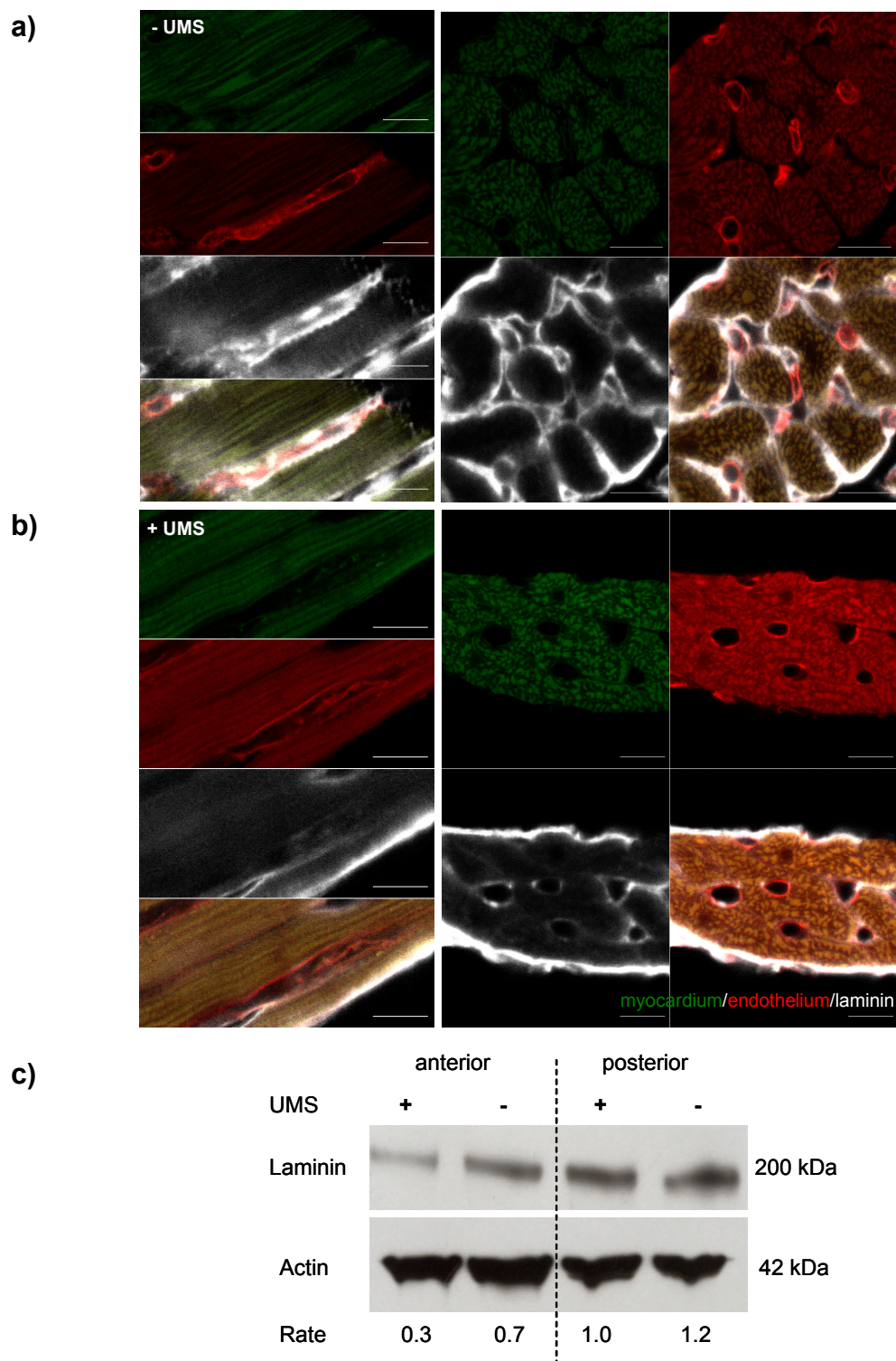
Figure 38: Alteration of the basal lamina

a) and b) Confocal images of immunohistochemical laminin staining revealed inhomogeneous distribution pattern and absolute reduction of the basal lamina 2 hours after UMS (b) compared to untreated controls (a). Note the undamaged endothelium. Green: myocardial autofluorescence, Red: endothelium (Rhodamine-*Griffonia simplicifolia* Lectin I), White: laminin (Cy5). Scale bar: 10 µm

Legend to Figure 38, continued:

c) Protein expression of laminin in anterior and posterior walls of untreated or UMS treated hearts demonstrated by western immunoblot analysis. After application of UMS to anteroseptal myocardium myocardial laminin content (shown is the characteristic laminin band of 200 kDa) was decreased. The density of the actin band (42 kDa) served as internal standard. Densitometric ratios of laminin/actin values validated the reduction of laminin content in the anterior wall induced by UMS.
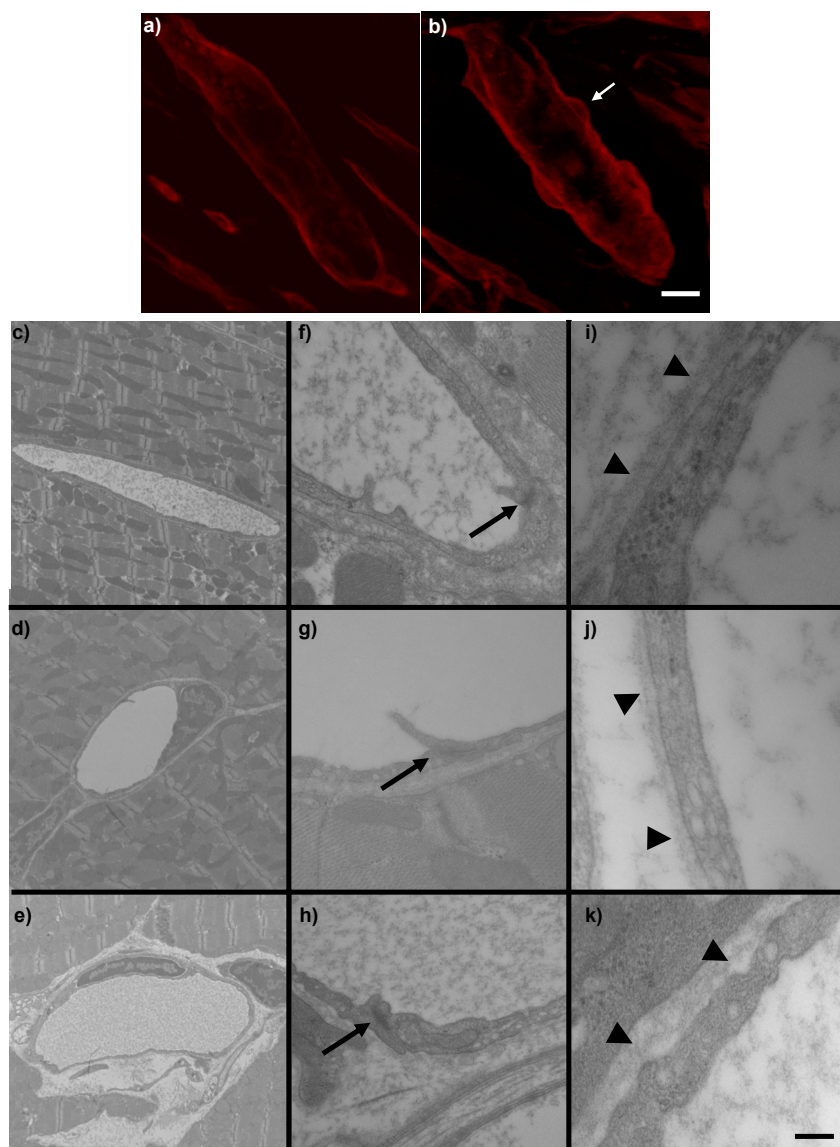
Figure 39: Morphology of the myocardial endothelium

a) Fluorescence microscopy of myocardial endothelium not pre-exposed to ultrasound-mediated destruction of microbubbles (UMS). Note the smooth and even surface of the endothelial wall.

b) After UMS the endothelium appeared more rough (bubbly, distended, swollen, bloated) and increased in its surface (arrow), but showed no signs of damage in its integrity. [continued on next page]

Legend to Figure 39, continued:

> Red: endothelium Rhodamine-*Griffonia Simplicifolia* Lectin I. Bar: 10 µm.
>
> c)-k) Electron micrographs of myocardium of the anterior left-ventricular wall treated with focussed ultrasound-mediated microbubble stimulation (UMS) (c,f,i) and untreated myocardium from posterior ventricular wall of the same heart (d,g,j) as well as from an untreated control heart (e,h,k). Hearts were harvested 2 hours after UMS application. Physiological vessel shape and structural integrity were obtained in treated (c) and untreated myocardium (d,e). No endothelial damage was visible at higher magnification; cell-cell-contacts (arrows) looked unchanged. Moreover, the morphological integrity of the basement membrane (arrowheads) remained intact after UMS.
>
> Scale bars: c-e: 2 µm; f-h: 250 nm; i-k: 100 nm.

Moreover, regional cytokine array analyses revealed a significant gradient of several cytokine levels between anterior myocardial tissue after focussed insonication in non-ischemic myocardium as compared to non-insonicated myocardial tissue. The amount of IL-1α in the anterior wall standardized on the amount in the posterior wall increased 2.2-fold after UMS compared to untreated tissue. In addition, the amount of IL-1β increased 3.8-fold, TNF-α 1.6-fold and GM-CSF 1.7-fold. IL-4, IL-6 and IL-10 were not detected in non-insonicated tissue, while insonicated myocardium contained these cytokines.

Eosinophily of cardiomyocytes, capillary rupture and erythrocyte extravasation could not be observed histologically as signs of UMS-induced mechanical bioeffects. Increased rate of apoptotic cardiomyocytes and myocardial endothelium could be ruled out with TUNEL assays. No increase in TUNEL^{+} cells was detected within regions of the myocardium pre-treated with UMS as compared to control myocardium and tissue outside the UMS focus (see Figure 40).
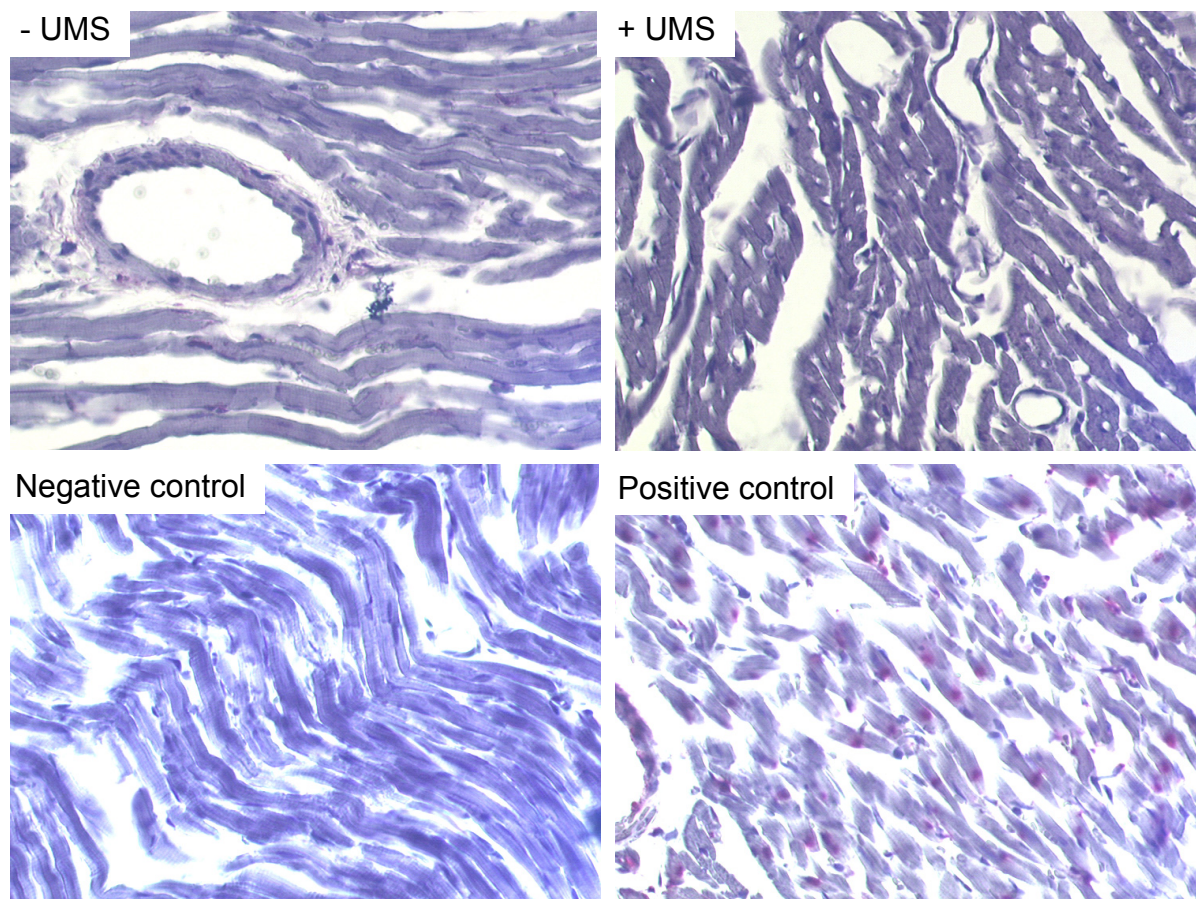
Figure 40: TUNEL assay of myocardium under the influence of UMS

No increase in TUNEL^{+} cells (pink staining) was detected within regions of the myocardium pre-treated with UMS as compared to control myocardium and tissue outside the UMS focus. Negative controls were incubated in the absence of terminal desoxynucleotidyl-transferase. Positive controls were treated with DNAse. Magnification 20x.

Additionally, after UMS – focussed on anteroseptal myocardium – gelatinase activity was regionally increased in vessels within the anteroseptal, but not in vessels within the posterolateral myocardium (see Figure 41).

anterior   posterior

- inhibitor

+ inhibitor
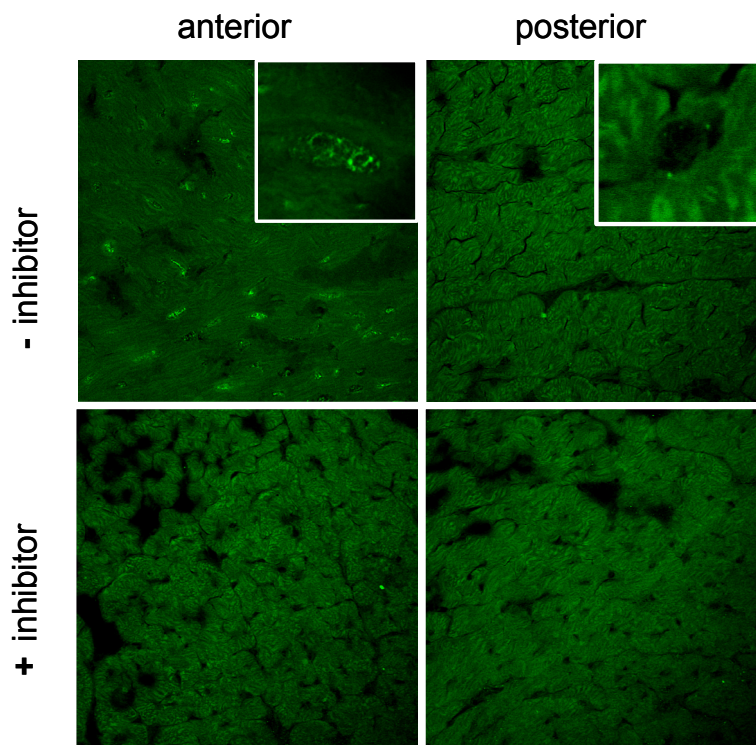
Figure 41: Induction of gelatinase activity by UMS

In situ zymography of non-ischemic murine cardiac tissue clearly showed the presence of active gelatinases (green fluorescence) in vessels within the anteroseptal wall after focussed UMS insonication. No gelatinase activity was detected in the untreated posterior myocardium. In control experiments 1,10-phenanthroline (inhibitor) prevented gelatinase activity. Small pictures illustrate one vessel at higher magnification.

4. Discussion

The use of mesenchymal stem cells (MSCs) for cellular replacement therapy has emerged as a novel strategy for the treatment of a variety of diseases. The systemic delivery by intravenous or intracoronary injection facilitates a minimal-invasive administration of MSCs. However, the prerequisite for a successful systemic stem cell therapy is that MSCs exit the blood circulation and home into the target tissue. This vascular recruitment of MSCs comprises (1) the cell attraction, (2) the rolling of MSCs along the endothelium, (3) the firm adhesion, (4) the transmigration of MSCs across the endothelial barrier and finally (5) their invasion into the target tissue. To date, the mechanisms underlying the two final steps – transmigration and invasion – of the homing of MSCs from the vasculature to the desired tissue are poorly understood. However, elevating our knowledge on these core processes might help to optimize stem cell based therapies. Therefore, the first part of the present study focussed on characterizing some of the key mechanisms involved in transmigration and invasion of MSCs. The second part of the study investigated two possible options for enhancing the efficiency of MSC-based therapy. First, the genetic manipulation of MSCs by infection with a CXCR4 overexpressing adenovirus and second, the selected pretreatment of endothelium by a novel technique using ultrasound-mediated microbubble stimulation.

4.1 Characterization of MSCs

Prior to the experiments MSCs were routinely subjected to defined quality controls. By microscopic assessments cultured MSCs appeared fibroblastic-like and homogenous in size and morphology by the second passage. It was, however, important to prove with different approaches that the plastic-adherent expanded human cells possessed the described characteristics of MSCs. Therefore, flow cytometry, colony-forming unit assays as well as three differentiation assays were performed.

Flow cytometry was used to determine the surface molecules in the expanded cell population. Hematopoietic cells were discriminated by at least one of the following markers: CD14 (expressed on monocytes and macrophages), CD34 (expressed on hematopoietic progenitor cells) or CD45 (leukocyte-common antigen). The most frequently used set of markers to detect MSCs are SH2 and SH3 (Pittenger *et al.*,

1999). Theses antibodies recognize CD105 (endoglin) (Barry *et al.*, 1999) and CD73 (ecto-5´-nucleotidase) (Klinz *et al.*, 2005). Both antigens are constitutively expressed on MSCs, but also on endothelial cells (Gougos *et al.*, 1988; Airas *et al.*, 1995). In light of this fact, for the present study a combination of CD105 and CD106 (VCAM-1) was preferred as markers (Klinz *et al.*, 2005; Schmidt *et al.*, 2006a; Schmidt *et al.*, 2006b). CD106 is constitutively expressed on MSCs (Pittenger *et al.*, 1999), whereas endothelial cells are negative for CD106 and only become positive by cytokine induction during inflammation (Osborn *et al.*, 1989).

For example a representative flow cytometric analysis demonstrated that in the second passage 64.5% of all cells were double positive for CD105 and CD106 and additionally triple negative for CD14, CD34 and CD45 (section 3.1). This indicated that most of the cultured cells expressed surface markers of mesenchymal lineages, but not the selected hematopoietic markers and therefore could be referred to as MSCs. However, in the above example about one third of the cultivated cells did not comprise the predicted surface characteristics. One possible reason is a contamination of the culture with hematopoietic cells. Although, the ability of MSCs to adhere to plastic surfaces is an accepted defining feature of these cells (Docheva *et al.*, 2007), it should be kept in mind that pre-B-cell progenitor cells and granulocytic/monocytic precursor cells also show plastic adherence (Phinney *et al.*, 1999). Furthermore, MSCs do not possess a unique marker that can be reliably used for their identification (Docheva *et al.*, 2007). Also, controversy about the surface characteristics of MSCs still exists (Docheva *et al.*, 2007). Therefore, one cannot strictly exclude that in the above example the remaining percentage (35.5%) of the cultured cells still represented MSCs even though they expressed a different set of surface markers. These remaining cells might form a stem cell subpopulation which does not comprise the whole predicted surface characteristics of MSCs. Therefore, multiple research groups refer their expanded cells to as bone marrow mononuclear stem cells (Strauer *et al.*, 2001; Strauer *et al.*, 2002; Perin *et al.*, 2003; Tse *et al.*, 2003a; Imada *et al.*, 2005; Li *et al.*, 2005a; Sasaki *et al.*, 2006; Kaminski *et al.*, 2007). However, all of the cells which were microscopically evaluated in the present study held the typical MSC morphology and size and could therefore reliably be termed MSCs. Furthermore, the observed amount of MSCs in culture was comparable to results of previous flow cytometric reports (Pittenger *et al.*, 1999; Klinz *et al.*, 2005; Schmidt *et al.*, 2006a; Schmidt *et al.*, 2006b).

Although, most of the isolated MSCs expressed characteristic surface markers and showed fibroblastic morphology the functionality of the stem cells needed to be confirmed. Therefore, the abilities of the MSCs to produce daughter cells as well as to differentiate into multiple phenotypes had to be assayed (Pittenger and Martin, 2004). First, to evaluate their expansion capacity, colony-forming unit assays were performed. Here, single cells continued to divide and thereby formed clonal cell colonies which determined the proliferation potential of the MSCs. However, differences in the expansion potential of MSCs derived from different donors existed. With increasing age the growth capacity of MSCs seemed to decrease. This is consistent with the findings of other research groups. For example, Majors *et al.* demonstrated that although MSCs are present throughout lifetime, their total number is inversely correlated to the age of the donor and depends upon the site of extraction and the systemic disease state of the patient (Majors *et al.*, 1997).

Second, the multi-lineage differentiation potential of isolated and cultured MSCs was assayed by culturing the cells under conditions favourable for adipogenic, osteogenic and chondrogenic differentiation. *In vitro* adipogenic induction of MSCs required specific supplementations, including dexamethasone and indomethacin (Tuan *et al.*, 2002). Indomethacin, a non-steroidal anti-inflammatory drug, binds to and activates the transcription factor peroxisome proliferator-activated receptor gamma (PPAR-γ), which is crucial for adipogenesis (Lehmann *et al.*, 1997). During osteogenesis treatment with the synthetic glucocorticoid dexamethasone stimulated the proliferation of MSCs and supported their osteogenic lineage differentiation (Liu *et al.*, 2002). Organic phosphates, such as β-glycerophosphate, also supported osteogenesis by playing a role in the mineralization and modulation of osteoblast activities (Chung *et al.*, 1992). The induction of chondrogenesis in MSCs depends on the coordinated activities of many parameters, including the cell density and various growth factors (Tuan *et al.*, 2002). Therefore, culture conditions conductive for chondrogenic induction of MSCs required high-density pelleting of the cells and growth in serum-free medium containing regulatory factors such as TGF-β which increased the amount of matrix proteoglycan produced (Sekiya *et al.*, 2001; Tuan *et al.*, 2002). In the present study, the three differentiation assays revealed that the cultured MSCs easily differentiated into adipocytes, osteocytes and chondrocytes, which served as representative mesenchymal cell lineages.

Of particular importance for the growth and differentiation potential of MSCs was the lot of fetal calf serum (FCS) selected for the MSC growth medium (Martin *et al.*, 1997). It became obvious that different charges of FCS had a strong impact on MSCs in culture. Alas, since the growth requirements of MSCs are not fully understood, a serum-free medium with defined growth factor composition has not been developed yet (Pittenger and Martin, 2004).

To summarize, the isolation technique used for the present study resulted in a population of MSCs with required surface characteristics, high expansion as well as differentiation potential. These reproducible characteristics which are obtained in many different research laboratories qualify MSCs as good candidates for a therapeutic usage (Pittenger and Martin, 2004).

4.2 Discussion of the morphological aspects and time course of MSC transmigration

The endothelium forms the main barrier for the passage of macromolecules and cells from the blood to the surrounding tissues. A prerequisite for a successful systemic therapeutic usage of MSCs is that the cells exit the blood circulation *via* transmigration across the endothelium and subsequently invade their target tissue. To understand the underlying mechanisms and to describe the morphology of transmigration and invasion in detail co-culture experiments, three different three-dimensional model systems as well as *in vivo* experiments were established.

4.2.1 Co-culture experiments

The co-culture experiments demonstrated that MSCs quickly flattened and integrated into a confluent endothelial monolayer. The integration was accompanied by morphological changes of the MSCs, especially the formation of long plasmic podia. Endothelial cells even started to grow on top of the MSCs to seal their confluent monolayer (see Figure 11).

In a previous work of our laboratory, different staining methods were used for the co-culture experiments of MSCs and endothelial cells (Schmidt *et al.*, 2006b). Here, MSCs were stained using PKH67 whereas endothelial cells either remained unstained or were stained *via* immunohistochemical detection of platelet-endothelial

cell adhesion molecule (PECAM)-1. On the one hand, working with unstained endothelial monolayer did not allow an analysis of the status of MSC integration. On the other hand, the staining of endothelial cells by the antibody PECAM-1 prior to co-cultivation may have affected the natural interaction of surface molecules. Thus, for the present study another technique for visualizing MSCs and endothelial cells was established. Staining the cells with CellTracker Green and Red respectively fulfilled all requirements (section 2.3.2). The CellTracker staining technique was easy to handle and facilitated a more stable and durable staining of the cells; PKH67 was emitted into the media and the surrounding cells at the latest after three hours in co-cultivation experiments. Furthermore, as described by the manufacturer PKH67 anchors into the cell membrane thereby causing a dotted staining. In contrast, by using the CellTracker labeling the cell margins and even very thin plasmic podia were clearly definable. As described by the manufacturer CellTracker reagents are fluorescent chloromethyl derivatives which freely diffuse through the membranes of living cells. Once inside the cell, these mildly thiol-reactive probes undergo a glutathione S-transferase-mediated reaction to produce membrane impermeable glutathione-fluorescent dye adducts. Moreover, the peptide-fluorescent dye adducts contain amino groups and can therefore be covalently linked to surrounding biomolecules by fixation. This property permitted long-term storage of the labeled co-cultures.

Numerous studies have used co-cultivation experiments to investigate the interaction of two cell types (Pawlowski *et al.*, 1988; Maschio *et al.*, 1996; Alter *et al.*, 2003; Schmidt *et al.*, 2006b; Bauer *et al.*, 2007). Advantages of co-cultivation experiments are that they are feasible to handle, easy to reproduce and that the experiments can be accomplished in large numbers. Therefore, in the present study co-culture experiments allowed to examine the effects of different conditions or substances on the interaction of MSCs and endothelial cells. Nevertheless, a major limitation of co-culture experiments is that MSCs and endothelial cell are more or less only able to interact with each other in a two-dimensional fashion, because MSCs are arrested by the coverslips underneath the endothelial monolayer. Thus, more complex model systems which mimicked the *in vivo* situation more closely than monolayer cultures were established to analyze the interaction of MSCs and endothelial cells three-dimensionally.

4.2.2 Three-dimensional model systems

First, to investigate the process of transmigration in a three-dimensional fashion, experiments with endothelial cell spheroids were designed. It is known that endothelial spheroids establish a two-compartment system consisting of a surface monolayer of differentiated endothelial cells and a center of unorganized cells (Korff and Augustin, 1998). The surface layer consists of a continuous monolayer with well-differentiated cell-cell contacts (Korff and Augustin, 1998). The co-culture experiments of MSCs with endothelial spheroids demonstrated that MSC came into contact with the spheroids after two hours, but MSCs still remained in a spherical shape. After four hours MSCs invaded into the inner mass of the spheroids by the extension of plasmic podia. However, these experiments were conducted in the presence of carboxymethyl cellulose. The cellulose facilitated the preservation of the spheroids, but also could affect the transmigratory activity of the MSCs. Therefore, additional three-dimensional models were established.

Second, to evaluate morphological aspects of the transendothelial migration of MSCs in the presence of extracellular matrix proteins, collagen invasion assays were performed. Collagen invasion assays are well established for the analysis of invasive tumor cells (Bauer *et al.*, 2007). Moreover, growth of HUVECs on a collagen gel matrix is known to promote the development of intercellular junctions (Pawlowski *et al.*, 1988), thus mimicking an intact endothelium. In our study, the collagen gel not only enabled the MSCs to integrate into the endothelial monolayer, but also to invade the matrix below the monolayer. Again after two hours, MSCs came into contact with the endothelial monolayer still retaining a spherical shape. Later, MSCs integrated into the monolayer, transmigrated and invaded the collagen gel. These processes were accompanied by the formation of plasmic podia. From ultrastructural analysis co-culture experiments of monocytes and endothelial monolayers on collagen gels it is known that monocytes first establish an extensive membrane contact with the surface of the endothelial cells (Pawlowski *et al.*, 1988). Here, the penetration of the monolayer also begins with the insertion of a pseudopod between two endothelial cells (Pawlowski *et al.*, 1988). Therefore, monocyte and MSC transmigration appear to hold similar morphological characteristics.

However, both model systems – co-cultivation experiments using endothelial spheroids as well as collagen invasion assays – did not reflect the complexity present

in a complete target organ. Therefore, *ex vivo* mouse heart perfusions were conducted to analyze the transmigration of MSCs in an isolated organ. The observed morphology of transmigrating MSCs was comparable to the other more simplified models. MSCs also penetrated the endothelial barrier *via* the insertion of plasmic podia. After 90 minutes of perfusion, more than one third of the MSCs started to transmigrate across the endothelium. However, no event of completed transmigration was noted. Thus, after 90 minutes parts of the cell bodies of the MSCs still resided inside the vessels, indicating that transmigration of MSCs is no rapid event. However, after longer perfusion times one would expect the MSCs to completely transmigrate. In contrast, for the transmigration of leukocytes it is known that this process can be accomplished within minutes (Marchesi *et al.*, 1960).

As already indicated by the two-dimensional co-culture experiments, the three different three-dimensional models revealed that the processes of penetration of the endothelial barrier and invasion of MSCs into the surrounding tissue were guided by the formation of plasmic podia. All model systems showed a time delay compared to the two-dimensional monolayer co-culture, emphasizing that the time course of interaction of MSCs and endothelial cells is depending on the complexity of the model system. In summary, microscopic assessment of different systems revealed that MSCs quickly came into contact with the endothelium, but still possessed a spherical shape. Subsequently, the MSCs penetrated the endothelial barrier and finally invaded the surrounding tissue. Transmigration and invasion of MSCs were accompanied by the insertion of plasmic podia. Recently, Ruster and co-workers characterized the rolling and adherence of MSCs on endothelial cells (Ruster *et al.*, 2006). They showed that both processes are accompanied by a rapid extension of plasmic podia. In accordance, the present study observed that the final step of penetrating the endothelial barrier was also guided by the insertion of plasmic podia. Furthermore, as it has been described for leukocytes (Wang *et al.*, 2006), the results presented here imply that MSCs use endothelial tri- or bicellular corners to transmigrate across the endothelial barrier.

4.2.3 Transmigration of MSCs *in vivo*

The reports of successful clinical trials especially for the infarcted heart indicate the transmigratory activity of MSCs. As described in section 3.2.2.3 the process of

transmigration of MSCs could be monitored *ex vivo* by performing isolated mouse heart perfusions. Thus far, no direct *in vivo* evidence for the transmigration of MSCs in the heart existed. The present study validated that MSCs indeed transmigrate *in vivo* under physiological conditions. This transmigration phenomenon was observed in native as well as in infarcted myocardium and possessed the same morphological characteristics as described for the other model systems. However, *in vivo* experiments demonstrated a slower process of transmigration kinetics as compared to the *ex vivo* and *in vitro* situation. *In vivo*, after 60 minutes no signs of beginning transmigration were monitored. Therefore, for *in vivo* cardiomyoplasty the hearts were harvested after 120 minutes. The deceleration of the transmigration process may partly be attributed to the blood flow and blood pressure as well as to the complexity of emerging events *in vivo*. Additionally, the experiments demonstrated that the number and concentration of MSCs can play a major role in coronary cell delivery. Experiments using different numbers of MSCs revealed that application of 500.000 MSCs into the aortic root – as used for *ex vivo* experiments – resulted in wall motion abnormalities and decrease in systolic function. These complications after the delivery of high MSC amounts were most likely due to ischemic events which could be explained best with intravascular cell aggregation and consecutive microembolisms. Therefore, the amount of MSCs applied during clinical trials should be evaluated carefully. For all *in vivo* cardiomyoplasty experiments of the present study the number of MSCs was reduced to 150.000. More results obtained under *in vivo* conditions will be discussed in section 4.9.

4.3 Integrins and their role in transendothelial migration

Integrins are known to play a key role in cell adhesion, migration and chemotaxis (Gao *et al.*, 1997; Werr *et al.*, 1998; Imhof *et al.*, 2004). An individual integrin receptor consist of two non-covalently bound subunits – α and β. Therefore, integrins are categorized as heterodimeric receptors (Docheva *et al.*, 2007). For example, the localization of leukocytes to extravascular sites of inflammation is accompanied by repeated adhesive and de-adhesive events along the endothelium (Lauffenburger *et al.*, 1996). The surface molecules very late antigen-4 (VLA-4, α4β1 integrin) and its most important ligand vascular cell adhesion molecule-1 (VCAM-1) are involved in leukocyte transendothelial migration (Ridger *et al.*, 2001). The VLA-4 antigen is

expressed by MSCs (Ip *et al.*, 2007). Recently, Ruster *et al.* verified that human MSCs bind to endothelial cells in a P-selectin dependent manner and that rolling of MSCs engage VLA-4/VCAM-1 to mediate their firm adhesion on the endothelial cells (Ruster *et al.*, 2006). In the present study, blocking experiments additionally identified VCAM-1 and VLA-4 as key receptors for the transendothelial migration of human MSCs (section 3.4). Taking these findings together MSCs not only require VCAM-1 and VLA-4 to firmly adhere to the endothelium, but also to transmigrate across the barrier.

Since the interaction of MSCs and endothelial cells was not completely blocked by anti-VCAM-1 and antibodies specific for the integrin α4-chain, it is possible that other integrin α-chains might be involved in the transmigration. Lately, it was confirmed that MSCs not only express integrin α4β1, but also other combinations of integrin subunits such as integrin α6β1, α8β1 and α9β1 (Ip *et al.*, 2007). Future studies should focus on identifying which additional integrins facilitate the process of MSC transmigration.

Moreover, immunohistochemistry confirmed that co-cultivation of MSCs with endothelial cells triggered a massive and distinct clustering of β1 integrins. Because integrins function as transmembrane linkers between the extracellular matrix and the actin cytoskeleton the integrin-mediated signaling regulates a variety of cellular events including migration and invasiveness (Ellerbroek *et al.*, 1999). For example, aggregation of integrin receptors is sufficient to induce a prompt transmembrane accumulation of a large class of at least 20 signal transduction molecules, including c-Src, c-Fyn, RhoA, Racl, Ras, GAP, MEK1, ERK1, ERK2 and JNK1. Furthermore, integrin occupancy and aggregation are required for integrin-induced accumulation of the cytoskeletal components F-actin, paxillin and filamin (Miyamoto *et al.*, 1995). In addition, aggregation of β1 integrins stimulates the activation of matrix metalloproteinase-2 (Ellerbroek *et al.*, 1999). Results about the key role of matrix metalloproteinase-2 for the invasion of MSCs will be discussed in section 4.4. To further evaluate this aspect future studies should focus on downstream effects of β1 integrin in the signal transduction and cytoskeleton organization of MSCs during transmigration. However, one could reasonably speculate that the massive clustering of β1 integrins in MSCs triggered by their co-cultivation with endothelial cells might effect the signal transduction and cytoskeleton organization of MSCs and thereby modulate their transmigratory activity.

Recent data suggested that MSCs may be mobilized from the bone marrow, migrate to the infarcted myocardium and differentiate into cardiac myocytes (Kawada *et al.*, 2004). Lately, it has been demonstrated that for intramyocardial trafficking of MSCs integrin β1 is crucial, but not integrin α4 (Ip *et al.*, 2007). Ip and co-workers demonstrated that injection of MSCs pretreated with blocking antibodies against integrin β1 (CD29) into the ischemic myocardium of mice reduced the intramyocardial migration of stem cells in the ischemic myocardium by 45% compared with control experiments. When using blocking antibodies against CD49d (integrin α4) no significant difference in the quantity of MSCs in the infracted myocardium was observed. These data suggest a crucial role of CD29 (integrin β1) in stem cell cardiac trafficking (Ip *et al.*, 2007). Consistent with these finding, a recent study showed that blockade of CD49d in endothelial progenitor cells did not affect their homing into ischemic sites in hearts or limbs (Qin *et al.*, 2006). However, as demonstrated in the present study, for the vascular transmigration of MSCs integrin α4 does plays a key role, thus pointing out that intravascular migration and vascular transmigration are two distinct processes which have to be distinguished.

4.4 Role of matrix metalloproteinases for the invasion of MSCs

A successful and efficient invasion of MSCs into a target tissue not only requires their transmigration across the endothelial barrier, but also across the basement membrane. The basement membrane is the first barrier encountered by all emigrating cells subsequent to the penetration of the vascular endothelial monolayer (Agrawal *et al.*, 2006). For transmigration of leukocytes it has been validated that integrin α4β1 on the surface of the leukocytes binds to VCAM-1 on the endothelial surface of inflamed vessels and subsequently induces matrix metalloproteinase (MMP)-2 expression in T cells (Graesser *et al.*, 2000). This mechanism is proposed to facilitate the invasion of leukocytes into the subendothelial matrix. The gelatinases MMP-2 and MMP-9 were identified as the major proteases active at sites of leukocyte infiltration into the brain parenchyma (Agrawal *et al.*, 2006).

Results of the present study obtained by ELISA validated on protein level that MSCs secreted active MMP-2, but not MMP-9. Therefore, in contrast to infiltrating leukocytes (Agrawal *et al.*, 2006) MSCs do not express MMP-9. Moreover, in the present study *in situ* zymography was used as technique to detect gelatinases in

tissue slides. Alternative methods such as immunohistochemistry and western blot do not provide information on the activity of proteases in the tissue because many of these enzymes are synthesized in an inactive or proenzyme form. Moreover, *in situ* zymography is a technique to specifically localize proteolytic activity in tissue sections (Yan *et al.*, 2003). Here, active gelatinases were located in the heart at sites of transmigrating and invading MSCs. This indicated that during invasion into cardiac tissue, MSCs secrete active proteinases – for instance MMP-2 –, which might be crucial for penetrating the basement membrane and invading the surrounding extracellular matrix. Indeed, MMP-2 has the capacity to degrade for example collagen IV, laminin and gelatine, major constituents of the basement membrane (De Becker *et al.*, 2007).

In accordance, a recent study demonstrated *in vitro* that bone marrow and cord blood derived mesenchymal stem cells from early up to late passages express MMP-2 and membrane type 1 MMP (MT1-MMP) mRNA (Son *et al.*, 2006). However, MMP-9 mRNA was not detected. Ries and co-workers analyzed bone marrow-derived human MSCs and detected strong expression and synthesis of MMP-2 and MT1-MMP as well, and, additionally, that of tissue inhibitor of metalloproteinase 1 (TIMP-1) and TIMP-2 (Ries *et al.*, 2007). The ability of MSCs to traverse reconstituted human basement membranes was effectively blocked in the presence of synthetic MMP inhibitors. RNA interference revealed that gene knock-down of MMP-2, MT1-MMP or TIMP-2 substantially impaired MSC invasion (Ries *et al.*, 2007). Furthermore, De Becker *et al.* showed in invasion assays that MSCs have the potential to migrate through bone marrow endothelium and that this process involves MMP-2 (De Becker *et al.*, 2007). By RT-PCR they demonstrated that MSCs express MMP-2 mRNA while no transcripts for MMP-9 were detected (De Becker *et al.*, 2007). Neutralizing MMP-2 with a blocking antibody or MMP-2 siRNA impaired the migration capacity of MSCs *in vitro*. A rewarding future task might be to discover whether MSC invasion into myocardium can be completely blocked by MMP inhibitors. One novel possibility to facilitate a regional activation of MMPs in the heart will be discussed in section 4.9.4.

4.5   Importance of the endothelial phenotype for transmigration

The endothelium, once viewed as homogenous mass of passive cells, is now appreciated to possess regionally specific phenotypic responses (Isenberg *et al.*, 2005). Therefore, in various regions of the vascular tree, the endothelium is functionally different and its barrier function varies accordingly (Dejana *et al.*, 1995). Recent advantages have been made in localizing specific endothelial cell subpopulations *via* surface expression mapping techniques (Demeule *et al.*, 2004; Schluesener *et al.*, 2004). Thus, different endothelial phenotypes hold functional differences (Dejana *et al.*, 1995). For example, variances in the amount of intercellular tight junctions exist at different points along the vascular tree and cause differences in the endothelial permeability. Human brain-derived endothelial cells have reduced levels of adhesion molecules under basal culture conditions and therefore represent a less permissive barrier to cell migration than human umbilical vein endothelial cells (Wong *et al.*, 1999). Furthermore, it has been reported that different phenotypes of endothelial cells produce different amounts of nitric oxide (Altland *et al.*, 2004). The results of the present study indicated not only that differences exist in the MSC transmigration capacity within the vasculature, but also that the morphology of MSCs during transmigration is strongly influenced by the endothelial phenotype. Coronary artery endothelium enabled the fastest MSC integration *in vitro* and resulted in the highest percentage of plasmic podia. In contrast, over time the transmigration of MSCs across venous endothelium was most efficient. Aortic endothelium facilitated the slowest transmigration of MSCs. Consequently, MSCs preferably transmigrated across venous and avoided transmigrating across the aortic endothelium. Thus, the results indicate that the transmigration and invasion efficiency of MSCs into different organs can vary in accordance with the surrounding type of vessels.

Contrary to our results obtained with human MSCs it has been reported that the adherence of rat MSCs to aortic endothelial cells and cardiac microvascular endothelial cells does not differ significantly (Segers *et al.*, 2006). This suggests that rat-derived MSCs – in contrast to human MSCs – do not discriminate between different endothelial phenotypes. Consistent with our results for MSC transmigration, it has been discussed for leukocytes that endothelial cells not only play an important

role in regulating the leukocyte attachment, but also actively modulate their diapedesis (Dejana *et al.*, 1996).

The observations presented in this study were obtained *in vitro* under static conditions without applying shear stress. Therefore, the observed differences of the time course of MSC interaction with different endothelial monolayers did not depend on variances of the shear rate, but were only influenced by the phenotype of the endothelial cells. *In vivo* different flow conditions within the blood circulation should also influence the transmigration efficiency. For example, the rolling of leukocytes is reduced by increasing shear rates (Bienvenu *et al.*, 1993) as is the adhesion of rat-derived MSCs to cardiac microvascular endothelium (Segers *et al.*, 2006). Future studies should try to elucidate the role of the endothelial phenotype for MSC transmigration *in vivo*.

4.6   Role of cytokines

Cytokines are known to increase the expression of adhesion molecules in endothelial cells (Mantovani *et al.*, 1992) and play a key role in the homing of hematopoietic stem cells (Yong *et al.*, 1998). Moreover, cytokines such as interleukin (IL)-6 and vascular endothelial growth factor (VEGF) are up-regulated after myocardial infarction (Ip *et al.*, 2007). A previous study of our laboratory validated that the migratory activity of MSCs is increased by cytokines, in particular basic fibroblast growth factor (bFGF), but also IL-6 and VEGF (Schmidt *et al.*, 2006a). Therefore, the present study focussed on the effect of cytokines on the transmigration of MSCs. It was demonstrated that in contrast to migration, transmigration was only marginally influenced by bFGF. After 15 minutes, bFGF, VEGF, erythropoietin (EPO) and IL-6 accelerated transmigration, whereas in the remaining experiments the process was mostly slowed down by bFGF. EPO and VEGF improved the transmigration capacity for up to 120 minutes. Therefore, transmigration might only be influenced by cytokines at early time points. Comparing the current findings with the previous migration study (Schmidt *et al.*, 2006a) again provides evidence that migration and transmigration are processes with unique characteristics that are differentially regulated and diversely influenced by cytokines.

The effect of the angiogenic cytokine EPO during skeletal myoblast transplantation was evaluated by Chanseaume and colleagues (Chanseaume *et al.*, 2007). In this

study, EPO failed to improve myoblast engraftment and postinfarction leftventricular function. Lately, MSCs were shown to express the cognate EPO receptor (Zwezdaryk *et al.*, 2007). Here, EPO increased the chemotaxis, migration and activation of matrix metalloprotease-2 of MSCs. These findings are in accordance with the present study which demonstrated an increase of transmigration induced by EPO. Recently, Chen *et al.* investigated that cord blood plasma induces transendothelial and trans-Matrigel migration of stem cells *in vitro* (Chen *et al.*, 2007). This migration was inhibited by a VEGF-neutralizing antibody and antibodies against the VEGF-receptor-1. For bFGF it is known that after spinal cord injury a transplantation of MSCs in combination with bFGF infusion improved the functional outcome (Kim *et al.*, 2006). Whether this might be an effect of the number of MSCs homed to the neural tissue has not been investigated. A recent study demonstrated that IL-6 is released into the systemic circulation in response to exercise which might result in increased stem cell recruitment after exercises (Schmidt *et al.*, 2007).

Taken together, for the therapeutic usage a local increase of cytokines for example induced by a myocardial infarction might not only improve the cell attraction to the tissue, but also influence the transmigration and invasion efficiency of MSCs at early time points. The local increase of cytokines *via* ultrasound and its effect on MSC attraction will be discussed in section 4.9.3.

4.7   Involvement of nitric oxide and free oxygen radicals

4.7.1 Nitric oxide

The blood-endothelial cell interface is a region of significant importance for many physiological and pathological processes. Macromolecules and cells gain access to the subendothelial space and the extravascular tissues by traversing the endothelium (Isenberg *et al.*, 2005). Yet the various factors responsible for modulation of this process remain only partially elucidated. Several agents were found to be involved in this process, including nitric oxide (NO) (Isenberg *et al.*, 2005).

In the present study co-cultivation experiments validated that the integration of MSCs into endothelial monolayers was accelerated by the NO-donor DETA NONOate especially at early points in time. NOS-inhibition *via* L-NAME decreased the integration. Furthermore, NO-measurements by DAF fluorometry revealed that the NO-release by MSCs was increased upon contact with endothelial cells while

endothelial cells obviously did not change their NO-production upon contact with MSCs. Therefore, one could speculate that not only NO produced by the vasculature, but also the release of NO by MSCs might influence their transmigration. Potentially, MSCs regionally manipulate the endothelial permeability by their endogenous NO-release. Isenberg and co-workers reported that stimulated endothelial layers alter their permeability to low-density mononuclear cells in the presence of exogenous NO (Isenberg, 2003). Furthermore, they demonstrated that NO can modify the endothelial permeability to macromolecules and low-density mononuclear cells in the absence of an inflammatory prestimulation (Isenberg *et al.*, 2005). By using Transwell chamber experiments they demonstrated that confluent monolayers of HUVECs increase their permeability to low-density mononuclear cells in the presence of spermine-NO. This response was dose-dependent, with low doses promoting and high doses inhibiting transendothelial cellular migration. Nonselective NOS-inhibition with L-NAME had no effect upon permeability to low-density mononuclear cells (Isenberg *et al.*, 2005). Moreover, it has been reported that NO alters the expression of the adhesion protein VE-cadherin, leading to a decrease of the same (Gonzalez *et al.*, 2003). This decrease of VE-cadherin at the adherent junctions between endothelial cells was correlated with an increased vascular permeability *in vivo* to the Evans blue dye in mice. Gonzalez and colleagues demonstrated that NO decreases β- and γ-catenin, known to make up – along with VE-cadherin – the adherent junction complexes between endothelial cells (Gonzalez *et al.*, 2003). Catenin proteins anchor the adherens junctional proteins to the actin cytoskeleton (Aberle *et al.*, 1996). Such a loss of inter- and intracellular junctional proteins – induced by NO – could allow for cellular retraction along the actin cytoskeleton and result in increased paracellular space for cellular transmigration (Isenberg *et al.*, 2005). Moreover, Sasaki and co-workers showed the crucial specific involvement of NO-producing enzymes in the migratory activity of bone marrow mononuclear cells *in vivo* (Sasaki *et al.*, 2006).

Recently, Kaminski *et al.* investigated the adhesion of c-kit[+] bone marrow stem cells to endothelial cells *in vivo* by intravital fluorescence microscopy of murine cremaster muscles (Kaminski *et al.*, 2007). They showed that firm endothelial adhesion of c-kit^{+} cells was entirely abrogated in wildtype mice treated with the arginine analog and nonselective NOS-inhibitor L-NAME as well as in eNOS-knockout mice. The fact that MSCs also express the endothelial nitric oxide synthase eNOS has recently been validated (Klinz *et al.*, 2005). Klinz *et al.* demonstrated that proliferating MSCs

accumulate eNOS phosphorylated at Serin-114 in the nuclear compartment, whereas eNOS phosphorylated at Serin-1177 was localized at filamentous structures in the perinuclear region of MSCs (Klinz *et al.*, 2005). Indeed, it has been confirmed that MSCs produce NO as an immunomodulatory mediator and to suppress T-cell proliferation (Oh *et al.*, 2007; Sato *et al.*, 2007). Furthermore, Ladage *et al.* showed that MSCs produce soluble factors which increased endothelial NO synthase (eNOS) activity by translocation and by phosphorylation in human umbilical vein endothelial cells (Ladage *et al.*, 2007). Thus, MSCs seem to emit soluble factors which alter the endothelial barrier mediated by the regulation of endothelial NO-release (Ladage *et al.*, 2007). Additionally, as it was confirmed in the present study MSCs increase their own NO-release upon contacting endothelial cells. Concluding, NO might be one important factor produced by MSCs which could regulate their transmigratory capacity by influencing the permeability of the endothelial barrier.

4.7.2 Reactive oxygen species

Reactive oxygen species (ROS) are a class of molecules that are derived from the metabolism of oxygen and include free radical and nonradical species that are generally capable of oxidizing molecular targets (Ardanaz *et al.*, 2006). Numerous studies have demonstrated the ability of a variety of vascular cells, including endothelial cells, to produce reactive oxygen species (ROS) (Ardanaz and Pagano, 2006). Herein, we present that MSCs are also capable of producing ROS. Fischer and colleagues demonstrated that H_2O_2 is able to induce an increased endothelial permeability (Fischer *et al.*, 2005). H_2O_2 as it was used by Fischer and in the present study to induce an oxidative stress situation under co-culture conditions is a cell-permeable and highly stable ROS (Ardanaz and Pagano, 2006). Although H_2O_2 is classified as a ROS, unlike O_2^- it is not a free radical, in that it does not possess an unpaired electron in its outer shell (Ardanaz and Pagano, 2006). This renders H_2O_2 more stable and less reactive with other tissue radicals and, thus, a more likely paracrine ROS (Ardanaz and Pagano, 2006). Steady-state H_2O_2 levels in vascular tissue are tightly regulated by the endogenous scavengers catalase and glutathione peroxidase (Suttorp *et al.*, 1986). It is known that in patients suffering from hypertension, plasma levels of H_2O_2 do rise (Lacy *et al.*, 1998). Since the superoxide anion O_2^- has the ability to directly attenuate the biological activity of nitric oxide by

the formation of peroxynitrite (Ardanaz and Pagano, 2006), ROS have been shown to contribute to vascular dysfunction partly by reducing the bioavailability of NO (Yung *et al.*, 2006).

In the present study, it was validated that the integration of MSCs into endothelial monolayers was impaired by H_2O_2, but enhanced by the radical scavenger N-acetylcysteine. This is in accordance with a study from Montoya and colleagues (Montoya *et al.*, 1997). They showed that under flow conditions treatment with antioxidants enhanced the adhesion of polymorphonuclear leukocytes to human umbilical vein endothelial cells activated with tumor necrosis factor-alpha. This adhesion was mediated by β2 integrins (Montoya *et al.*, 1997). Hung *et al.* found evidence that short-term exposure of MSCs to low oxygen conditions of 1% augmented expression of certain chemokine receptors thus increasing *in vitro* migration (Hung *et al.*, 2007).

Moreover, in the present study APF fluorometry demonstrated that MSCs themselves produce a large quantity of ROS. Their ROS-levels were about four-fold greater than the release by the endothelial cells and increased upon contact with endothelial cells. Parts of this production might be peroxynitrite – which is detected by the APF fuorometry – produced from the reaction with NO. To summarize, one could speculate that ROS decrease the transmigratory activity of MSCs by reducing the bioavailability of NO which itself positively influences transmigration. The simultaneous production of NO and ROS by MSCs could represent a negative feed-back mechanism as only a certain range of NO might be adequate to optimally influence the endothelial permeability for MSC transmigration. However, cardiomyoplasty in the presence of free radical scavengers and NO-donors could help to elevate the therapeutic efficiency.

4.8   Genetic manipulation of MSCs *via* adenoviral infection

Myocardial infarction is a leading cause of heart failure and death in developed countries (Ip *et al.*, 2007). In several trials the application of cell-based therapies for the treatment of heart disease has shown promising results (Strauer *et al.*, 2001; Assmus *et al.*, 2002; Britten *et al.*, 2003; Perin *et al.*, 2003; Stamm *et al.*, 2003; Tse *et al.*, 2003a). However, enhancing the efficiency of stem cell therapy is a major goal of current research.

Genetic modification of stem cells may represent one important strategic advancement in regenerative medicine (Dzau *et al.*, 2005). In future, by combining gene with stem cell therapy, one may be able to enhance the stem cell function. Indeed, genetic modification can improve the survival, the metabolic characteristics, the proliferative capacity and the differentiation of stem cells (Dzau *et al.*, 2005). Therefore, genetic modification of MSCs could elevate their therapeutic efficacy (Dzau *et al.*, 2005). For example, Mangi and co-workers demonstrated that the genetic modification of MSCs with the anti-apoptotic gene Akt1 (Akt-MSCs) increased their post-transplantation viability (Mangi *et al.*, 2003). Intramyocardial injection of Akt-MSCs led to the prevention of ventricular remodeling and to the restoration of cardiac function. Following studies demonstrated that the functional improvement of Akt-MSC transplantation occurred within 72 hours, which raised the hypothesis that paracrine actions instead of differentiation into cardiomyocytes might be important for tissue repair (Gnecchi *et al.*, 2006). Recently, secreted frizzled related protein 2 has been identified as the key paracrine factor released by Akt-modified MSCs mediating myocardial survival and repair (Mirotsou *et al.*, 2007).

Given its essential role in the hematopoietic system including bone marrow homing and recruitment (Jo *et al.*, 2000), stromal-derived factor (SDF)-1 (also known as CXCL12) and its receptor CXC chemokine receptor 4 (CXCR4) are candidates to promote stem cells recruitment to the heart (Pyo *et al.*, 2006). The SDF-1/CXCR4 system, which is implicated in migration, proliferation, differentiation and survival of hematopoietic stem and progenitor cells (Lapidot *et al.*, 2002), probably plays a significant role in stem cell homing after myocardial infarction (Barbash *et al.*, 2006).

Son and co-workers demonstrated that the CXCR4 transcript is strongly expressed in both bone marrow- and cord blood-derived MSCs (Son *et al.*, 2006). Additionally, it was reported that SDF-1 increases the migratory activity of MSCs (Schmidt *et al.*, 2006a). A recent study demonstrated that a small subpopulation of bone marrow-adherent cells that are small in size, seen in the colonies of earliest passages, express high levels of CXCR4 and exhibit greater engraftment into the hippocampal region after systemic infusion (Lee *et al.*, 2006). In a rat model it has been shown that SDF-1-CXCR4 interactions mediate the homing of bone marrow-derived MSCs to impaired sites in the brain (Ji *et al.*, 2004). Taken together, utilization of the SDF-1/CXCR4 system might be a potential target to improve the homing efficacy of MSCs (Barbash and Leor, 2006). Therefore, in the present study MSCs were adenovirally

infected to study the impact of overexpression of the SDF-1 receptor CXCR4 on the transmigration of MSCs in the murine heart.

Successful adenoviral infection of MSCs has been described in different studies (Barbash *et al.*, 2003; Mangi *et al.*, 2003; Gnecchi *et al.*, 2005; Gnecchi *et al.*, 2006; Mirotsou *et al.*, 2007). For example, an adenoviral infection efficiency of MSCs of >95% was achieved using a recombinant adenovirus enconding the reporter gene *LacZ* (Barbash *et al.*, 2003). However, in the present study the efficiency of adenoviral infection of MSCs with Ad.CXCR4.GFP was worse than it has been described for adult rat cardiac myocytes (Pyo *et al.*, 2006). The present study and Pyo *et al.* used the same adenovirus. However, Pyo and colleagues reported that after 48 hours even at the lowest virus concentration (MOI 1) almost 100% of the adult rat cardiac myocytes were infected as visualized by GFP fluorescence. The infection efficiency of MSCs using the Ad.CXCR4.GFP adenovirus was significantly inferior compared to the adult rat cardiac myocytes. Even by using high virus concentrations (MOI 80) only about 60% of the MSCs were infected. Nonetheless, the amount of CXCR4 protein in infected MSC lysates was strongly increased. Contrary to the expectation, the migratory activity of MSCs infected with Ad.CXCR4.GFP was significantly reduced as compared to MSCs infected with the control virus Ad.GFP. Addition of SDF-1 could not abrogate this discrepancy.

A study from Bhakta and co-workers also describes the transduction of MSCs using either CXCR4 and GFP or GFP alone (Bhakta *et al.*, 2006). Here, in contrast to the present study MSCs were retrovirally transduced. By performing flow cytometry they showed that on average 83% of the transduced MSCs expressed CXCR4. In contrast to the present work, MSCs transduced with CXCR4 exhibited significantly more migration toward SDF-1, threefold greater after 3 hours and more than fivefold greater after 6 hours compared with control MSCs (Bhakta *et al.*, 2006). Son and co-workers demonstrated that the surface expression of the CXCR4 antigen both on bone marrow- and cord blood derived MSCs was quite low, suggesting that this protein can be expressed intracellularly rather than on the cell surface (Son *et al.*, 2006). They assume that CXCR4 sequestered intracellularly in MSCs is mobilized to the cell surface, for example, during cytokine stimulation (Wynn *et al.*, 2004). Therefore, in the present study the overexpressed CXCR4 receptor might not have been transported sufficiently to the cell surface. However, this fact would still not explain why the migratory activity of MSCs infected with Ad.CXCR4.GFP was

significantly reduced as compared to MSCs infected with the control virus Ad.GFP. The presented data rather imply that adenoviral infection of MSCs using the Ad.CXCR4.GFP virus disturbed the physiological behavior of the cells. To summarize, on the one hand as demonstrated in the present study infection of MSCs using the Ad.CXCR4.GFP adenovirus impaired their migratory motility. On the other hand, infection with a CXCR4 expressing retrovirus is able to augment MSC motility (Bhakta *et al.*, 2006). Thus, a retroviral mediated CXCR4 transduction of MSCs might be the better alternative to increase their therapeutic potential.

In addition, the transmigratory activity of Ad.CXCR4.GFP infected MSCs with or without SDF-1 was not significantly altered as compared to the GFP-control cells. However, transmigration of MSCs infected with Ad.GFP tended to be increased in the presence of SDF-1. Thus, a genetic manipulation of MSCs by overexpressing CXCR4 was not beneficial for the transmigration of MSCs. Experiments of the present study were conducted in the presence of 50 ng/ml SDF-1 as described for transendothelial migration assays of human breast cancer cells across human brain microvascular endothelial cell monolayers (Lee *et al.*, 2004a). However, a recent study validated that high concentrations of SDF-1 between 100 and 600 ng/ml might be more efficient to increase the migratory activity of c-kit$^+$ bone marrow stem cells (Kaminski *et al.*, 2007). Nonetheless, Bhakta and colleagues observed a significant increase of the migration of CXCR4-expressing MSCs even in the presence of 30 ng/ml (Bhakta *et al.*, 2006).

Kaminski *et al.* recently demonstrated that for the firm adhesion of c-kit$^+$ bone marrow stem cells to endothelial cells the presence of both SDF-1 chemoattractant activity and inflammatory endothelial activation by TNF-α were required (Kaminski *et al.*, 2007). SDF-1 alone induced a transient c-kit$^+$ cell-endothelium interaction (rolling), but not their firm adhesion. This might explain why in the present study SDF-1 alone was not sufficient to increase the transmigration of MSCs in the isolated mouse heart. Furthermore, Kaminski and co-workers validated that ICAM-1 and CXCR4 on the vascular endothelium were crucial for the firm adhesion of the c-kit$^+$ cells. In accordance with the present study, Ip and co-workers demonstrated that injection of MSCs pretreated with blocking antibodies against CXCR4 into the ischemic myocardium of mice did not affect the amount of stem cells in the ischemic myocardium compared with control experiments (Ip *et al.*, 2007). Furthermore, Abbott and co-workers confirmed that SDF-1 plays a critical role in stem cell recruitment to

the heart after myocardial infarction, but that it is not sufficient to induce homing in the absence of injury. In this context, it would be interesting to investigate the efficiency of CXCR4 overexpressing MSCs in ischemic myocardium.

It is known that SDF-1 becomes up-regulated at sites of tissue damage (Ponomaryov *et al.*, 2000). For instance, levels of the chemokine SDF-1 and its receptor CXCR4 were elevated in patients with heart failure (Shioi *et al.*, 1997; Aukrust *et al.*, 1998; Aukrust *et al.*, 2001). This up-regulation of SDF-1 – also in the ischemic myocardium – mediates the homing of hematopoietic stem cells *via* its direct interaction with CXCR4 on the stem cells (Askari *et al.*, 2003; Abbott *et al.*, 2004). Furthermore, local manipulations to increase levels of SDF-1 in the myocardium have been shown to increase stem cells homing following myocardial infarction (Askari *et al.*, 2003). In addition, SDF-1 has been shown to not only regulate the adhesion of hematopoietic stem and progenitor cells to the endothelium (Grabovsky *et al.*, 2000), but also to control the expression of basement membrane degrading matrix metalloproteinases (Kijowski *et al.*, 2001). A recent study indicated that up-regulation of SDF-1 by hypoxic endothelial cells was required for the attachment and transendothelial migration of circulating CXCR4-positive endothelial progenitor cells (Ceradini *et al.*, 2004).

To conclude, the amount of CXCR4 receptor expressed on MSCs might not be the limiting factor for an efficient homing to the heart, while the concentration of SDF-1 could be important for the intravascular trafficking of MSCs. Furthermore, an adenoviral overexpression of CXCR4 in MSCs does not increase their myocardial homing potential. However, future studies should further examine the role of SDF-1 for the recruitment of MSCs into the heart.

4.9 Preconditioning of the endothelium by ultrasound-mediated microbubble stimulation triggers attraction, transmigration and invasion of MSCs

4.9.1 Systemic delivery of MSCs

A critical step for the clinical success of a stem cell-based therapy for myocardial repair is an efficient method for cell delivery (Barbash *et al.*, 2003). Intramyocardial transplantation of MSCs has been shown to promote cardiac repair with resulting

functional improvement and reduced infarct size (Kocher *et al.*, 2001; Mangi *et al.*, 2003; Amado *et al.*, 2005). Different groups reported good results after direct intracardiac injection of autologous bone marrow or skeletal myoblast cells during coronary artery bypass surgery. However, in contrast to skeletal myoblasts differentiated MSCs may have the capacity for electromechanical coupling (Nagaya *et al.*, 2004). Of note is that, although the patients had improved myocardial performance after stem cell therapy, increased arrhythmogenic potential has been reported, necessitating the implantation of internal defibrillators (Assmus *et al.*, 2002; Strauer *et al.*, 2002; Chen *et al.*, 2004). Moreover, this way of administration holds a considerable the risk for calcifications in the heart (Breitbach *et al.*, 2007). Instead of a direct transplantation, the mobilization of MSCs with cytokines such as granulocyte stimulating factor (G-CSF) and SDF-1 has been reported to enhance myocardial repair and improve cardiac function (Anversa and Nadal-Ginard, 2002; Askari *et al.*, 2003). Stem and progenitor cells have been shown to circulate in the peripheral blood and home to ischemic tissue (Asahara *et al.*, 1997). These results raise the possibility that intravenously administrated MSCs could participate in the repair of ischemic myocardium. Saito *et al.* were the first to demonstrate that MSCs administered intravenously engraft within regions of myocardial infarction (Saito *et al.*, 2002). Therefore, intravenous delivery of bone marrow-derived stem cells, as performed during bone marrow transplantation, to patients recovering from myocardial infarction is an alternative and attractive non-invasive strategy that allows repeated administrations of large numbers of cells (Barbash *et al.*, 2003). This systemic cellular transplantation could be achieved by the injection of cells either intracoronary during coronary interventions or intravenously (Barbash and Leor, 2006). Furthermore, it may be applicable to patients with diffuse myocardial disease, such as the idiopathic dilated cardiomyopathy (Barbash *et al.*, 2003). Once delivered, the cells would migrate through the systemic circulation, resettle in the infarcted myocardium and receive local signals that would direct myogenic differentiation (Orlic *et al.*, 2002; Toma *et al.*, 2002). Strauer and colleagues were the first to show the feasibility of intracoronary injection of enriched autologous mononuclear bone marrow cells in patients with acute myocardial infarction (Strauer *et al.*, 2002).

A positive effect of intravenously administrated MSCs on rats subjected to traumatic brain injury has been observed (Lu *et al.*, 2001). Here, MSCs preferentially entered and migrated into the parenchyma of the injured brain and significantly reduced

motor and neurological deficits. Another study performing a systemic MSC transplantation in a pig model of chronic ischemia showed significant functional improvements in the postinfarcted heart (Krause *et al.*, 2007). Here, systemic administration of MSCs reduced the infarct size and improved the hemodynamics. The authors speculate whether increased myocardial thickness, due to local infiltration of transplanted cells in the area of scarring, may have decreased the wall stress, resulting in a more compliant, less stiff ventricle with improved diastolic filling (Krause *et al.*, 2007).

However, Dai and colleagues reported for a postinfarcted rat model that although MSCs were detected 4 weeks after transplantation in the infarct scar, differentiation of MSCs to cardiomyocytes was incomplete because only immature myofibrillar organization was developed (Dai *et al.*, 2005). Therefore, mechanisms apart from cell differentiation contribute to the early functional effects of MSC transplantation (Krause *et al.*, 2007). Paracrine effects seem to be a plausible explanation because it has been shown that MSCs secrete a great number of growth factors and cytokines (Kinnaird *et al.*, 2004). Paracrine factors released from MSCs were recently been shown to promote antiapoptotic effects in cardiomyocytes subjected to hypoxia (Gnecchi *et al.*, 2005).

Barbash and co-workers investigated the engraftment of MSCs in the ischemic myocardium after systemic delivery (Barbash *et al.*, 2003). For gamma camera *in vivo* imaging and organ counting MSCs were labeled with the radioactive tracer isotope technetium-99m. Furthermore, they tested the feasibility of different systemic application routes: systemic intravenous delivery, infusion into the left ventricular cavity and infusion into the right ventricular cavity. However, shortly after infusion into the right ventricular cavity, Barbash and colleagues report that all animals died of massive pulmonary embolisms. Relative specific activity of labeled MSCs revealed that intravenous infusion of MSCs resulted predominately in lung uptake and lower uptake in liver, heart and spleen. In contrast, infusion into the left ventricular cavity was significantly more effective with lower lung uptake and increased uptake in the heart. However, gamma camera imaging indicated that even after intracoronary cardiomyoplasty within the first hours less than 1% of the infused cells resided in the infarcted heart (Barbash *et al.*, 2003). Furthermore, they identified clusters of infused cells at the boderzone. Thus, the main findings of Barbash and colleagues were that systemic intravenous delivery of MSCs is limited by the entrapment of donor cells

mainly in the lungs and that MSCs delivered by left ventricular cavity infusion migrate to and colonize the infracted heart in significantly higher amounts (Barbash *et al.*, 2003). Furthermore, a study which assessed the homing capabilities of bone marrow-derived stem cells in humans using three-dimensional positron-emitted tomography discovered that 1.3-2.6% of injected cells homed into the myocardium after intracoronary injection and no cells were found following intravenous injection (Hofmann *et al.*, 2005). Nagaya and co-workers investigated whether intravenously transplanted MSCs induce angiogenesis and myogenesis and improve cardiac function in rats with acute myocardial infarction (Nagaya *et al.*, 2004). Here, transplanted MSCs were preferentially attracted to the infarcted, but not the non-infarcted myocardium. The engrafted MSCs were positive for some cardiac markers. Capillary density was markedly increased and cardiac infarct size was significantly decreased after MSC transplantation. The fraction of left ventricular ejection was also higher in the MSC than in the control group. Semiquantitative analysis of the hearts demonstrated that about 3% of the transplanted MSCs were incorporated into the heart 24 hours after transplantation. At 4 weeks after transplantation, MSCs were incorporated predominantely into the borderzone of infarcts. These results suggested that intravenously administrated MSCs are capable of engraftment in the ischemic myocardium and that transplantation improves cardiac function after acute myocardial infarction through enhancement of angiogenesis and myogenesis in ischemic myocardium (Nagaya *et al.*, 2004). However, only a low percentage of transplanted MSCs incorporated into the heart (Nagaya *et al.*, 2004), which could be explained by MSC apoptosis (Mangi *et al.*, 2003) or tacking in the lung (Barbash *et al.*, 2003). To summarize, only a small percentage of MSCs home to the desired tissue after a systemic delivery. Thus, the development of a method to increase the cell engraftment by modulating the process of transmigration of MSCs in a site-specific manner would be of great clinical benefit.

4.9.2 Ultrasound-mediated microbubble stimulation

One possible technique to influence the interaction of MSCs and the endothelium could be ultrasound-mediated microbubble stimulation (UMS). Ultrasound is commonly used for diagnostic imaging and physiotherapy (Altland *et al.*, 2004). Contrast agent microbubbles have been currently used for therapeutic purposes (Zen

et al., 2006). UMS in the capillary lumen elicited arteriogenesis and enhanced the hyperaemic blood flow in normal and ischemic rat skeletal muscle (Skyba *et al.*, 1998; Song *et al.*, 2004). However, UMS is also used as a novel gene- and cell-delivery system which depends on intravenous application of gas-filled microbubbles and their cardiopulmonary circulation through intravascular space until ultrasound-induced bubble-tissue interaction in the target organ (Shohet *et al.*, 2000). UMS was used for cell-delivery in skeletal muscle and myocardium (Imada *et al.*, 2005; Zen *et al.*, 2006). The study of Imada and co-workers demonstrated that the release of pro-inflammatory factors activated by UMS plays a key role in the attachment of transplanted bone marrow-derived mononuclear cells onto the endothelial layer (Imada *et al.*, 2005). Zen and co-workers obtained increased cardiac function *via* an angiogenic response 12 weeks after application of UMS and intravenous infusion of endothelial progenitor cells in a cardiomyopathy model. Both, gene- and cell-therapeutic approaches revealed no significant delivery in the controls using ultrasound or microbubbles alone (Bekeredjian *et al.*, 2003; Imada *et al.*, 2005). Therefore, exposure of defined regions of the heart to UMS prior to systemic administration of MSCs may be well suited to non-invasively augment MSC recruitment to non-ischemic and ischemic myocardium.

UMS is known to administrate a mechanical action on endothelial and vascular smooth muscle cells *via* a so called sonoporation resulting in the formation of transient pores which revert to normal appearance within 24 hours (Taniyama *et al.*, 2002a). However, this technique can also cause fatal bioeffects, such as capillary rupture and extravasation of erythrocytes as well as eosinophily and cardiomyocyte necrosis which are positively associated with ultrasound emission power (Chen *et al.*, 2002; Chen *et al.*, 2003; Miller *et al.*, 2007). However, the ultrasound emission power used in the present study was well defined and did not result in obvious vasculature and tissue damage. For the treatment of non-ischemic myocardium the anterior wall was selected as the target tissue. In ischemic myocardium the borderzone of infarcts served as UMS target. It has been described previously that transplanted MSCs were preferentially attracted to and retained in the borderzone of infarcts (Barbash *et al.*, 2003; Nagaya *et al.*, 2004). Therefore, the borderzone of infracted myocardium should be a sufficient target tissue for stem cell therapy.

In the present study, the effect of UMS applied shortly before cardiomyoplasty was evaluated by calculating the cell attraction (section 3.11.3) and the transmigration of

MSCs (section 3.11.4). Furthermore, the impact of UMS on cytokine levels, apoptosis, protease activity as well as endothelium and basement membrane morphology was studied (section 3.11.5).

4.9.3 Effect of UMS on cell attraction and cytokine levels

The number of MSCs attracted into the ischemic myocardium was significantly higher than the number of cells in non-ischemic myocardium. However, focussed pre-treatment of the anterior wall resulted in a significant increase in the absolute number of MSCs per heart slide in ischemic as well as in non-ischemic myocardium. It has been previously described that MSCs are preferentially attracted to ischemic myocardium (Nagaya *et al.*, 2004). Earlier studies showed that endothelial progenitor cells are mobilized from the bone marrow into the peripheral blood in response to tissue ischemia and home to and incorporate into sites of neovascularization (Asahara *et al.*, 1997). Although, the underlying mechanisms remain unclear, ischemic tissue may express specific receptors or ligands to facilitate trafficking, adhesion and infiltration of MSCs in ischemic sites (Nagaya *et al.*, 2004). In the present study investigations of MSC cell therapy in non-ischemic myocardium were performed since its cytokine and chemokine activity and therefore intrinsic attraction of MSCs is the lowest and might therefore resemble the chronic state of an idiopathic cardiomyopathy.

To approximate the myocardial transplantation efficacy, the absolute amount of MSCs per rat heart was estimated and related to the left-ventricular volume (Ghanem *et al.*, 2006). For example, in ischemic, non-insonicated myocardium 3.800 MSCs retained in the left-ventricle, normalized to 100.000 transplanted MSCs. The corresponding transplantation efficacy of 3.8% is comparable to previous observations in experimental (Barbash *et al.*, 2003) and clinical studies (Hofmann *et al.*, 2005). However, UMS preconditioning significantly increased the transplantation efficacy to 5.2%. This UMS-induced improvement of cell attraction in ischemic as well as in non-ischemic myocardium could be explained with the transient endothelial alteration and with well known shear forces generated through the transient ultrasound-induced pressure pulse (Hsu *et al.*, 2004). Ruster and co-workers showed that P-selectin is involved in the rolling of MSCs on endothelial cells (Ruster *et al.*, 2006). However, Imada *et al.* demonstrated that UMS quickly induced the expression

of adhesive molecules such as P-selectin in treated endothelial cells (Imada *et al.*, 2005). Therefore, the increased cell attraction of MSCs induced by UMS could also be explained by an alteration of the P-selectin expression on the endothelial cells, which might result in an increase of the rolling and adhesion behavior of MSCs.

Furthermore, ultrasound exposure was reported to cause a rapid response in nitric oxide synthesis by endothelial cells (Altland *et al.*, 2004). This increase of nitric oxide release within the first minutes after insonication (Altland *et al.*, 2004) might allow an additional mechanistic explanation of the increased attraction and adhesion of MSCs after UMS. Kaminski and co-workers showed for eNOS-knockout mice that the firm adhesion of c-kit[+] bone marrow stem cells was entirely abrogated (Kaminski *et al.*, 2007). Moreover, the present study implies that nitric oxide also plays a key role during the transmigration of MSCs (section 3.8 and 4.7.1).

On the other hand, in the present study regional analyses of non-ischemic anterior and posterior myocardial segments of the same rat hearts by cytokine arrays, done immediately after UMS, revealed that UMS acutely induced a local pro-inflammatory response resulting in an anterior-to-posterior gradient of cytokines as compared to control tissue. Interleukin (IL)-1α, IL-1β, tumor necrosis factor (TNF)-α and granulocyte macrophage stimulating factor (GM-CSF) were significantly increased by UMS. IL-4, IL-6 and IL-10 were not detected in non-insonicated tissue, while insonicated myocardium contained these cytokines. Previous studies already described the induction of cytokine expression after UMS (Imada *et al.*, 2005; Zen *et al.*, 2006). These experiments studied cytokine levels a minimum of 3 days after insonication; to our knowledge the present study is the first investigation of acute UMS effects on cytokine levels. The study of Imada and co-workers demonstrated that the release of pro-inflammatory factors activated by UMS plays a key role in the attachment of transplanted bone marrow-derived mononuclear cells onto the endothelial layer (Imada *et al.*, 2005). Moreover, UMS markedly elevated the expression of inflammatory chemokines and cytokines (IL-1β, TNF-α, monocyte chemoattractant protein (MCP)-1, VEGF and bFGF) three days after insonication (Zen *et al.*, 2006). In accordance with the present study, cytokines were mainly expressed in UMS-treated myocardium.

In this study hearts were harvested within 10 minutes after UMS application. Thus, up-regulation of protein expression cannot explain the observed differences in

cytokine levels. The cytokines could rather be released from extracellular matrix storages or secreted by activated cells. Ultrasound has been shown to increase the production of IL-1β and VEGF by monocytes (Reher *et al.*, 1999). To speculate, UMS could also have induced a loosening of matrix-bound cytokines (Park *et al.*, 1993); and these free cytokines might be detected more sufficiently by the cytokine array as compared to matrix-bound cytokines (oral information provided by the manufacturer). This hypothesis is supported by the observation that UMS regionally activated proteases which will be discussed in the following section. Indeed, previous studies obtained for example fibronectin-bound TNF-α which allowed stimulation of cellular MMP-9 expression and consecutively regulated the chemotaxis of monocytes (Vaday *et al.*, 2000; Vaday *et al.*, 2001). One of the most interesting characteristics of MSCs is their ability to home to sites of tissue damage or inflammation (Devine *et al.*, 2001). Therefore, by regionally increasing the cytokine level UMS might imitate an inflammatory situation and thereby increase MSC attraction to insonicated regions. Recently, Segers and co-workers demonstrated an increase of cardiac infiltration of MSCs after activation with TNF-α or IL-1β before cell interaction (Segers *et al.*, 2006). In addition, rolling and adhesion of MSCs was found to be increased after pre-stimulation of endothelial cells with TNF-α (Ruster *et al.*, 2006). Furthermore, Kaminski and colleagues validated that activation of the endothelium by TNF-α and SDF-1 led to a relevant attraction of c-kit[+] bone marrow stem cells (Kaminski *et al.*, 2007). Wang *et al.* showed a significant increase in the attachment of neutrophils to endothelial cells after application of IL-1β (Wang *et al.*, 2006) and IL-1α increases the expression of matrix metalloproteinases and thereby mediates matrix degradation (Wisithphrom *et al.*, 2006). Cho *et al.* demonstrated that GM-CSF treatment mobilized endothelial progenitor cells, accelerated reendothelialization and reduced monocytes infiltration after intravascular radiation therapy (Cho *et al.*, 2003). Moreover, MSCs have been mobilized from the bone marrow by G-CSF and SDF-1, which has been reported to enhance myocardial repair and improve cardiac function (Anversa and Nadal-Ginard, 2002; Askari *et al.*, 2003).

To summarize, the present findings lead to the hypothesis that UMS – apart from other bioeffects – induced a regional cytokine release, which triggered an intravascular trafficking of MSCs to the target zone. This increase of cytokines might also influence the transendothelial migration of MSCs.

4.9.4 Effect of UMS on transmigration, basement membrane and protease activity

To evaluate the effect of UMS on the transmigration of MSCs the percentage of transmigrating MSCs in the target tissue in native and ischemic myocardium with and without UMS preconditioning was calculated. UMS significantly increased the number of transmigrating MSCs in native as well as in ischemic hearts. Therefore, UMS not only increased the number of MSCs attracted to the target tissue, but also the number of actually transmigrating and invading MSCs. In accordance, UMS has previously been reported to induce an opening of cell-cell-contacts in a chorioallantoic membrane model and thereby increasing the vascular permeability (Stieger *et al.*, 2007).

UMS was used for cell-delivery in the skeletal muscle and myocardium (Imada *et al.*, 2005; Zen *et al.*, 2006). Zen and co-workers obtained increased cardiac function *via* an angiogenic response 12 weeks after application of UMS and endothelial progenitor cells in a cardiomyopathy model. Those findings were related to an approximately 2.5-fold increase in expression of the adhesion molecules VCAM-1 and ICAM-1 (Zen *et al.*, 2006). In addition, Hsu *et al.* propose that ultrasound activates endothelial integrins (Hsu *et al.*, 2006). Since the present study identified VCAM-1 and integrins as key surface molecules for the transmigration of MSCs, the activation of surface molecules *via* ultrasound might be one possible explanation for UMS-induced increase of transmigration. However, in contrast to Imada and Zen *et al.*, the present study investigated the acute impact of UMS on cell infiltration as well as endothelial and basal membrane alterations, since post-ischemic remodeling can be positively influenced best at an early stage.

Altland and co-workers demonstrated that exposure of endothelial cells to low-frequency ultrasound increased their NO production through up-regulation of eNOS activity within minutes (Altland *et al.*, 2004). Hsu and Huang published that the enhanced NO release by endothelial cells was maintained up till days after ultrasound treatment (Hsu and Huang, 2004). Since in the present study NO has been shown to increase transmigration this might be another possible and important explanation for the enhanced transmigratory activity of MSCs after UMS.

Since degradation of the basement membrane is a critical step for the invasion of MSCs into the myocardium (section 3.5 and 4.4) the expression of the basement

membrane component laminin was investigated after UMS exposure. Thus, heart sections were immunostained for laminin. The expression of laminin 2 hours after UMS insonication was decreased as demonstrated by reduced fluorescence intensity, indicating a reduced level of immunoreactive laminin. This UMS-mediated decrease of laminin was confirmed by western blot analysis. Wang and co-workers lately identified regions within the venular wall, where the expression of certain basement membrane constituents such as laminin and collagen IV was lower than the average vascular level (Wang *et al.*, 2006). These regions were highly associated with gaps between pericytes and appeared to be preferentially used by transmigrating neutrophils. One potential mechanism by which neutrophils may increase the size of low expression regions of extracellular matrix proteins is *via* proteolytic cleavage (Wang *et al.*, 2006).

However, in the present study by performing electron microscopy no visual alterations of the basement membrane and the endothelium on an ultrastructural level were observed. Studies investigating the emigration of leukocytes also did not note visible damage of the basement membrane at sites of leukocyte transmigration (Marchesi and Florey, 1960; Hurley, 1963). Therefore, it is possible that ultrastructural analysis did not enable us to visualize those transient changes in extracellular matrix protein expression caused by UMS. Perhaps, UMS induced – by activating proteases – a transient remodeling of the basement membrane and thereby enabled regionally a more efficient transmigration and invasion of MSCs without gross and irreversible disruption of the vascular wall structure. Such a transient basement membrane remodeling has been observed at sites of emigrating neutrophils (Wang *et al.*, 2006). Here, the above mentioned low expression regions of extracellular matrix proteins do not lack the basement membrane, but are regions in which there is less expression of selective basement membrane constituents (Wang *et al.*, 2006). Neutrophils traverse the vessel wall preferentially at those regions (Wang *et al.*, 2006).

To investigate whether the observed changes in the extracellular matrix protein expression might be caused by the activation of proteases, *in situ* zymographies were conducted. They allowed localizing gelatinase activity in heart slides after UMS treatment. Localized protease activity in the targeted myocardium within the anteroseptal wall was observed after focussed insonication, while no gelatinase activity was detected in the untreated posterior myocardium. Thus, UMS locally

induced the activation of proteases, which might explain the observed transient reduction of basement membrane components. The activity of proteases was shown to be crucial for invasion of MSCs into the basement membrane of bone marrow (De Becker *et al.*, 2007; Ries *et al.*, 2007) and as demonstrated in the present study for the invasion into myocardial tissue (section 3.5 and 4.4). Therefore, the described finding of MMP-activation *via* UMS might contribute substantially to the improved myocardial engraftment of MSCs after exposition to UMS.

However, UMS is known to cause bioeffects on endothelial cells, such as capillary rupture and extravasation of erythrocytes, and cardiomyocytes, for example eosinophily and cardiomyocyte necrosis, which are positively associated with the used ultrasound emission power (Chen *et al.*, 2002). Recently, Miller and colleagues demonstrated an early onset of apoptosis within hours after UMS at high emission power and histological signs of myocardial necrosis days after insonication (Miller *et al.*, 2007). However, extensive endothelial damage was not observed in the present study as supported by the observations of lack of early apoptosis by TUNEL staining and microscopic as well as ultrastructural assessments. These discrepancies are likely due to the differences in the insonication protocol as well as microbubble properties and concentration. In this study, UMS was performed for 60 pulses at a duty cycle of >1%. It is also worth to mention that this is the first study using SonoVue microbubbles. As described by the manufacturer, even at higher emission power its microbubble shell did not increase in size and thereby did not cause potential capillary disruption. Therefore, UMS with the described insonication protocol and microbubble properties did not produce an intolerable level of side effects in the treated myocardium and vasculature.

In conclusion, the presented study proved that myocardial MSC attraction, transmigration and invasion after systemic stem cell therapy can be enhanced locally by means of focussed UMS in native and ischemic myocardium. Therefore, exposure of hearts to the non-invasive UMS prior to a systemic stem cell therapy may be well suited to augment the stem cell recruitment to non-ischemic as well as ischemic myocardium. Whether this UMS-mediated MSC recruitment and incorporation leads to a functional improvement of impaired heart function needs to be assessed by subsequent studies.

It will be one of the major future tasks to find the most practical and specific way of evolving and targeting the healing potency of stem cells for tissue regeneration (Wollert *et al.*, 2005).

5. Summary

Stem cell therapy using human adult mesenchymal stem cells (MSCs) has emerged as a novel strategy for the treatment of a variety of damaged tissues. For a successful systemic stem cell therapy MSCs have to exit the blood circulation by transmigrating across the endothelium and invading into the target tissue. Elevating our knowledge on these core processes might help to optimize stem cell based therapies. The first part of the present study provides insights into key mechanisms involved in the transmigration and invasion of MSCs. Different model systems as well as *in vivo* studies revealed that MSCs quickly come into contact with the endothelium and subsequently exit the blood circulation by (1) integrating into the endothelium, (2) transmigrating across the endothelial barrier *via* the insertion of plasmic podia, (3) penetrating the basement membrane and subsequently invading the surrounding tissue.

Additionally, it was proven that transmigration of human MSCs not only requires the interaction of very late antigen-4 (VLA-4, $\alpha4\beta1$ integrin) and its most important ligand vascular cell adhesion molecule-1 (VCAM-1), but also triggers a clustering of $\beta1$ integrins. Furthermore, upon invading into cardiac tissue MSCs secrete active matrix metalloproteinase (MMP)-2, but not MMP-9.

This study also demonstrates that both the time course and the morphological aspects of MSC transmigration differ depending on the endothelial phenotype, thus indicating, that a variable capacity for transendothelial migration exists within the vasculature. Furthermore, addition of cytokines, mainly vascular endothelial growth factor (VEGF) and erythropoietin (EPO), accelerate the transmigration of MSCs at early stages. Moreover, nitric oxide (NO) and reactive oxygen species (ROS) are released by MSCs upon contact with endothelial cells; manipulating the NO and ROS system by donors and inhibitors resulted in alterations of the transmigratory capacity of MSCs.

The second part of the study deals with two possible strategies to enhance the transmigration of MSCs and thereby their therapeutic effectiveness. First, the results demonstrate that genetic modification of MSCs using adenoviral overexpression of the chemokine receptor CXCR4 does not lead to an increase in the transmigration efficiency. Second, focussed pretreatment of the endothelium by a novel and non-invasive technique using ultrasound-mediated microbubble stimulation (UMS) induces a targeted improvement of MSC attraction, transmigration and invasion into

non-ischemic as well as into ischemic myocardium. This effect was most likely due to the release of nitric oxide, cytokines and the regional activation of proteases. Thus, UMS represents a forward-looking possibility to increase the efficiency of MSC engraftment by modulating the process of transmigration in a targeted and non-invasive manner.

6.   References

Abbott, J.D., Huang, Y., Liu, D., Hickey, R., Krause, D.S. and Giordano, F.J. (2004). Stromal cell-derived factor-1alpha plays a critical role in stem cell recruitment to the heart after myocardial infarction but is not sufficient to induce homing in the absence of injury. *Circulation* 110, 3300-3305.

Aberle, H., Schwartz, H. and Kemler, R. (1996). Cadherin-catenin complex: protein interactions and their implications for cadherin function. *J Cell Biochem* 61, 514-523.

Agrawal, S., Anderson, P., Durbeej, M., van Rooijen, N., Ivars, F., Opdenakker, G. and Sorokin, L.M. (2006). Dystroglycan is selectively cleaved at the parenchymal basement membrane at sites of leukocyte extravasation in experimental autoimmune encephalomyelitis. *J Exp Med* 203, 1007-1019.

Airas, L., Hellman, J., Salmi, M., Bono, P., Puurunen, T., Smith, D.J. and Jalkanen, S. (1995). CD73 is involved in lymphocyte binding to the endothelium: characterization of lymphocyte-vascular adhesion protein 2 identifies it as CD73. *J Exp Med* 182, 1603-1608.

Alderton, W.K., Cooper, C.E. and Knowles, R.G. (2001). Nitric oxide synthases: structure, function and inhibition. *Biochem J* 357, 593-615.

Alter, A., Duddy, M., Hebert, S., Biernacki, K., Prat, A., Antel, J.P., Yong, V.W., Nuttall, R.K., Pennington, C.J., Edwards, D.R. and Bar-Or, A. (2003). Determinants of Human B Cell Migration Across Brain Endothelial Cells. *The Journal of Immunology* 170, 4497-4505.

Altland, O.D., Dalecki, D., Suchkova, V.N. and Francis, C.W. (2004). Low-intensity ultrasound increases endothelial cell nitric oxide synthase activity and nitric oxide synthesis. *J Thromb Haemost* 2, 637-643.

Amado, L.C., Saliaris, A.P., Schuleri, K.H., St John, M., Xie, J.S., Cattaneo, S., Durand, D.J., Fitton, T., Kuang, J.Q., Stewart, G., Lehrke, S., Baumgartner, W.W., Martin, B.J., Heldman, A.W. and Hare, J.M. (2005). Cardiac repair with intramyocardial injection of allogeneic mesenchymal stem cells after myocardial infarction. *Proc Natl Acad Sci U S A* 102, 11474-11479.

Anversa, P. and Nadal-Ginard, B. (2002). Myocyte renewal and ventricular remodelling. *Nature* 415, 240-243.

Ardanaz, N. and Pagano, P.J. (2006). Hydrogen peroxide as a paracrine vascular mediator: regulation and signaling leading to dysfunction. *Exp Biol Med (Maywood)* 231, 237-251.

Arnhold, S., Klein, H., Klinz, F.J., Absenger, Y., Schmidt, A., Schinkothe, T., Brixius, K., Kozlowski, J., Desai, B., Bloch, W. and Addicks, K. (2006). Human bone marrow stroma cells display certain neural characteristics and integrate in the subventricular compartment after injection into the liquor system. *Eur J Cell Biol* 85, 551-565.

Asahara, T., Murohara, T., Sullivan, A., Silver, M., van der Zee, R., Li, T., Witzenbichler, B., Schatteman, G. and Isner, J.M. (1997). Isolation of putative progenitor endothelial cells for angiogenesis. *Science* 275, 964-967.

Askari, A.T., Unzek, S., Popovic, Z.B., Goldman, C.K., Forudi, F., Kiedrowski, M., Rovner, A., Ellis, S.G., Thomas, J.D., DiCorleto, P.E., Topol, E.J. and Penn, M.S. (2003). Effect of stromal-cell-derived factor 1 on stem-cell homing and tissue regeneration in ischaemic cardiomyopathy. *Lancet* 362, 697-703.

Assmus, B., Schachinger, V., Teupe, C., Britten, M., Lehmann, R., Dobert, N., Grunwald, F., Aicher, A., Urbich, C., Martin, H., Hoelzer, D., Dimmeler, S. and Zeiher, A.M. (2002). Transplantation of Progenitor Cells and Regeneration Enhancement in Acute Myocardial Infarction (TOPCARE-AMI). *Circulation* 106, 3009-3017.

Aukrust, P., Ueland, T., Muller, F., Andreassen, A.K., Nordoy, I., Aas, H., Kjekshus, J., Simonsen, S., Froland, S.S. and Gullestad, L. (1998). Elevated circulating levels of C-C chemokines in patients with congestive heart failure. *Circulation* 97, 1136-1143.

Aukrust, P., Damas, J.K., Gullestad, L. and Froland, S.S. (2001). Chemokines in myocardial failure -- pathogenic importance and potential therapeutic targets. *Clin Exp Immunol* 124, 343-345.

Azizi, S.A., Stokes, D., Augelli, B.J., DiGirolamo, C. and Prockop, D.J. (1998). Engraftment and migration of human bone marrow stromal cells implanted in the brains of albino rats--similarities to astrocyte grafts. *Proc Natl Acad Sci U S A* 95, 3908-3913.

Barbash, I.M., Chouraqui, P., Baron, J., Feinberg, M.S., Etzion, S., Tessone, A., Miller, L., Guetta, E., Zipori, D., Kedes, L.H., Kloner, R.A. and Leor, J. (2003). Systemic delivery of bone marrow-derived mesenchymal stem cells to the infarcted myocardium: feasibility, cell migration, and body distribution. *Circulation* 108, 863-868.

Barbash, I.M. and Leor, J. (2006). Myocardial regeneration by adult stem cells. *Isr Med Assoc J* 8, 283-287.

Barry, F.P., Boynton, R.E., Haynesworth, S., Murphy, J.M. and Zaia, J. (1999). The monoclonal antibody SH-2, raised against human mesenchymal stem cells, recognizes an epitope on endoglin (CD105). *Biochem Biophys Res Commun* 265, 134-139.

Bauer, K., Mierke, C. and Behrens, J. (2007). Expression profiling reveals genes associated with transendothelial migration of tumor cells: A functional role for alphavbeta3 integrin. *Int J Cancer*.

Bekeredjian, R., Chen, S., Frenkel, P.A., Grayburn, P.A. and Shohet, R.V. (2003). Ultrasound-targeted microbubble destruction can repeatedly direct highly specific plasmid expression to the heart. *Circulation* 108, 1022-1026.

Bhakta, S., Hong, P. and Koc, O. (2006). The surface adhesion molecule CXCR4 stimulates mesenchymal stem cell migration to stromal cell-derived factor-1 in vitro but does not decrease apoptosis under serum deprivation. *Cardiovasc Revasc Med* 7, 19-24.

Bienvenu, K. and Granger, D.N. (1993). Molecular determinants of shear rate-dependent leukocyte adhesion in postcapillary venules. *Am J Physiol* 264, H1504-1508.

Bittner, R.E., Schofer, C., Weipoltshammer, K., Ivanova, S., Streubel, B., Hauser, E., Freilinger, M., Hoger, H., Elbe-Burger, A. and Wachtler, F. (1999). Recruitment of bone-marrow-derived cells by skeletal and cardiac muscle in adult dystrophic mdx mice. *Anat Embryol (Berl)* 199, 391-396.

Breitbach, M., Bostani, T., Roell, W., Xia, Y., Dewald, O., Nygren, J.M., Fries, J.W., Tiemann, K., Bohlen, H., Hescheler, J., Welz, A., Bloch, W., Jacobsen, S.E. and Fleischmann, B.K. (2007). Potential risks of bone marrow cell transplantation into infarcted hearts. *Blood*.

Brenner, S., Whiting-Theobald, N., Kawai, T., Linton, G.F., Rudikoff, A.G., Choi, U., Ryser, M.F., Murphy, P.M., Sechler, J.M. and Malech, H.L. (2004). CXCR4-transgene expression significantly improves marrow engraftment of cultured hematopoietic stem cells. *Stem Cells* 22, 1128-1133.

Britten, M.B., Abolmaali, N.D., Assmus, B., Lehmann, R., Honold, J., Schmitt, J., Vogl, T.J., Martin, H., Schachinger, V., Dimmeler, S. and Zeiher, A.M. (2003). Infarct remodeling after intracoronary progenitor cell treatment in patients with acute myocardial infarction (TOPCARE-AMI): mechanistic insights from serial contrast-enhanced magnetic resonance imaging. *Circulation* 108, 2212-2218.

Caplan, A.I. and Bruder, S.P. (2001). Mesenchymal stem cells: building blocks for molecular medicine in the 21st century. *Trends Mol Med* 7, 259-264.

Caskey, C.F., Stieger, S.M., Qin, S., Dayton, P.A. and Ferrara, K.W. (2007). Direct observations of ultrasound microbubble contrast agent interaction with the microvessel wall. *J Acoust Soc Am* 122, 1191-1200.

Ceradini, D.J., Kulkarni, A.R., Callaghan, M.J., Tepper, O.M., Bastidas, N., Kleinman, M.E., Capla, J.M., Galiano, R.D., Levine, J.P. and Gurtner, G.C. (2004). Progenitor cell trafficking is regulated by hypoxic gradients through HIF-1 induction of SDF-1. *Nat Med* 10, 858-864.

Chanseaume, S., Azarnoush, K., Maurel, A., Bellamy, V., Peyrard, S., Bruneval, P., Hagege, A.A. and Menasche, P. (2007). Can erythropoietin improve skeletal myoblast engraftment in infarcted myocardium? *Interact Cardiovasc Thorac Surg* 6, 293-297.

Chen, C.P., Lee, M.Y., Huang, J.P., Aplin, J.D., Wu, Y.H., Hu, C.S., Chen, P.C., Li, H., Hwang, S.M., Liu, S.H. and Yang, Y.C. (2007). Trafficking of Multipotent

Mesenchymal Stromal Cells From Maternal Circulation Through the Placenta Involves VEGFR-1 and Integrins. *Stem Cells*.

Chen, S., Kroll, M.H., Shohet, R.V., Frenkel, P., Mayer, S.A. and Grayburn, P.A. (2002). Bioeffects of myocardial contrast microbubble destruction by echocardiography. *Echocardiography* 19, 495-500.

Chen, S., Shohet, R.V., Bekeredjian, R., Frenkel, P. and Grayburn, P.A. (2003). Optimization of ultrasound parameters for cardiac gene delivery of adenoviral or plasmid deoxyribonucleic acid by ultrasound-targeted microbubble destruction. *J Am Coll Cardiol* 42, 301-308.

Chen, S., Liu, Z., Tian, N., Zhang, J., Yei, F., Duan, B., Zhu, Z., Lin, S. and Kwan, T.W. (2006). Intracoronary transplantation of autologous bone marrow mesenchymal stem cells for ischemic cardiomyopathy due to isolated chronic occluded left anterior descending artery. *J Invasive Cardiol* 18, 552-556.

Chen, S.L., Fang, W.W., Ye, F., Liu, Y.H., Qian, J., Shan, S.J., Zhang, J.J., Chunhua, R.Z., Liao, L.M., Lin, S. and Sun, J.P. (2004). Effect on left ventricular function of intracoronary transplantation of autologous bone marrow mesenchymal stem cell in patients with acute myocardial infarction. *Am J Cardiol* 94, 92-95.

Cho, H.J., Kim, H.S., Lee, M.M., Kim, D.H., Yang, H.J., Hur, J., Hwang, K.K., Oh, S., Choi, Y.J., Chae, I.H., Oh, B.H., Choi, Y.S., Walsh, K. and Park, Y.B. (2003). Mobilized endothelial progenitor cells by granulocyte-macrophage colony-stimulating factor accelerate reendothelialization and reduce vascular inflammation after intravascular radiation. *Circulation* 108, 2918-2925.

Christensen, M.M., Danscher, G., Ellermann-Eriksen, S., Schionning, J.D. and Rungby, J. (1992). Autometallographic silver-enhancement of colloidal gold particles used to label phagocytic cells. *Histochemistry* 97, 207-211.

Chung, C.H., Golub, E.E., Forbes, E., Tokuoka, T. and Shapiro, I.M. (1992). Mechanism of action of beta-glycerophosphate on bone cell mineralization. *Calcif Tissue Int* 51, 305-311.

Dai, W., Hale, S.L., Martin, B.J., Kuang, J.Q., Dow, J.S., Wold, L.E. and Kloner, R.A. (2005). Allogeneic mesenchymal stem cell transplantation in postinfarcted rat myocardium: short- and long-term effects. *Circulation* 112, 214-223.

De Bari, C., Dell'Accio, F., Vandenabeele, F., Vermeesch, J.R., Raymackers, J.M. and Luyten, F.P. (2003). Skeletal muscle repair by adult human mesenchymal stem cells from synovial membrane. *J Cell Biol* 160, 909-918.

De Becker, A., Van Hummelen, P., Bakkus, M., Vande Broek, I., De Wever, J., De Waele, M. and Van Riet, I. (2007). Migration of culture-expanded human mesenchymal stem cells through bone marrow endothelium is regulated by matrix metalloproteinase-2 and tissue inhibitor of metalloproteinase-3. *Haematologica* 92, 440-449.

Dejana, E., Corada, M. and Lampugnani, M.G. (1995). Endothelial cell-to-cell junctions. *Faseb J* 9, 910-918.

Dejana, E., Zanetti, A. and Del Maschio, A. (1996). Adhesive proteins at endothelial cell-to-cell junctions and leukocyte extravasation. *Haemostasis* 26 Suppl 4, 210-219.

Demeule, M., Regina, A., Annabi, B., Bertrand, Y., Bojanowski, M.W. and Beliveau, R. (2004). Brain endothelial cells as pharmacological targets in brain tumors. *Mol Neurobiol* 30, 157-183.

Devine, S.M., Bartholomew, A.M., Mahmud, N., Nelson, M., Patil, S., Hardy, W., Sturgeon, C., Hewett, T., Chung, T., Stock, W., Sher, D., Weissman, S., Ferrer, K., Mosca, J., Deans, R., Moseley, A. and Hoffman, R. (2001). Mesenchymal stem cells are capable of homing to the bone marrow of non-human primates following systemic infusion. *Exp Hematol* 29, 244-255.

Docheva, D., Popov, C., Mutschler, W. and Schieker, M. (2007). Human mesenchymal stem cells in contact with their environment: surface characteristics and the integrin system. *J Cell Mol Med* 11, 21-38.

Doetschman, T.C., Eistetter, H., Katz, M., Schmidt, W. and Kemler, R. (1985). The in vitro development of blastocyst-derived embryonic stem cell lines: formation of visceral yolk sac, blood islands and myocardium. *J Embryol Exp Morphol* 87, 27-45.

Dzau, V.J., Gnecchi, M. and Pachori, A.S. (2005). Enhancing stem cell therapy through genetic modification. *J Am Coll Cardiol* 46, 1351-1353.

Ellerbroek, S.M., Fishman, D.A., Kearns, A.S., Bafetti, L.M. and Stack, M.S. (1999). Ovarian carcinoma regulation of matrix metalloproteinase-2 and membrane type 1 matrix metalloproteinase through beta1 integrin. *Cancer Res* 59, 1635-1641.

Erices, A., Conget, P. and Minguell, J.J. (2000). Mesenchymal progenitor cells in human umbilical cord blood. *Br J Haematol* 109, 235-242.

Fassler, R., Rohwedel, J., Maltsev, V., Bloch, W., Lentini, S., Guan, K., Gullberg, D., Hescheler, J., Addicks, K. and Wobus, A.M. (1996). Differentiation and integrity of cardiac muscle cells are impaired in the absence of beta 1 integrin. *J Cell Sci* 109 (Pt 13), 2989-2999.

Faveeuw, C., Preece, G. and Ager, A. (2001). Transendothelial migration of lymphocytes across high endothelial venules into lymph nodes is affected by metalloproteinases. *Blood* 98, 688-695.

Fernandez, M., Simon, V., Herrera, G., Cao, C., Del Favero, H. and Minguell, J.J. (1997). Detection of stromal cells in peripheral blood progenitor cell collections from breast cancer patients. *Bone Marrow Transplant* 20, 265-271.

Fischer, S., Wiesnet, M., Renz, D. and Schaper, W. (2005). H_2O_2 induces paracellular permeability of porcine brain-derived microvascular endothelial cells by activation of the p44/42 MAP kinase pathway. *Eur J Cell Biol* 84, 687-697.

Fleming, I. and Busse, R. (2003). Molecular mechanisms involved in the regulation of the endothelial nitric oxide synthase. *Am J Physiol Regul Integr Comp Physiol* 284, R1-12.

Fox, J.M., Chamberlain, G., Ashton, B.A. and Middleton, J. (2007). Recent advances into the understanding of mesenchymal stem cell trafficking. *Br J Haematol* 137, 491-502.

Friedenstein, A.J., Gorskaja, J.F. and Kulagina, N.N. (1976). Fibroblast precursors in normal and irradiated mouse hematopoietic organs. *Exp Hematol* 4, 267-274.

Friedenstein, A.J., Chailakhyan, R.K. and Gerasimov, U.V. (1987). Bone marrow osteogenic stem cells: in vitro cultivation and transplantation in diffusion chambers. *Cell Tissue Kinet* 20, 263-272.

Furchgott, R.F. and Zawadzki, J.V. (1980). The obligatory role of endothelial cells in the relaxation of arterial smooth muscle by acetylcholine. *Nature* 288, 373-376.

Gao, J.X. and Issekutz, A.C. (1997). The beta 1 integrin, very late activation antigen-4 on human neutrophils can contribute to neutrophil migration through connective tissue fibroblast barriers. *Immunology* 90, 448-454.

Ghanem, A., Roll, W., Hashemi, T., Dewald, O., Djoufack, P.C., Fink, K.B., Schrickel, J., Lewalter, T., Luderitz, B. and Tiemann, K. (2006). Echocardiographic assessment of left ventricular mass in neonatal and adult mice: accuracy of different echocardiographic methods. *Echocardiography* 23, 900-907.

Ghanem, A., Troatz, C., Elhafi, N., Dewald, O., Heeschen, C., Nickenig, G., Stypmann, J. and Tiemann, K. (2007). Quantitation Of Myocardial Borderzone Using Reconstructive 3-D Echocardiography After Chronic Infarction In Rats-Incremental Value Of Low-Dose Dobutamine. *Ultrasound Med Biol*.

Gnecchi, M., He, H., Liang, O.D., Melo, L.G., Morello, F., Mu, H., Noiseux, N., Zhang, L., Pratt, R.E., Ingwall, J.S. and Dzau, V.J. (2005). Paracrine action accounts for marked protection of ischemic heart by Akt-modified mesenchymal stem cells. *Nat Med* 11, 367-368.

Gnecchi, M., He, H., Noiseux, N., Liang, O.D., Zhang, L., Morello, F., Mu, H., Melo, L.G., Pratt, R.E., Ingwall, J.S. and Dzau, V.J. (2006). Evidence supporting paracrine hypothesis for Akt-modified mesenchymal stem cell-mediated cardiac protection and functional improvement. *Faseb J* 20, 661-669.

Gonzalez, D., Herrera, B., Beltran, A., Otero, K., Quintero, G. and Rojas, A. (2003). Nitric oxide disrupts VE-cadherin complex in murine microvascular endothelial cells. *Biochem Biophys Res Commun* 304, 113-118.

Goodell, M.A., Jackson, K.A., Majka, S.M., Mi, T., Wang, H., Pocius, J., Hartley, C.J., Majesky, M.W., Entman, M.L., Michael, L.H. and Hirschi, K.K. (2001). Stem cell plasticity in muscle and bone marrow. *Ann N Y Acad Sci* 938, 208-218; discussion 218-220.

Gougos, A. and Letarte, M. (1988). Identification of a human endothelial cell antigen with monoclonal antibody 44G4 produced against a pre-B leukemic cell line. *J Immunol* 141, 1925-1933.

Grabovsky, V., Feigelson, S., Chen, C., Bleijs, D.A., Peled, A., Cinamon, G., Baleux, F., Arenzana-Seisdedos, F., Lapidot, T., van Kooyk, Y., Lobb, R.R. and Alon, R. (2000). Subsecond induction of alpha4 integrin clustering by immobilized chemokines stimulates leukocyte tethering and rolling on endothelial vascular cell adhesion molecule 1 under flow conditions. *J Exp Med* 192, 495-506.

Graesser, D., Mahooti, S. and Madri, J.A. (2000). Distinct roles for matrix metalloproteinase-2 and alpha4 integrin in autoimmune T cell extravasation and residency in brain parenchyma during experimental autoimmune encephalomyelitis. *J Neuroimmunol* 109, 121-131.

Haynesworth, S.E., Goshima, J., Goldberg, V.M. and Caplan, A.I. (1992). Characterization of cells with osteogenic potential from human marrow. *Bone* 13, 81-88.

He, T.C., Zhou, S., da Costa, L.T., Yu, J., Kinzler, K.W. and Vogelstein, B. (1998). A simplified system for generating recombinant adenoviruses. *Proc Natl Acad Sci U S A* 95, 2509-2514.

Hofmann, M., Wollert, K.C., Meyer, G.P., Menke, A., Arseniev, L., Hertenstein, B., Ganser, A., Knapp, W.H. and Drexler, H. (2005). Monitoring of bone marrow cell homing into the infarcted human myocardium. *Circulation* 111, 2198-2202.

Horwitz, E.M., Prockop, D.J., Fitzpatrick, L.A., Koo, W.W., Gordon, P.L., Neel, M., Sussman, M., Orchard, P., Marx, J.C., Pyeritz, R.E. and Brenner, M.K. (1999). Transplantability and therapeutic effects of bone marrow-derived mesenchymal cells in children with osteogenesis imperfecta. *Nat Med* 5, 309-313.

Hsu, S.H. and Huang, T.B. (2004). Bioeffect of ultrasound on endothelial cells in vitro. *Biomol Eng* 21, 99-104.

Hsu, S.H., Huang, T.B., Chuang, S.C., Tsai, I.J. and Chen, D.C. (2006). Ultrasound preexposure improves endothelial cell binding and retention on biomaterial surfaces. *J Biomed Mater Res B Appl Biomater* 76, 85-92.

Hung, S.C., Pochampally, R.R., Hsu, S.C., Sanchez, C., Chen, S.C., Spees, J. and Prockop, D.J. (2007). Short-term exposure of multipotent stromal cells to low oxygen increases their expression of CX3CR1 and CXCR4 and their engraftment in vivo. *PLoS ONE* 2, e416.

Hurley, J.V. (1963). An electron microscopic study of leucocytic emigration and vascular permeability in rat skin. *Aust J Exp Biol Med Sci* 41, 171-186.

Imada, T., Tatsumi, T., Mori, Y., Nishiue, T., Yoshida, M., Masaki, H., Okigaki, M., Kojima, H., Nozawa, Y., Nishiwaki, Y., Nitta, N., Iwasaka, T. and Matsubara, H. (2005). Targeted delivery of bone marrow mononuclear cells by ultrasound

destruction of microbubbles induces both angiogenesis and arteriogenesis response. *Arterioscler Thromb Vasc Biol* 25, 2128-2134.

Imaizumi, T., Nejima, J., Kiuchi, K., Takeda, S., Seino, Y., Tanaka, K. and Takano, T. (2007). Dynamics and source of endothelin-1 and interleukin-6 following coronary reperfusion in patients with acute myocardial infarction. *J Nippon Med Sch* 74, 131-147.

Imhof, B.A. and Aurrand-Lions, M. (2004). Adhesion mechanisms regulating the migration of monocytes. *Nat Rev Immunol* 4, 432-444.

In 't Anker, P.S., Scherjon, S.A., Kleijburg-van der Keur, C., de Groot-Swings, G.M., Claas, F.H., Fibbe, W.E. and Kanhai, H.H. (2004). Isolation of mesenchymal stem cells of fetal or maternal origin from human placenta. *Stem Cells* 22, 1338-1345.

Ip, J.E., Wu, Y., Huang, J., Zhang, L., Pratt, R.E. and Dzau, V.J. (2007). Mesenchymal stem cells use integrin beta1 not CXC chemokine receptor 4 for myocardial migration and engraftment. *Mol Biol Cell* 18, 2873-2882.

Isenberg, J.S. (2003). Inhibition of nitric oxide synthase (NOS) conversion of L-arginine to nitric oxide (NO) decreases low density mononuclear cell (LD MNC) trans-endothelial migration and cytokine output. *J Surg Res* 114, 100-106.

Isenberg, J.S., Tabatabi, N. and Spinelli, H.M. (2005). Nitric Oxide Modulation of Low-density Mononuclear Cell Transendothelial Migration. *Inc. Microsurgery* 25, 452-456.

Jackson, K.A., Majka, S.M., Wang, H., Pocius, J., Hartley, C.J., Majesky, M.W., Entman, M.L., Michael, L.H., Hirschi, K.K. and Goodell, M.A. (2001). Regeneration of ischemic cardiac muscle and vascular endothelium by adult stem cells. *J Clin Invest* 107, 1395-1402.

Ji, J.F., He, B.P., Dheen, S.T. and Tay, S.S. (2004). Interactions of chemokines and chemokine receptors mediate the migration of mesenchymal stem cells to the impaired site in the brain after hypoglossal nerve injury. *Stem Cells* 22, 415-427.

Jiang, Y., Jahagirdar, B.N., Reinhardt, R.L., Schwartz, R.E., Keene, C.D., Ortiz-Gonzalez, X.R., Reyes, M., Lenvik, T., Lund, T., Blackstad, M., Du, J., Aldrich, S., Lisberg, A., Low, W.C., Largaespada, D.A. and Verfaillie, C.M. (2002). Pluripotency of mesenchymal stem cells derived from adult marrow. *Nature* 418, 41-49.

Jo, D.Y., Rafii, S., Hamada, T. and Moore, M.A. (2000). Chemotaxis of primitive hematopoietic cells in response to stromal cell-derived factor-1. *J Clin Invest* 105, 101-111.

Kaminski, A., Ma, N., Donndorf, P., Lindenblatt, N., Feldmeier, G., Ong, L.L., Furlani, D., C, A.S., Liebold, A., Vollmar, B. and Steinhoff, G. (2007). Endothelial NOS is required for SDF-1alpha/CXCR4-mediated peripheral endothelial adhesion of c-kit(+) bone marrow stem cells. *Lab Invest*.

Kang, H.J., Kim, H.S., Zhang, S.Y., Park, K.W., Cho, H.J., Koo, B.K., Kim, Y.J., Soo Lee, D., Sohn, D.W., Han, K.S., Oh, B.H., Lee, M.M. and Park, Y.B. (2004). Effects of intracoronary infusion of peripheral blood stem-cells mobilised with granulocyte-colony stimulating factor on left ventricular systolic function and restenosis after coronary stenting in myocardial infarction: the MAGIC cell randomised clinical trial. *Lancet* 363, 751-756.

Kanki-Horimoto, S., Horimoto, H., Mieno, S., Kishida, K., Watanabe, F., Furuya, E. and Katsumata, T. (2006). Implantation of mesenchymal stem cells overexpressing endothelial nitric oxide synthase improves right ventricular impairments caused by pulmonary hypertension. *Circulation* 114, I181-185.

Katritsis, D.G., Sotiropoulou, P.A., Karvouni, E., Karabinos, I., Korovesis, S., Perez, S.A., Voridis, E.M. and Papamichail, M. (2005). Transcoronary transplantation of autologous mesenchymal stem cells and endothelial progenitors into infarcted human myocardium. *Catheter Cardiovasc Interv* 65, 321-329.

Kawada, H., Fujita, J., Kinjo, K., Matsuzaki, Y., Tsuma, M., Miyatake, H., Muguruma, Y., Tsuboi, K., Itabashi, Y., Ikeda, Y., Ogawa, S., Okano, H., Hotta, T., Ando, K. and Fukuda, K. (2004). Nonhematopoietic mesenchymal stem cells can be mobilized and differentiate into cardiomyocytes after myocardial infarction. *Blood* 104, 3581-3587.

Kawamoto, A., Tkebuchava, T., Yamaguchi, J., Nishimura, H., Yoon, Y.S., Milliken, C., Uchida, S., Masuo, O., Iwaguro, H., Ma, H., Hanley, A., Silver, M., Kearney, M., Losordo, D.W., Isner, J.M. and Asahara, T. (2003). Intramyocardial transplantation of autologous endothelial progenitor cells for therapeutic neovascularization of myocardial ischemia. *Circulation* 107, 461-468.

Kijowski, J., Baj-Krzyworzeka, M., Majka, M., Reca, R., Marquez, L.A., Christofidou-Solomidou, M., Janowska-Wieczorek, A. and Ratajczak, M.Z. (2001). The SDF-1-CXCR4 axis stimulates VEGF secretion and activates integrins but does not affect proliferation and survival in lymphohematopoietic cells. *Stem Cells* 19, 453-466.

Kim, K.N., Oh, S.H., Lee, K.H. and Yoon, D.H. (2006). Effect of human mesenchymal stem cell transplantation combined with growth factor infusion in the repair of injured spinal cord. *Acta Neurochir Suppl* 99, 133-136.

Kim, S.C., Ghanem, A., Stapel, H., Tiemann, K., Knuefermann, P., Hoeft, A., Meyer, R., Grohe, C., Knowlton, A.A. and Baumgarten, G. (2007). Toll-like receptor 4 deficiency: smaller infarcts, but no gain in function. *BMC Physiol* 7, 5.

Kinnaird, T., Stabile, E., Burnett, M.S., Shou, M., Lee, C.W., Barr, S., Fuchs, S. and Epstein, S.E. (2004). Local delivery of marrow-derived stromal cells augments collateral perfusion through paracrine mechanisms. *Circulation* 109, 1543-1549.

Klinz, F.J., Schmidt, A., Schinkothe, T., Arnhold, S., Desai, B., Popken, F., Brixius, K., Schwinger, R., Mehlhorn, U., Staib, P., Addicks, K. and Bloch, W. (2005). Phospho-eNOS Ser-114 in human mesenchymal stem cells: constitutive

phosphorylation, nuclear localization and upregulation during mitosis. *Eur J Cell Biol* 84, 809-818.

Kocher, A.A., Schuster, M.D., Szabolcs, M.J., Takuma, S., Burkhoff, D., Wang, J., Homma, S., Edwards, N.M. and Itescu, S. (2001). Neovascularization of ischemic myocardium by human bone-marrow-derived angioblasts prevents cardiomyocyte apoptosis, reduces remodeling and improves cardiac function. *Nat Med* 7, 430-436.

Koike, N., Fukumura, D., Gralla, O., Au, P., Schechner, J.S. and Jain, R.K. (2004). Tissue engineering: creation of long-lasting blood vessels. *Nature* 428, 138-139.

Kojima, H., Nakatsubo, N., Kikuchi, K., Kawahara, S., Kirino, Y., Nagoshi, H., Hirata, Y. and Nagano, T. (1998). Detection and imaging of nitric oxide with novel fluorescent indicators: diaminofluoresceins. *Anal Chem* 70, 2446-2453.

Kopen, G.C., Prockop, D.J. and Phinney, D.G. (1999). Marrow stromal cells migrate throughout forebrain and cerebellum, and they differentiate into astrocytes after injection into neonatal mouse brains. *Proc Natl Acad Sci U S A* 96, 10711-10716.

Korff, T. and Augustin, H.G. (1998). Integration of endothelial cells in multicellular spheroids prevents apoptosis and induces differentiation. *J Cell Biol* 143, 1341-1352.

Krampera, M., Glennie, S., Dyson, J., Scott, D., Laylor, R., Simpson, E. and Dazzi, F. (2003). Bone marrow mesenchymal stem cells inhibit the response of naive and memory antigen-specific T cells to their cognate peptide. *Blood* 101, 3722-3729.

Krause, U., Harter, C., Seckinger, A., Wolf, D., Reinhard, A., Bea, F., Dengler, T., Hardt, S., Ho, A., Katus, H.A., Kuecherer, H. and Hansen, A. (2007). Intravenous delivery of autologous mesenchymal stem cells limits infarct size and improves left ventricular function in the infarcted porcine heart. *Stem Cells Dev* 16, 31-37.

Kuwabara, K., Ogawa, S., Matsumoto, M., Koga, S., Clauss, M., Pinsky, D.J., Lyn, P., Leavy, J., Witte, L., Joseph-Silverstein, J. and et al. (1995). Hypoxia-mediated induction of acidic/basic fibroblast growth factor and platelet-derived growth factor in mononuclear phagocytes stimulates growth of hypoxic endothelial cells. *Proc Natl Acad Sci U S A* 92, 4606-4610.

Kuznetsov, S.A., Krebsbach, P.H., Satomura, K., Kerr, J., Riminucci, M., Benayahu, D. and Robey, P.G. (1997). Single-colony derived strains of human marrow stromal fibroblasts form bone after transplantation in vivo. *J Bone Miner Res* 12, 1335-1347.

Lacy, F., O'Connor, D.T. and Schmid-Schonbein, G.W. (1998). Plasma hydrogen peroxide production in hypertensives and normotensive subjects at genetic risk of hypertension. *J Hypertens* 16, 291-303.

Ladage, D., Brixius, K., Steingen, C., Mehlhorn, U., Schwinger, R.H., Bloch, W. and Schmidt, A. (2007). Mesenchymal stem cells induce endothelial activation via paracine mechanisms. *Endothelium* 14, 53-63.

Laflamme, M.A. and Murry, C.E. (2005). Regenerating the heart. *Nat Biotechnol* 23, 845-856.

Laitinen, L. (1987). Griffonia simplicifolia lectins bind specifically to endothelial cells and some epithelial cells in mouse tissues. *Histochem J* 19, 225-234.

Lapidot, T. and Kollet, O. (2002). The essential roles of the chemokine SDF-1 and its receptor CXCR4 in human stem cell homing and repopulation of transplanted immune-deficient NOD/SCID and NOD/SCID/B2m(null) mice. *Leukemia* 16, 1992-2003.

Lauffenburger, D.A. and Horwitz, A.F. (1996). Cell migration: a physically integrated molecular process. *Cell* 84, 359-369.

Le Blanc, K., Tammik, L., Sundberg, B., Haynesworth, S.E. and Ringden, O. (2003). Mesenchymal stem cells inhibit and stimulate mixed lymphocyte cultures and mitogenic responses independently of the major histocompatibility complex. *Scand J Immunol* 57, 11-20.

Le Blanc, K., Rasmusson, I., Sundberg, B., Gotherstrom, C., Hassan, M., Uzunel, M. and Ringden, O. (2004). Treatment of severe acute graft-versus-host disease with third party haploidentical mesenchymal stem cells. *Lancet* 363, 1439-1441.

Lee, B.C., Lee, T.H., Avraham, S. and Avraham, H.K. (2004a). Involvement of the chemokine receptor CXCR4 and its ligand stromal cell-derived factor 1alpha in breast cancer cell migration through human brain microvascular endothelial cells. *Mol Cancer Res* 2, 327-338.

Lee, R.H., Kim, B., Choi, I., Kim, H., Choi, H.S., Suh, K., Bae, Y.C. and Jung, J.S. (2004b). Characterization and expression analysis of mesenchymal stem cells from human bone marrow and adipose tissue. *Cell Physiol Biochem* 14, 311-324.

Lee, R.H., Hsu, S.C., Munoz, J., Jung, J.S., Lee, N.R., Pochampally, R. and Prockop, D.J. (2006). A subset of human rapidly self-renewing marrow stromal cells preferentially engraft in mice. *Blood* 107, 2153-2161.

Lehmann, J.M., Lenhard, J.M., Oliver, B.B., Ringold, G.M. and Kliewer, S.A. (1997). Peroxisome proliferator-activated receptors alpha and gamma are activated by indomethacin and other non-steroidal anti-inflammatory drugs. *J Biol Chem* 272, 3406-3410.

Leppert, D., Waubant, E., Galardy, R., Bunnett, N.W. and Hauser, S.L. (1995). T cell gelatinases mediate basement membrane transmigration in vitro. *J Immunol* 154, 4379-4389.

Li, T.S., Hayashi, M., Ito, H., Furutani, A., Murata, T., Matsuzaki, M. and Hamano, K. (2005a). Regeneration of infarcted myocardium by intramyocardial implantation of ex vivo transforming growth factor-beta-preprogrammed bone marrow stem cells. *Circulation* 111, 2438-2445.

Li, W.J., Tuli, R., Okafor, C., Derfoul, A., Danielson, K.G., Hall, D.J. and Tuan, R.S. (2005b). A three-dimensional nanofibrous scaffold for cartilage tissue engineering using human mesenchymal stem cells. *Biomaterials* 26, 599-609.

Lieber, A., Sandig, V. and Strauss, M. (1993). A mutant T7 phage promoter is specifically transcribed by T7-RNA polymerase in mammalian cells. *Eur J Biochem* 217, 387-394.

Liu, F., Aubin, J.E. and Malaval, L. (2002). Expression of leukemia inhibitory factor (LIF)/interleukin-6 family cytokines and receptors during in vitro osteogenesis: differential regulation by dexamethasone and LIF. *Bone* 31, 212-219.

Lohmaier, S., Ghanem, A., Veltmann, C., Sommer, T., Bruce, M. and Tiemann, K. (2004). In vitro and in vivo studies on continuous echo-contrast application strategies using SonoVue in a newly developed rotating pump setup. *Ultrasound Med Biol* 30, 1145-1151.

Lowry, O.H., Rosebrough, N.J., Farr, A.L. and Randall, R.J. (1951). Protein measurement with the Folin phenol reagent. *J Biol Chem* 193, 265-275.

Lu, D., Mahmood, A., Wang, L., Li, Y., Lu, M. and Chopp, M. (2001). Adult bone marrow stromal cells administered intravenously to rats after traumatic brain injury migrate into brain and improve neurological outcome. *Neuroreport* 12, 559-563.

Majors, A.K., Boehm, C.A., Nitto, H., Midura, R.J. and Muschler, G.F. (1997). Characterization of human bone marrow stromal cells with respect to osteoblastic differentiation. *J Orthop Res* 15, 546-557.

Mangi, A.A., Noiseux, N., Kong, D., He, H., Rezvani, M., Ingwall, J.S. and Dzau, V.J. (2003). Mesenchymal stem cells modified with Akt prevent remodeling and restore performance of infarcted hearts. *Nat Med* 9, 1195-1201.

Mantovani, A., Bussolino, F. and Dejana, E. (1992). Cytokine regulation of endothelial cell function. *Faseb J* 6, 2591-2599.

Marchesi, V.T. and Florey, H.W. (1960). Electron micrographic observations on the emigration of leucocytes. *Q J Exp Physiol Cogn Med Sci* 45, 343-348.

Martin, I., Muraglia, A., Campanile, G., Cancedda, R. and Quarto, R. (1997). Fibroblast growth factor-2 supports ex vivo expansion and maintenance of osteogenic precursors from human bone marrow. *Endocrinology* 138, 4456-4462.

Maschio, A.D., Zanetti, A., Corada, M., Rival, Y., Ruco, L., Lampugnani, M.G. and Dejana, E. (1996). Polymorphonuclear Leukocyte Adhesion Triggers the Disorganization of Endothelial Cell-to-Cell Adherens Junctions. *The Journal of Cell Biology* 135, 497-510.

Meinel, L., Karageorgiou, V., Fajardo, R., Snyder, B., Shinde-Patil, V., Zichner, L., Kaplan, D., Langer, R. and Vunjak-Novakovic, G. (2004a). Bone tissue engineering

using human mesenchymal stem cells: effects of scaffold material and medium flow. *Ann Biomed Eng* 32, 112-122.

Meinel, L., Karageorgiou, V., Hofmann, S., Fajardo, R., Snyder, B., Li, C., Zichner, L., Langer, R., Vunjak-Novakovic, G. and Kaplan, D.L. (2004b). Engineering bone-like tissue in vitro using human bone marrow stem cells and silk scaffolds. *J Biomed Mater Res A* 71, 25-34.

Miller, D.L., Li, P., Dou, C., Armstrong, W.F. and Gordon, D. (2007). Evans Blue Staining Of Cardiomyocytes Induced By Myocardial Contrast Echocardiography In Rats: Evidence For Necrosis Instead Of Apoptosis. *Ultrasound Med Biol*.

Minguell, J.J., Erices, A. and Conget, P. (2001). Mesenchymal stem cells. *Exp Biol Med (Maywood)* 226, 507-520.

Mirotsou, M., Zhang, Z., Deb, A., Zhang, L., Gnecchi, M., Noiseux, N., Mu, H., Pachori, A. and Dzau, V. (2007). Secreted frizzled related protein 2 (Sfrp2) is the key Akt-mesenchymal stem cell-released paracrine factor mediating myocardial survival and repair. *Proc Natl Acad Sci U S A* 104, 1643-1648.

Mitchell, M.D., Laird, R.E., Brown, R.D. and Long, C.S. (2007). IL-1beta stimulates rat cardiac fibroblast migration via MAP kinase pathways. *Am J Physiol Heart Circ Physiol* 292, H1139-1147.

Miyamoto, S., Teramoto, H., Coso, O.A., Gutkind, J.S., Burbelo, P.D., Akiyama, S.K. and Yamada, K.M. (1995). Integrin function: molecular hierarchies of cytoskeletal and signaling molecules. *J Cell Biol* 131, 791-805.

Montoya, M.C., Luscinskas, F.W., del Pozo, M.A., Aragones, J. and de Landazuri, M.O. (1997). Reduced intracellular oxidative metabolism promotes firm adhesion of human polymorphonuclear leukocytes to vascular endothelium under flow conditions. *Eur J Immunol* 27, 1942-1951.

Muller-Ehmsen, J., Schmidt, A., Krausgrill, B., Schwinger, R.H. and Bloch, W. (2006). Role of erythropoietin for angiogenesis and vasculogenesis: from embryonic development through adulthood. *Am J Physiol Heart Circ Physiol* 290, H331-340.

Nagase, H. and Woessner, J.F., Jr. (1999). Matrix metalloproteinases. *J Biol Chem* 274, 21491-21494.

Nagaya, N., Fujii, T., Iwase, T., Ohgushi, H., Itoh, T., Uematsu, M., Yamagishi, M., Mori, H., Kangawa, K. and Kitamura, S. (2004). Intravenous administration of mesenchymal stem cells improves cardiac function in rats with acute myocardial infarction through angiogenesis and myogenesis. *Am J Physiol Heart Circ Physiol* 287, H2670-2676.

Nossuli, T.O., Lakshminarayanan, V., Baumgarten, G., Taffet, G.E., Ballantyne, C.M., Michael, L.H. and Entman, M.L. (2000). A chronic mouse model of myocardial ischemia-reperfusion: essential in cytokine studies. *Am J Physiol Heart Circ Physiol* 278, H1049-1055.

Nygren, J.M., Jovinge, S., Breitbach, M., Sawen, P., Roll, W., Hescheler, J., Taneera, J., Fleischmann, B.K. and Jacobsen, S.E. (2004). Bone marrow-derived hematopoietic cells generate cardiomyocytes at a low frequency through cell fusion, but not transdifferentiation. *Nat Med* 10, 494-501.

Oh, I., Ozaki, K., Sato, K., Meguro, A., Tatara, R., Hatanaka, K., Nagai, T., Muroi, K. and Ozawa, K. (2007). Interferon-gamma and NF-kappaB mediate nitric oxide production by mesenchymal stromal cells. *Biochem Biophys Res Commun* 355, 956-962.

Oh, L.Y., Larsen, P.H., Krekoski, C.A., Edwards, D.R., Donovan, F., Werb, Z. and Yong, V.W. (1999). Matrix metalloproteinase-9/gelatinase B is required for process outgrowth by oligodendrocytes. *J Neurosci* 19, 8464-8475.

Ohnishi, S., Ohgushi, H., Kitamura, S. and Nagaya, N. (2007). Mesenchymal stem cells for the treatment of heart failure. *Int J Hematol* 86, 17-21.

Orlic, D., Kajstura, J., Chimenti, S., Jakoniuk, I., Anderson, S.M., Li, B., Pickel, J., McKay, R., Nadal-Ginard, B., Bodine, D.M., Leri, A. and Anversa, P. (2001a). Bone marrow cells regenerate infarcted myocardium. *Nature* 410, 701-705.

Orlic, D., Kajstura, J., Chimenti, S., Limana, F., Jakoniuk, I., Quaini, F., Nadal-Ginard, B., Bodine, D.M., Leri, A. and Anversa, P. (2001b). Mobilized bone marrow cells repair the infarcted heart, improving function and survival. *Proc Natl Acad Sci U S A* 98, 10344-10349.

Orlic, D., Hill, J.M. and Arai, A.E. (2002). Stem cells for myocardial regeneration. *Circ Res* 91, 1092-1102.

Osborn, L., Hession, C., Tizard, R., Vassallo, C., Luhowskyj, S., Chi-Rosso, G. and Lobb, R. (1989). Direct expression cloning of vascular cell adhesion molecule 1, a cytokine-induced endothelial protein that binds to lymphocytes. *Cell* 59, 1203-1211.

Paravicini, T.M. and Touyz, R.M. (2006). Redox signaling in hypertension. *Cardiovasc Res* 71, 247-258.

Park, J.E., Keller, G.A. and Ferrara, N. (1993). The vascular endothelial growth factor (VEGF) isoforms: differential deposition into the subepithelial extracellular matrix and bioactivity of extracellular matrix-bound VEGF. *Mol Biol Cell* 4, 1317-1326.

Pasqui, A.L., Di Renzo, M., Bova, G., Maffei, S., Pompella, G., Auteri, A. and Puccetti, L. (2006). Pro-inflammatory/anti-inflammatory cytokine imbalance in acute coronary syndromes. *Clin Exp Med* 6, 38-44.

Pawlowski, N.A., Kaplan, G., Abraham, E. and Chon, Z.A. (1988). The Selective Binding and Transmigration of Monocytes through the Junctional Complexes of Human Endothelium. *J. Exp. Med.* 168, 1865-1882.

Perin, E.C., Dohmann, H.F., Borojevic, R., Silva, S.A., Sousa, A.L., Mesquita, C.T., Rossi, M.I., Carvalho, A.C., Dutra, H.S., Dohmann, H.J., Silva, G.V., Belem, L.,

Vivacqua, R., Rangel, F.O., Esporcatte, R., Geng, Y.J., Vaughn, W.K., Assad, J.A., Mesquita, E.T. and Willerson, J.T. (2003). Transendocardial, autologous bone marrow cell transplantation for severe, chronic ischemic heart failure. *Circulation* 107, 2294-2302.

Phinney, D.G., Kopen, G., Isaacson, R.L. and Prockop, D.J. (1999). Plastic adherent stromal cells from the bone marrow of commonly used strains of inbred mice: variations in yield, growth, and differentiation. *J Cell Biochem* 72, 570-585.

Pittenger, M.F., Mackay, A.M., Beck, S.C., Jaiswal, R.K., Douglas, R., Mosca, J.D., Moorman, M.A., Simonetti, D.W., Craig, S. and Marshak, D.R. (1999). Multilineage Potential of Adult Human Mesenchymal Stem Cells. *Science* 284, 143-147.

Pittenger, M.F., Mosca, J.D. and McIntosh, K.R. (2000). Human mesenchymal stem cells: progenitor cells for cartilage, bone, fat and stroma. *Curr Top Microbiol Immunol* 251, 3-11.

Pittenger, M.F. and Martin, B.J. (2004). Mesenchymal stem cells and their potential as cardiac therapeutics. *Circ Res* 95, 9-20.

Ponomaryov, T., Peled, A., Petit, I., Taichman, R.S., Habler, L., Sandbank, J., Arenzana-Seisdedos, F., Magerus, A., Caruz, A., Fujii, N., Nagler, A., Lahav, M., Szyper-Kravitz, M., Zipori, D. and Lapidot, T. (2000). Induction of the chemokine stromal-derived factor-1 following DNA damage improves human stem cell function. *J Clin Invest* 106, 1331-1339.

Porter, G.A., Palade, G.E. and Milici, A.J. (1990). Differential binding of the lectins Griffonia simplicifolia I and Lycopersicon esculentum to microvascular endothelium: organ-specific localization and partial glycoprotein characterization. *Eur J Cell Biol* 51, 85-95.

Price, M.J., Chou, C.C., Frantzen, M., Miyamoto, T., Kar, S., Lee, S., Shah, P.K., Martin, B.J., Lill, M., Forrester, J.S., Chen, P.S. and Makkar, R.R. (2006). Intravenous mesenchymal stem cell therapy early after reperfused acute myocardial infarction improves left ventricular function and alters electrophysiologic properties. *Int J Cardiol* 111, 231-239.

Pyo, R.T., Sui, J., Dhume, A., Palomeque, J., Blaxall, B.C., Diaz, G., Tunstead, J., Logothetis, D.E., Hajjar, R.J. and Schecter, A.D. (2006). CXCR4 modulates contractility in adult cardiac myocytes. *J Mol Cell Cardiol* 41, 834-844.

Qin, G., Ii, M., Silver, M., Wecker, A., Bord, E., Ma, H., Gavin, M., Goukassian, D.A., Yoon, Y.S., Papayannopoulou, T., Asahara, T., Kearney, M., Thorne, T., Curry, C., Eaton, L., Heyd, L., Dinesh, D., Kishore, R., Zhu, Y. and Losordo, D.W. (2006). Functional disruption of alpha4 integrin mobilizes bone marrow-derived endothelial progenitors and augments ischemic neovascularization. *J Exp Med* 203, 153-163.

Reher, P., Doan, N., Bradnock, B., Meghji, S. and Harris, M. (1999). Effect of ultrasound on the production of IL-8, basic FGF and VEGF. *Cytokine* 11, 416-423.

Reyes, M., Dudek, A., Jahagirdar, B., Koodie, L., Marker, P.H. and Verfaillie, C.M. (2002). Origin of endothelial progenitors in human postnatal bone marrow. *J Clin Invest* 109, 337-346.

Ridger, V.C., Wagner, B.E., Wallace, W.A. and Hellewell, P.G. (2001). Differential effects of CD18, CD29, and CD49 integrin subunit inhibition on neutrophil migration in pulmonary inflammation. *J Immunol* 166, 3484-3490.

Ries, C., Egea, V., Karow, M., Kolb, H., Jochum, M. and Neth, P. (2007). MMP-2, MT1-MMP, and TIMP-2 are essential for the invasive capacity of human mesenchymal stem cells: differential regulation by inflammatory cytokines. *Blood* 109, 4055-4063.

Ruster, B., Gottig, S., Ludwig, R.J., Bistrian, R., Muller, S., Seifried, E., Gille, J. and Henschler, R. (2006). Mesenchymal stem cells (MSCs) display coordinated rolling and adhesion behavior on endothelial cells. *Blood*.

Saito, T., Kuang, J.Q., Bittira, B., Al-Khaldi, A. and Chiu, R.C. (2002). Xenotransplant cardiac chimera: immune tolerance of adult stem cells. *Ann Thorac Surg* 74, 19-24; discussion 24.

Sasaki, K., Heeschen, C., Aicher, A., Ziebart, T., Honold, J., Urbich, C., Rossig, L., Koehl, U., Koyanagi, M., Mohamed, A., Brandes, R.P., Martin, H., Zeiher, A.M. and Dimmeler, S. (2006). Ex vivo pretreatment of bone marrow mononuclear cells with endothelial NO synthase enhancer AVE9488 enhances their functional activity for cell therapy. *Proc Natl Acad Sci U S A* 103, 14537-14541.

Sasaki, Y., Kawamoto, A., Iwano, M., Kurioka, H., Takase, E., Kawata, H., Tsujimura, S., Fukuhara, S., Akai, Y., Hashimoto, T. and Dohi, K. (2001). Vascular endothelial growth factor mRNA synthesis by peripheral blood mononuclear cells in patients with acute myocardial infarction. *Int J Cardiol* 81, 51-60.

Sato, K., Ozaki, K., Oh, I., Meguro, A., Hatanaka, K., Nagai, T., Muroi, K. and Ozawa, K. (2007). Nitric oxide plays a critical role in suppression of T-cell proliferation by mesenchymal stem cells. *Blood* 109, 228-234.

Schachinger, V., Assmus, B., Britten, M.B., Honold, J., Lehmann, R., Teupe, C., Abolmaali, N.D., Vogl, T.J., Hofmann, W.K., Martin, H., Dimmeler, S. and Zeiher, A.M. (2004). Transplantation of progenitor cells and regeneration enhancement in acute myocardial infarction: final one-year results of the TOPCARE-AMI Trial. *J Am Coll Cardiol* 44, 1690-1699.

Schluesener, H.J. and Xianglin, T. (2004). Selection of recombinant phages binding to pathological endothelial and tumor cells of rat glioblastoma by in-vivo display. *J Neurol Sci* 224, 77-82.

Schmidt, A. (2003). The vascular development is modulated by endostatin and restin, University of Cologne, Cologne.

Schmidt, A., Addicks, K. and Bloch, W. (2004a). Opposite effects of endostatin on different endothelial cells. *Cancer Biol Ther* 3, 1162-1166; discussion 1167-1168.

Schmidt, A., Wenzel, D., Ferring, I., Kazemi, S., Sasaki, T., Hescheler, J., Timpl, R., Addicks, K., Fleischmann, B.K. and Bloch, W. (2004b). Influence of endostatin on embryonic vasculo- and angiogenesis. *Dev Dyn* 230, 468-480.

Schmidt, A., Ladage, D., Schinkothe, T., Klausmann, U., Ulrichs, C., Klinz, F.J., Brixius, K., Arnhold, S., Desai, B., Mehlhorn, U., Schwinger, R.H., Staib, P., Addicks, K. and Bloch, W. (2006a). Basic fibroblast growth factor controls migration in human mesenchymal stem cells. *Stem Cells* 24, 1750-1758.

Schmidt, A., Ladage, D., Steingen, C., Brixius, K., Schinkothe, T., Klinz, F.J., Schwinger, R.H., Mehlhorn, U. and Bloch, W. (2006b). Mesenchymal stem cells transmigrate over the endothelial barrier. *Eur J Cell Biol* 85, 1179-1188.

Schmidt, A., Bierwirth, S., Weber, S., Platen, P., Schinkothe, T. and Bloch, W. (2007). Short intensive exercise increase the migratory activity of mesenchymal stem cells. *Br J Sports Med*.

Seely, A.J., Pascual, J.L. and Christou, N.V. (2003). Science review: Cell membrane expression (connectivity) regulates neutrophil delivery, function and clearance. *Crit Care* 7, 291-307.

Segers, V.F., Van Riet, I., Andries, L.J., Lemmens, K., Demolder, M.J., De Becker, A.J., Kockx, M.M. and De Keulenaer, G.W. (2006). Mesenchymal stem cell adhesion to cardiac microvascular endothelium: activators and mechanisms. *Am J Physiol Heart Circ Physiol* 290, H1370-1377.

Sekiya, I., Colter, D.C. and Prockop, D.J. (2001). BMP-6 enhances chondrogenesis in a subpopulation of human marrow stromal cells. *Biochem Biophys Res Commun* 284, 411-418.

Shih, D.T., Lee, D.C., Chen, S.C., Tsai, R.Y., Huang, C.T., Tsai, C.C., Shen, E.Y. and Chiu, W.T. (2005). Isolation and characterization of neurogenic mesenchymal stem cells in human scalp tissue. *Stem Cells* 23, 1012-1020.

Shioi, T., Matsumori, A., Kihara, Y., Inoko, M., Ono, K., Iwanaga, Y., Yamada, T., Iwasaki, A., Matsushima, K. and Sasayama, S. (1997). Increased expression of interleukin-1 beta and monocyte chemotactic and activating factor/monocyte chemoattractant protein-1 in the hypertrophied and failing heart with pressure overload. *Circ Res* 81, 664-671.

Shohet, R.V., Chen, S., Zhou, Y.T., Wang, Z., Meidell, R.S., Unger, R.H. and Grayburn, P.A. (2000). Echocardiographic destruction of albumin microbubbles directs gene delivery to the myocardium. *Circulation* 101, 2554-2556.

Shur, I., Reish, O., Ezra, E. and Benayahu, D. (2004). Analysis of mesenchymal cells derived from an chondrodysplasia punctuate patient and donors. *J Cell Biochem* 93, 112-119.

Simionescu, M. and Simionescu, N. (1991). Endothelial transport of macromolecules: transcytosis and endocytosis. A look from cell biology. *Cell Biol Rev* 25, 1-78.

Skyba, D.M., Price, R.J., Linka, A.Z., Skalak, T.C. and Kaul, S. (1998). Direct in vivo visualization of intravascular destruction of microbubbles by ultrasound and its local effects on tissue. *Circulation* 98, 290-293.

Son, B.R., Marquez-Curtis, L.A., Kucia, M., Wysoczynski, M., Turner, A.R., Ratajczak, J., Ratajczak, M.Z. and Janowska-Wieczorek, A. (2006). Migration of bone marrow and cord blood mesenchymal stem cells in vitro is regulated by stromal-derived factor-1-CXCR4 and hepatocyte growth factor-c-met axes and involves matrix metalloproteinases. *Stem Cells* 24, 1254-1264.

Song, J., Cottler, P.S., Klibanov, A.L., Kaul, S. and Price, R.J. (2004). Microvascular remodeling and accelerated hyperemia blood flow restoration in arterially occluded skeletal muscle exposed to ultrasonic microbubble destruction. *Am J Physiol Heart Circ Physiol* 287, H2754-2761.

Sorokin, L., Girg, W., Gopfert, T., Hallmann, R. and Deutzmann, R. (1994). Expression of novel 400-kDa laminin chains by mouse and bovine endothelial cells. *Eur J Biochem* 223, 603-610.

Stamm, C., Westphal, B., Kleine, H.D., Petzsch, M., Kittner, C., Klinge, H., Schumichen, C., Nienaber, C.A., Freund, M. and Steinhoff, G. (2003). Autologous bone-marrow stem-cell transplantation for myocardial regeneration. *Lancet* 361, 45-46.

Stavri, G.T., Zachary, I.C., Baskerville, P.A., Martin, J.F. and Erusalimsky, J.D. (1995). Basic fibroblast growth factor upregulates the expression of vascular endothelial growth factor in vascular smooth muscle cells. Synergistic interaction with hypoxia. *Circulation* 92, 11-14.

Sternlicht, M.D. and Werb, Z. (2001). How matrix metalloproteinases regulate cell behavior. *Annu Rev Cell Dev Biol* 17, 463-516.

Stieger, S.M., Caskey, C.F., Adamson, R.H., Qin, S., Curry, F.R., Wisner, E.R. and Ferrara, K.W. (2007). Enhancement of vascular permeability with low-frequency contrast-enhanced ultrasound in the chorioallantoic membrane model. *Radiology* 243, 112-121.

Strauer, B.E., Brehm, M., Zeus, T., Gattermann, N., Hernandez, A., Sorg, R.V., Kogler, G. and Wernet, P. (2001). [Intracoronary, human autologous stem cell transplantation for myocardial regeneration following myocardial infarction]. *Dtsch Med Wochenschr* 126, 932-938.

Strauer, B.E., Brehm, M., Zeus, T., Kostering, M., Hernandez, A., Sorg, R.V., Kogler, G. and Wernet, P. (2002). Repair of infarcted myocardium by autologous intracoronary mononuclear bone marrow cell transplantation in humans. *Circulation* 106, 1913-1918.

Suttorp, N., Toepfer, W. and Roka, L. (1986). Antioxidant defense mechanisms of endothelial cells: glutathione redox cycle versus catalase. *Am J Physiol* 251, C671-680.

Taniyama, Y., Tachibana, K., Hiraoka, K., Aoki, M., Yamamoto, S., Matsumoto, K., Nakamura, T., Ogihara, T., Kaneda, Y. and Morishita, R. (2002a). Development of safe and efficient novel nonviral gene transfer using ultrasound: enhancement of transfection efficiency of naked plasmid DNA in skeletal muscle. *Gene Ther* 9, 372-380.

Taniyama, Y., Tachibana, K., Hiraoka, K., Namba, T., Yamasaki, K., Hashiya, N., Aoki, M., Ogihara, T., Yasufumi, K. and Morishita, R. (2002b). Local delivery of plasmid DNA into rat carotid artery using ultrasound. *Circulation* 105, 1233-1239.

Templin, C., Kotlarz, D., Marquart, F., Faulhaber, J., Brendecke, V., Schaefer, A., Tsikas, D., Bonda, T., Hilfiker-Kleiner, D., Ohl, L., Naim, H.Y., Foerster, R., Drexler, H. and Limbourg, F.P. (2006). Transcoronary delivery of bone marrow cells to the infarcted murine myocardium: feasibility, cellular kinetics, and improvement in cardiac function. *Basic Res Cardiol* 101, 301-310.

Timpl, R. (1996). Macromolecular organization of basement membranes. *Curr Opin Cell Biol* 8, 618-624.

Toma, C., Pittenger, M.F., Cahill, K.S., Byrne, B.J. and Kessler, P.D. (2002). Human mesenchymal stem cells differentiate to a cardiomyocyte phenotype in the adult murine heart. *Circulation* 105, 93-98.

Toma, J.G., Akhavan, M., Fernandes, K.J., Barnabe-Heider, F., Sadikot, A., Kaplan, D.R. and Miller, F.D. (2001). Isolation of multipotent adult stem cells from the dermis of mammalian skin. *Nat Cell Biol* 3, 778-784.

Tomita, S., Li, R.K., Weisel, R.D., Mickle, D.A., Kim, E.J., Sakai, T. and Jia, Z.Q. (1999). Autologous transplantation of bone marrow cells improves damaged heart function. *Circulation* 100, II247-256.

Tse, H.F., Kwong, Y.L., Chan, J.K., Lo, G., Ho, C.L. and Lau, C.P. (2003a). Angiogenesis in ischaemic myocardium by intramyocardial autologous bone marrow mononuclear cell implantation. *Lancet* 361, 47-49.

Tse, W.T., Pendleton, J.D., Beyer, W.M., Egalka, M.C. and Guinan, E.C. (2003b). Suppression of allogeneic T-cell proliferation by human marrow stromal cells: implications in transplantation. *Transplantation* 75, 389-397.

Tuan, R.S., Boland, G. and Tuli, R. (2002). Adult mesenchymal stem cells and cell-based tissue engineering. *Arthritis Research and Therapy* 5, 32-45.

Vaday, G.G., Hershkoviz, R., Rahat, M.A., Lahat, N., Cahalon, L. and Lider, O. (2000). Fibronectin-bound TNF-alpha stimulates monocyte matrix metalloproteinase-9 expression and regulates chemotaxis. *J Leukoc Biol* 68, 737-747.

Vaday, G.G., Franitza, S., Schor, H., Hecht, I., Brill, A., Cahalon, L., Hershkoviz, R. and Lider, O. (2001). Combinatorial signals by inflammatory cytokines and chemokines mediate leukocyte interactions with extracellular matrix. *J Leukoc Biol* 69, 885-892.

Wang, J.S., Shum-Tim, D., Galipeau, J., Chedrawy, E., Eliopoulos, N. and Chiu, R.C. (2000). Marrow stromal cells for cellular cardiomyoplasty: feasibility and potential clinical advantages. *J Thorac Cardiovasc Surg* 120, 999-1005.

Wang, J.S., Shum-Tim, D., Chedrawy, E. and Chiu, R.C. (2001). The coronary delivery of marrow stromal cells for myocardial regeneration: pathophysiologic and therapeutic implications. *J Thorac Cardiovasc Surg* 122, 699-705.

Wang, S., Voisin, M.B., Larbi, K.Y., Dangerfield, J., Scheiermann, C., Tran, M., Maxwell, P.H., Sorokin, L. and Nourshargh, S. (2006). Venular basement membranes contain specific matrix protein low expression regions that act as exit points for emigrating neutrophils. *J Exp Med* 203, 1519-1532.

Werr, J., Xie, X., Hedqvist, P., Ruoslahti, E. and Lindbom, L. (1998). beta1 integrins are critically involved in neutrophil locomotion in extravascular tissue In vivo. *J Exp Med* 187, 2091-2096.

Wisithphrom, K., Murray, P.E. and Windsor, L.J. (2006). Interleukin-1 alpha alters the expression of matrix metalloproteinases and collagen degradation by pulp fibroblasts. *J Endod* 32, 186-192.

Wollert, K.C., Meyer, G.P., Lotz, J., Ringes-Lichtenberg, S., Lippolt, P., Breidenbach, C., Fichtner, S., Korte, T., Hornig, B., Messinger, D., Arseniev, L., Hertenstein, B., Ganser, A. and Drexler, H. (2004). Intracoronary autologous bone-marrow cell transfer after myocardial infarction: the BOOST randomised controlled clinical trial. *Lancet* 364, 141-148.

Wollert, K.C. and Drexler, H. (2005). Clinical applications of stem cells for the heart. *Circ Res* 96, 151-163.

Wong, D., Prameya, R. and Dorovini-Zis, K. (1999). In vitro adhesion and migration of T lymphocytes across monolayers of human brain microvessel endothelial cells: regulation by ICAM-1, VCAM-1, E-selectin and PECAM-1. *J Neuropathol Exp Neurol* 58, 138-152.

Wynn, R.F., Hart, C.A., Corradi-Perini, C., O'Neill, L., Evans, C.A., Wraith, J.E., Fairbairn, L.J. and Bellantuono, I. (2004). A small proportion of mesenchymal stem cells strongly expresses functionally active CXCR4 receptor capable of promoting migration to bone marrow. *Blood* 104, 2643-2645.

Yan, S.J. and Blomme, E.A. (2003). In situ zymography: a molecular pathology technique to localize endogenous protease activity in tissue sections. *Vet Pathol* 40, 227-236.

Yong, K.L., Watts, M., Shaun Thomas, N., Sullivan, A., Ings, S. and Linch, D.C. (1998). Transmigration of CD34+ cells across specialized and nonspecialized endothelium requires prior activation by growth factors and is mediated by PECAM-1 (CD31). *Blood* 91, 1196-1205.

Yoon, Y.S., Wecker, A., Heyd, L., Park, J.S., Tkebuchava, T., Kusano, K., Hanley, A., Scadova, H., Qin, G., Cha, D.H., Johnson, K.L., Aikawa, R., Asahara, T. and Losordo, D.W. (2005). Clonally expanded novel multipotent stem cells from human bone marrow regenerate myocardium after myocardial infarction. *J Clin Invest* 115, 326-338.

Yung, L.M., Leung, F.P., Yao, X., Chen, Z.Y. and Huang, Y. (2006). Reactive oxygen species in vascular wall. *Cardiovasc Hematol Disord Drug Targets* 6, 1-19.

Zen, K., Okigaki, M., Hosokawa, Y., Adachi, Y., Nozawa, Y., Takamiya, M., Tatsumi, T., Urao, N., Tateishi, K., Takahashi, T. and Matsubara, H. (2006). Myocardium-targeted delivery of endothelial progenitor cells by ultrasound-mediated microbubble destruction improves cardiac function via an angiogenic response. *J Mol Cell Cardiol* 40, 799-809.

Zuk, P.A., Zhu, M., Ashjian, P., De Ugarte, D.A., Huang, J.I., Mizuno, H., Alfonso, Z.C., Fraser, J.K., Benhaim, P. and Hedrick, M.H. (2002). Human adipose tissue is a source of multipotent stem cells. *Mol Biol Cell* 13, 4279-4295.

Zwezdaryk, K.J., Coffelt, S.B., Figueroa, Y.G., Liu, J., Phinney, D.G., LaMarca, H.L., Florez, L., Morris, C.B., Hoyle, G.W. and Scandurro, A.B. (2007). Erythropoietin, a hypoxia-regulated factor, elicits a pro-angiogenic program in human mesenchymal stem cells. *Exp Hematol* 35, 640-652.

Danksagung

Die vorliegende Arbeit wurde am Institut für Kreislaufforschung und Sportmedizin, Abteilung für Molekulare und Zelluläre Sportmedizin, der Deutschen Sporthochschule Köln unter der Anleitung von Herrn Professor Dr. W. Bloch angefertigt.

Herrn Professor Dr. W. Bloch danke ich für die Überlassung des interessanten Themas und die große Freiheit, die mir bei der Bearbeitung zuteil geworden ist. Sehr herzlich bedanke ich mich für seine Unterstützung und Förderung, sowie für die vielen hilfreichen Gespräche und Anregungen.

Herrn Professor Dr. M. Pasparakis danke ich für die Übernahme des Koreferats.

Herrn Professor Dr. J. Schmidt und seinen Mitarbeitern am Dreifaltigkeitskrankenhaus danke ich für die gute Zusammenarbeit.

Zudem gilt mein Dank allen Mitarbeitern des Instituts für Molekulare und Zelluläre Sportmedizin für ihre Hilfe und das freundschaftliche Arbeitsklima. Insbesondere danke ich **Frau Anika Voß** und **Frau Mojgan Ghilav** für ihre technische Assistenz. Zudem gilt mein Dank **Frau Dr. Annette Schmidt**, die mir stets fachlich und freundschaftlich zur Seite stand. **Frau Dr. Klara Brixius** und **Frau Dr. Daniela Malan** danke ich für ihre zahlreichen Ratschläge. Besonders **Frau Yvonne Delhasse**, **Herrn Florian Brenig** und **Frau Laura Baumgartner** bin ich dankbar dafür, dass wir gemeinsam unsere kleine Stammzellgruppe gegründet haben. Was hätte ich nur ohne Euch gemacht? Ich hoffe wir bleiben in Kontakt!

Für zahlreiche Verbesserungsvorschläge und viele motivierende Worte danke ich **Herrn Dr. Christopher Rösch**.

Besonders herzlich bedanke ich mich bei **Herrn Dr. Alexander Ghanem**, der nicht nur meine Doktorarbeit, sondern mein ganzes Leben bereichert hat.

Schließlich möchte ich meinen Eltern, meinem Bruder Uli, meiner Oma und Jens für die große Unterstützung und Motivation während meines gesamten Studiums danken!

Ich versichere, dass ich die von mir vorgelegte Dissertation selbstständig angefertigt, die benutzten Quellen und Hilfsmittel vollständig angegeben und die Stellen der Arbeit – einschließlich Tabellen, Karten und Abbildungen –, die anderen Werken im Wortlaut oder dem Sinn nach entnommen sind, in jedem Einzelfall als Entlehnung kenntlich gemacht habe; dass diese Dissertation noch keiner anderen Fakultät oder Universität zur Prüfung vorgelegen hat; dass sie – abgesehen von unten angegebenen Teilpublikationen – noch nicht veröffentlicht worden ist sowie, dass ich eine solche Veröffentlichung vor Abschluss des Promotionsverfahrens nicht vornehmen werde. Die Bestimmungen der Promotionsverordnung sind mir bekannt. Die von mir vorgelegte Dissertation ist von Professor Dr. Wilhelm Bloch betreut worden.

Köln, 16. Januar 2008

Caroline Steingen

Lebenslauf

Name:	Caroline Steingen
Anschrift:	Säckinger Straße 29, 50935 Köln
Geburtsdatum:	18. April 1979
Geburtsort:	Köln
Eltern:	Rudolf Steingen und Carin Steingen-Zickendrath
Familienstand:	ledig
Konfession:	römisch-katholisch
Staatsangehörigkeit:	deutsch

Ausbildung

07.1985 – 06.1989	Gemeinschaftsgrundschule Freiligrathstraße, Köln
08.1989 – 06.1998	Städtisches Apostelgymnasium Köln
06.1998	Allgemeine Hochschulreife (Städtisches Apostelgymnasium Köln)
10.1998	Immatrikulation an der Universität zu Köln, Fachrichtung Biologie
10.2002 – 04.2004	Wissenschaftliche und studentische Hilfskraft am Institut für Botanik, Universität zu Köln
01.2004	Studienabschluss: Diplom in Biologie, Institut für Botanik, Universität zu Köln
Seit 05.2004	Doktorandin am Institut für Kreislaufforschung und Sportmedizin, Deutsche Sporthochschule Köln
Seit 11.2004	Teilnahme am Interdisziplinären Promotionsstudiengang Molekulare Medizin der Universität zu Köln
01.2005 – 12.2005	Promotionsstipendiatin von Köln Fortune, Forschungsförderungsprogramm der Universität zu Köln
Seit 01/2006	Promotionsstipendiatin der Jürgen Manchot Stiftung, Düsseldorf

Caroline Steingen